KEITH ANTHONY JOHNSON
High Resolution Mass Spectrometry of Metalloproteins: Studies by Electrospray Ionization Fourier Transform Ion Cyclotron Resonance Mass Spectrometry
(Under the Direction of IVES JONATHAN AMSTER)

ESI-FTICR mass spectrometry is used to determine the stoichiometry of iron-sulfur cluster proteins. The iron-sulfur clusters range from mononuclear iron-containing rubredoxin to ferredoxin that contains [2Fe-2S], [3Fe-4S] and [4Fe-4S] clusters as well as metal-substituted [3FeMn-4S] and [4Ga-4S] clusters. Positive and negative ionization mode mass spectra are compared for these metalloproteins. An increase in ion stability is observed in the mass spectra for some iron-sulfur cluster proteins in negative mode ESI compared to their spectra obtained in positive ion ESI.

High resolution and high mass accuracy are two characteristics of FTICR that make the technique useful for metalloprotein studies distinguishing between mass differences associated with disulfide bond formation, changes in oxidation state of the metal or metal cluster, and changes in mass due to post-translational modifications. The formation of disulfide bonds between free cysteine ligands upon metalloprotein denaturation leads to changes in protein molecular weight by as little as two mass units. The oxidation state of the metal or metal cluster in a metalloprotein is derived from the difference between the calculated and experimental masses, and the biologically relevant oxidation state of the metalloprotein is observed. Post-translational modifications such as glycosylation can greatly affect the measured molecular weight, whereas modifications such as amidation have only a small effect. The high potential iron-sulfur protein from *Chromatium vinosum* embodies all of these complications.

The chemically and on-line electrochemically reduced forms of several metalloproteins are observed using ESI-FTICR. Normal sample handling procedures produce mass spectra of metalloproteins in their oxidized forms. After chemical or electrochemical reduction and rigorous exclusion of oxygen, the reduced forms of metalloproteins are detected in the gas

phase. The oxidation state of the metal center is stable with respect to electrospray ionization in both positive and negative ionization modes.

INDEX WORDS: Fourier Transform Ion Cyclotron Resonance, FTICR; Electrospray Ionization, ESI; Metalloprotein; Iron-Sulfur Cluster; Oxidation; Reduction; High Potential Iron-Sulfur Protein; Positive Ions; Negative Ions; Electrochemical Cell; Post-Translational Modification

HIGH RESOLUTION MASS SPECTROMETRY OF METALLOPROTEINS: STUDIES BY ELECTROSPRAY IONIZATION FOURIER TRANSFORM ION CYCLOTRON RESONANCE MASS SPECTROMETRY

by

KEITH ANTHONY JOHNSON

B.S., University of Colorado at Denver, 1995

A Dissertation Submitted to the Graduate Faculty of The University of Georgia in Partial Fulfillment of the Requirements for the Degree

DOCTOR OF PHILOSOPHY

ATHENS, GEORGIA

2001

HIGH RESOLUTION MASS SPECTROMETRY OF METALLOPROTEINS: STUDIES BY ELECTROSPRAY IONIZATION FOURIER TRANSFORM ION CYCLOTRON RESONANCE MASS SPECTROMETRY

by

KEITH ANTHONY JOHNSON

Approved:

Major Professor: I. Jonathan Amster

Committee: Michael Johnson
James L. Anderson
Richard Dluhy
Ron Orlando

Electronic Version Approved:

Gordhan L Patel
Dean of the Graduate School
The University of Georgia
May 2001

DEDICATION

I would like to dedicate this work to my family and friends who have supported me, provided inspiration, and shaped my life in one form or another over the years. Thank you for always being there for me.

Phrase, Geraldine and Jeff Johnson

Lamar and Martha Covington

Adi, Emmi and Daniel Neuhauser

ACKNOWLEDGMENTS

Writing a dissertation begins with an interest in science that comes from more than just reading textbooks and solving mounds of homework problems. The interest is conceived from the dedication, knowledge and ability of others to guide a student along the way while maintaining the interest that drives the student to learn. First and foremost, I would like to acknowledge my family for providing the initial driving force for me to enjoy learning. The key turning point in my choice of graduate training came from my undergraduate analytical chemistry professor from the University of Colorado. Dr. Don Zapien taught chemistry with an enthusiasm that was contagious. He explored not only the small components of science in his class and laboratory, but also painted the bigger picture - how chemistry relates to other sciences. He explored how and why chemistry works with his students as if the fundamental concepts that he was demonstrating were being observed for the very first time. I admire his talent and his dedication.

I would also like to thank my major professor during graduate school, Dr. Jonathan Amster for his guidance, dedication, and patience during my studies in his laboratory at the University of Georgia. It is because of him that I have become a better scientist. During my graduate studies, there have been many professors at the University of Georgia who have guided my learning either directly or indirectly, and who should be acknowledged. These professors are Dr. Richard Dluhy, Dr. Ron Orlando, Dr. James Anderson, Dr. Michael Johnson and Dr. Jon Stickney.

I would also like to acknowledge my group members over the past few years who have come and gone and those that will still remain for a short period of time. These members include (in order of appearance) Cindy Pitsenberger, Mike Easterling, Kristi Taylor, Shubhada Kulkarni, Todd Mize, Gary Dent, David Silverstein, Michelle Trester, Julia Swancy, and Bryan

Parks. Other graduate students who have helped me survive my initial years in graduate school and enjoy my final years in graduate school include (in order of appearance) Karl Kirschner (TWP), Lorrie Howell, Shannon Garton, Brian Shira, Julia Swancy and Chad Galloway. All of the aforementioned graduate students must be acknowledged for their help for, in one or more ways, proofreading papers, assembling posters, solving problems, preparing for exams, collaborating on projects, teaching undergraduate lab courses, brainstorming, and sometimes just relaxing. I am deeply grateful for their friendship.

TABLE OF CONTENTS

CHAPTER 1

INTRODUCTION AND LITERATURE REVIEW

This dissertation describes studies by electrospray ionization Fourier transform ion cyclotron resonance mass spectrometry applied to metalloproteins. The high resolution and accuracy of FTICR mass spectrometry are used to deduce the changes in mass that accompany changes in metalloproteins, which may be structural or functional. These changes include amino acid modifications, post translational modifications, disulfide bond formation, metal substitution, and mass shifts that accompany redox reactions of metalloproteins.

I Mass Spectrometry of Metalloproteins

Proteins that contain metal centers or metal clusters play a significant role in biology. These metalloproteins aid in biochemical processes such as respiration, muscle contraction and relaxation, photosynthesis, and protein folding.[1-4] Substitutions of one metal or amino acid for another has been a common ways to study the structure - function relationships in metalloproteins. The three-dimensional structure of the protein is, in many cases, critical to the proper function of the metalloprotein as a whole.[2, 5]

Mass spectrometry has been used to identify these substitutions and mutations, and has also been used to uncover a wide range of metalloprotein characteristics. Mass spectrometry provides a means to study conformational changes that accompany metal binding, to observe metal-protein interactions, and to infer mechanisms for protein folding.[6-9] The metal or metal cluster is usually coordinated to the protein through only a few amino acids, however, slight changes in the three dimensional structure of the active site can cause significant changes in function.[10, 11] Therefore, the ionization method that is chosen for mass spectrometric analysis should be gentle, and not disturb the conformation of the three dimensional structure of the metalloprotein during transfer of the analyte into the gas-phase.[12-15] Many mass spectrometric procedures have been used to probe three dimensional structure in metalloproteins including H/D exchange[6, 16, 17] and by monitoring shifts in the charge state distribution in ESI caused by variations in solvent composition.[15, 18, 19] The stability of metalloproteins and their derivatives produced by site directed mutagenisis and by metal replacement has also been studied. Both

positive and negative ions have been generated and studied.[20-23] The derivation of the formal oxidation state of the metal centers of various metalloproteins has also been investigated, and both oxidized and reduced metal centers have been observed both by accurate mass measurements,[24, 25] and through tandem mass spectrometric dissociation methods that include collision induced dissociation (CID),[26] electron capture dissociation (ECD)[27] and infrared radiation multiphoton dissociation (IRMPD).[25]

II Denaturing versus Nondenaturing Ionzation Methods

There are several methods used in conjunction with mass spectrometry to ionize high molecular weight biomolecules. For metalloproteins, the most relevant methods are electrospray ionization (ESI) and matrix-assisted laser desorption/ionization (MALDI). ESI is rapidly becoming the most popular technique for metalloprotein studies since the intact metal-protein complex can be investigated in its native state. MALDI is also a soft ionization method that is used in some cases with metalloproteins, but is limited in applicability by the sample preparation methods which typically denature proteins. It is important to keep metalloproteins in their folded state during ionization, since the metal centers are typically bound to the protein through interactions with the side chains of several amino acids. These sites of interaction are close enough to coordinate the metal center when the protein is folded, but often are too distant from each other in the denatured protein to serve effectively as ligands. Most analyses of metalloproteins have required the sample to be introduced in a nondenaturing medium.

Electrospray ionization (ESI): A typical ESI source is illustrated in Figure 1. The setup begins with a syringe that contains analyte in a solution. The solution is pumped by a syringe pump for nanoelectrospray (electrospray at nL/hr flow rates). An electrical contact is made, normally on the stainless steel syringe tip, via a liquid electrical junction. The voltage applied to the needle usually varies according to the flow rate of the solution. For the proteins investigated here, the flow rates are between 1 and 10 μL/h and the voltages range between 600 and 1200

Figure 1.1 The electrospray source region of the FTICR mass spectrometry is shown (illustration not shown to scale). Solution is pumped at low flow rates from the syringe, where the high voltage contact is made, through a teflon tube, and into the nanoelectrospray capillary. The electrospray is oriented on the same axis as the heated metal capillary, which serves as the entrance to the mass spectrometer.

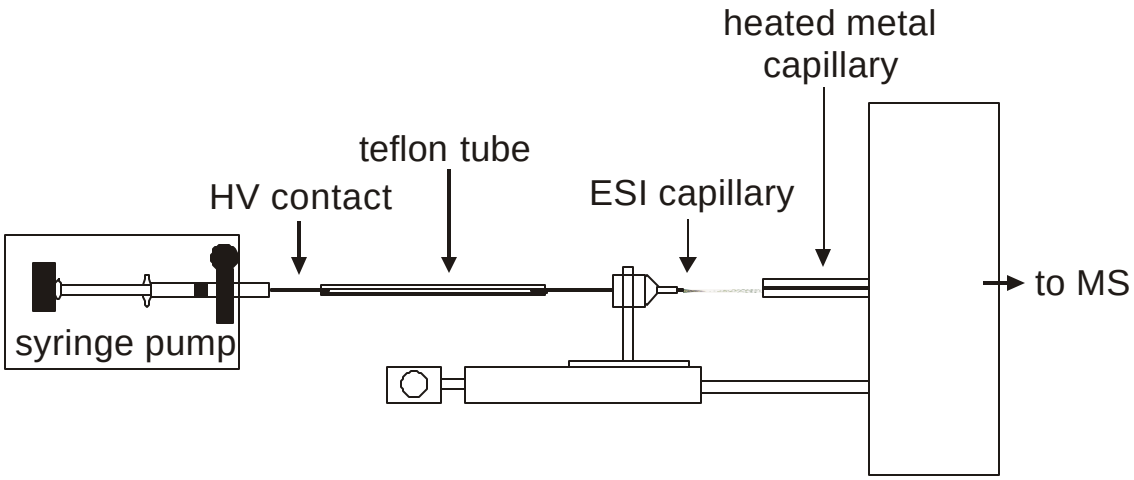
heated metal
capillary
teflon tube
HV contact
ESI capillary
to MS
syringe pump

V. The electrically charged solution is forced through a nanoelectrospray tip, which is positioned on axis toward a heated metal capillary, which is maintained at ground potential. This potential difference between the nanoelectrospray tip and the heated metal capillary causes a Taylor cone to form, from which a spray of solution is emitted. The charged droplets that are formed in the spray of solution produce gas-phase ions according to the charged residue model (CRM) of ion formation.[28] The CRM begins with the desolvation of the charged droplets. As the radii of the droplets decreases, the charge on the droplets increases. The Rayleigh limit defines the radius at which the charge on the droplet becomes greater than the surface tension that holds the droplet together.[29] At this point during desolvation, a coulombic fission event occurs, and destruction of the droplet creates smaller droplets. The newly created droplets repeat the process of desolvation and coulombic fission until each droplet contains a single protein ion. The remaining solvent evaporates from the ion, leaving the protein ion in the gas phase.

Electrospray ionization provides a means for introducing labile molecules into the gas phase for mass spectrometric analysis. The typical sample solvent (49% methanol, 49% water, 2% acetic acid) is highly denaturing, and usually causes the metal center to be lost from the protein, resulting in a mass spectrum of the apoprotein.[13, 14, 18, 30-35] Nondenaturing sample introduction to the mass spectrometer requires the use of low organic solvent content (< 10%) and neutral pH solutions. Introduction of such solutions by conventional electrospray is difficult, but is easily accomplished with pneumatic assistance[36-39] or by nanoelectrospray.[18, 35, 40, 41] Under nondenaturing conditions, metalloproteins which contain noncovalently bound metals or metal clusters can also be ionized without the loss of the noncovalently bound species.[14, 18, 19, 21, 22, 32, 33, 42-45] During electrospray ionization, ions are created by the addition of protons to basic sites along the peptide backbone to form positive ions or by loss of protons from acidic sites to form negative ions. The number of protons that accumulate on (or are extracted from) the metalloprotein during ion desolvation depends on the number of sites exposed to solution, and a distribution of charge states is normally seen in the mass spectrum. When the ions are

formed under nondenaturing solvent and ionization conditions it has been argued that the protein remains in a folded conformation in the gas phase.[5, 15, 46, 47] This is evidenced by the lower average charge state of the resulting distribution. For metalloproteins, the molecular weight that is derived from the experimental data corresponds to the mass of the amino acid constituents plus the weight of the metal center. When metalloproteins are exposed to denaturing solvent conditions such as extremes in pH or substantial concentrations of organic solvents, or aggressive ionization conditions such as a high nozzle-skimmer potential, the protein becomes denatured. When this occurs, the metal center is usually lost from the protein.

An example of the effect of solvent conditions on the mass spectrum of a metalloproteins is shown in Figure 2. The non-heme, iron-containing protein hemerythrin has been analyzed using ESI-FTICR mass spectrometry.[11] Metal binding was investigated under different solvent compositions to produce conditions necessary for the retention of the diiron center of hemerythrin. When using a solvent consisting of 10% methanol in water, metal attachment to hemerythrin was not disrupted, as shown in Figure 2, suggesting that the metalloprotein remains in a folded conformation under these conditions. The denatured mass spectrum was obtained after dissolving the metalloprotein in a solution containing methanol, water and acetic acid in the ratio of 49:49:2, shows a reduction in molecular weight corresponding to the mass of two iron atoms. The denaturation of a metalloprotein in mass spectrometry is accompanied by two characteristics in the mass spectrum. First, as the metalloprotein unfolds, a greater number of ionizable sites are exposed and become available for protonation (or deprotonation). This produces a shift in the mass spectrum toward lower mass-to-charge ratios and in some cases produces a broader charge state distribution, as can be seen in Figure 2. The second characteristic of a denatured metalloprotein is the loss of the metal. As the protein unfolds, the sites that bind the metal become more distant from each other and the metal or metal center is released, resulting in a measured mass that is lower than the molecular weight of the nondenatured metalloprotein by the mass of the metal or metal cluster that is contained therein.[15, 48]

Figure 1.2 The ESI-FTICR mass spectra for hemerythrin in denaturing solvent, 49% methanol, 49% water, 2% acetic acid (top), and in nondenaturing solvent, 10% methanol (bottom), are shown. The wider range of charge states in the top spectrum and the loss in mass of ~106 Da indicates that the protein in denaturing solvent is unfolded. The nondenatured metalloprotein maintains its folded conformation.

The observation of a metal ion complex in ESI mass spectrometry does not ensure that the metal is bound specifically to the protein active site. Nonspecific adduction of cations commonly occurs during ESI; however, nonspecifically bound metals are more easily displaced than a specifically bound metal. Adjustments in the ionization conditions during ESI can be used to reduce nonspecific interactions before detection.[49] Also, specifically bound metal atoms are resistant to dialysis or buffer exchange by ultrafiltration. Such procedures allow specific versus nonspecific binding of metals to be distinguished.

Matrix assisted laser desorption ionization (MALDI): The observation of noncovalent protein-metal and peptide-metal complexes has also been accomplished using matrix assisted laser desorption ionization (MALDI), although to a much lesser extent than for electrospray ionization. Several reviews have discussed the pros and cons of both ESI and MALDI as forms of ionization for metalloproteins and noncovalent complexes in general.[50, 51] Typically, the preparation of a sample for MALDI is conducted at low pH using a large excess of acidic matrix. These conditions denature a metalloprotein and disrupt the binding of the metal center in a protein-metal complex.[52-54]

MALDI-TOF mass spectrometry has been used to study zinc finger peptides under nondenaturing conditions by using solution preparation conditions which fall in the pH range 4-8 by dissolving the matrix, alpha-cyano-4-hydroxycinnamic acid in 1 M ammonium bicarbonate to neutralize the acid.[55] A similar method was used more recently to identify specific versus nonspecific binding in peptide-metal complexes.[56] The sample preparation conditions were kept at basic pH to prevent destruction of the metal-protein complex by using *p*-nitroanaline.

An iron-sulfur cluster intermediate has also been observed using MALDI-TOF mass spectrometry.[57] The high potential iron-sulfur protein from *Chromatium vinosum* has been of interest because of its [4Fe-4S] cluster and the mechanism of its formation. Mass spectrometry in combination with NMR spectroscopy has been used to characterize a stable [4Fe] intermediate in the metal-sulfur cluster formation. Using ^{1}H-^{15}N heteronuclear single quantum

coherence (HSQC) after the addition of Fe^{2+}, S^{2-} and dithiothreitol (DTT), a spectrum similar to the native spectrum was obtained, suggesting the possible formation of HiPIP with a [4Fe-4S] cluster. Similar experiments, but without the addition of S^{2-} were also performed and NMR spectra showing a change from apoprotein to protein with three dimensional structure were obtained. MALDI-TOF mass spectrometry was then used to confirm the addition of iron to the apoprotein. The stable intermediate mass corresponded to apoprotein, 4 equivalents of iron and 1 equivalents of DTT. ^{1}H NMR and electron paramagnetic resonance (EPR) data show that the addition of S^{2-} to the intermediate provides spectra that are indistinguishable from the native [4Fe-4S] containing protein.

MALDI-TOF mass spectrometry has more recently been adapted to analyze noncovalent interactions of metalloproteins by ionization from aqueous solutions of hemoglobin and calmodulin.[58, 59] In the hemoglobin experiments, the solution of 100 μM protein in 10 mM ammonium acetate buffer was injected into the high vacuum chamber of the mass spectrometer with a high pressure pump. The liquid beam extended ~10 cm into the mass spectrometer where it was then frozen onto a liquid nitrogen cool trap. The beam was intersected by a tunable infrared laser beam that imparted enough energy to the protein to aid in its escape from the liquid beam. The free ions were accelerated into the mass spectrometer. The intact tetramer of hemoglobin was detected in both negative and positive ion mode, with both singly and doubly charged ions observed in the spectra.[58] A more complete analysis of the technique applied to noncovalent complexes is outlined in a second study by Wattenberg et al.[59] In this study, calmodulin, a metalloprotein that regulates calcium dependent processes in various organisms, was examined using liquid beam ionization/desorption mass spectrometry (LILBID-MS). The properties of the calmodulin/melittin complex with calcium was studied by this method to observe the specificity of protein-substrate binding. The complex was shown not to form after addition of magnesium ions, but the intact complex was found to occur when calcium was added to the solution, demonstrating the specificity of the observed complex.

investigated to obtain parameters and nondenaturing conditions for use with other less stable iron-sulfur proteins. Rubredoxin is a small (MW~6000 Da) protein found in several different bacteria, including *Clostridium pasteurianum*. Although the function of rubredoxin is not known with certainty, it is thought to aid in electron transport. In its native state, rubredoxin contains an FeS_4 site. Petillot et al. used ESI-MS to examine rubredoxin purified from *C. pasteurianum* as well as rubredoxin which had been overexpressed in *E. coli*.[22] The study identified both iron and zinc forms of *Clostridium pasteurianum* rubredoxin and illustrated an increase in stability of both forms in the negative ion mode. They also showed that positive ions that were formylated showed greater stability (i.e. retention of the metal center) than the non-formylated forms based on the amount of apoprotein for each metalloprotein.

More complex iron-sulfur cluster proteins have also been studied in both modes of ionization. Wild type and mutated forms of ferredoxins from *Clostidium pasteurianum* containing a [2Fe-2S] cluster were shown to be more stable in the negative ion mode than in the positive ion mode.[45] The mass spectra for this metalloprotein showed that in addition to the apoprotein, a species existed whose mass matched the apoprotein plus two iron atoms and two sulfur atoms. The assembly of a [3Fe-2S] cluster was verified by other analytical methods. Ferredoxin from *Rhodobacter capsulatus* containing two intact [4Fe-4S] centers has also been observed as a stable negative ion.[66] The native ferredoxin isolated from *Rhodobacter capsulatus* contains one [3Fe-4S] cluster and one [4Fe-4S] cluster. However, overexpression of ferredoxin complete with metal centers yields only minimal amounts of protein. It was therefore necessary to express the protein in the apo form and then reconstitute it with the metal centers. The mass of the overexpressed apo-ferredoxin was identical to that purified from the native bacteria. After insertion of the metal, ESI-MS was used to characterize the protein. The mass of the recombinant protein matched that of the apo-protein plus two [4Fe-4S] clusters, rather than containing one [3Fe-4S] cluster as in the native form. This recombinant protein also showed much weaker enzyme activity, adding evidence for its erroneous composition. The results of these studies indicate that these proteins are more stable at neutral pH and are

converted to negative ions in this region. Wild type ferredoxin from *Anabaena* has been observed in positive and negative mode ESI and was shown to contain its intact [2Fe-2S] cluster only as a negative ion.[20] The positive mode spectrum contained only apoprotein. MALDI was also used to obtain conditions for which the iron-sulfur cluster could be observed. An acceleration voltage of 20 kV produced peaks showing losses of 1S, 2S, [1Fe-2S] or [2Fe-1S] from the cluster. Reduction of the acceleration voltage to 15 kV reduced the losses from the cluster and the protein containing the intact cluster was observed. Shifts in charge state distribution of the wild type and mutant forms of the protein using ESI in the negative mode have shown that the wild type protein is in a tightly folded conformation (lower charge states) and open conformations (higher charge states) for the mutant forms of the ferredoxin.

IV Investigation of Metal Content

The identity of a metal center or group of metals in a metalloprotein can be established by mass spectrometry. Identifying the metal that is coordinated to a wild type protein or investigating the stoichiometry of a metal cluster to determine the extent of metal binding in the active site of a metalloprotein are two common measurements. TOF, FTICR, and quadrupole mass spectrometry have been coupled with separation methods and various ionization methods to achieve the goal of investigating the metal content of many metalloproteins. Among the many metalloproteins studied for their stoichiometry are metallothioneins, zinc, copper and receptor metalloproteins.

Fabris et al. examined the thiol protons of metallothioneins with ESI-MS.[67] Several different classes of metallothioneins were studied, including protein purified from the native strain, recombinant protein, and a synthetic protein. In all the samples, the observed molecular masses were higher than those expected with complete deprotonation. Only enough protons were lost in each case to balance the charges of the divalent zinc atoms, suggesting partial retention of protons within the metal clusters.

Metalloproteins typically have one or two types of metals which they bind preferentially, and these specific metals are necessary for the proper functioning of the metalloprotein. However, it is often possible for the metalloprotein to bind other metals, although the affinity may be lower. It is also possible for proteins to interact with metals even though they are not primarily metalloproteins. Cooperative binding, in which the protein retains all of the metals associated with the metal center or none at all, is another type of metal binding in proteins. In many cases, cooperative binding is associated with a conformational change and this type of change in three dimensional structure can often be monitored by mass spectrometry.[4-6]

Veenstra et al. used ESI-MS to examine the zinc dependent binding of the vitamin D receptor DNA binding domain to the mouse osteopontin (mOP) vitamin D response element (VDRE).[4] In the presence of zinc, it was found that the vitamin D receptor bound the mOP VDRE in both a 1:1 and 2:1 stoichiometry. Both complexes contained two zinc atoms per protein. Addition of 100 μM zinc ion to the complex solution increased the amount of dimer/DNA complex relative to monomer/DNA complex, but addition of 200 μM zinc ion caused dissociation of the complex. In the absence of zinc, however, no binding to the mOP VDRE was observed. Cadmium, which also binds to zinc-finger domains, effected similar results. From these studies it is conjectured that metal binding to the two zinc-finger regions is necessary for DNA binding, but metal binding to the lower-affinity sites causes dissociation of the protein/DNA complexes.

V Metalloprotein Oxidation States Observed by Mass Spectrometry

The formal oxidation state of the metal center in metalloproteins has been examined by mass spectrometry. Gas phase studies of metalloproteins have been important in investigations of proteins, enzymes and metalloproteins and their similarities to solution studies have also been compared.[10, 57] The observation of the formal oxidation state carried by the metal centers of metalloproteins has been an important consideration especially for those proteins involved in redox chemistry, which carry out their biological function through the translocation of electrons.

Additional sequence structure of metalloproteins can be obtained by electrospray ionization mass spectrometry in combination with methods like collision-induced dissociation (CID), electron capture dissociation (ECD), and infrared radiation multiphoton dissociation (IRMPD). Each of these methods has been applied to various heme proteins in the gas phase and supplies the energy of activation necessary to activate the molecule causing a change in its conformation.

The zinc binding sites on engineered hemoglobin were investigated by ESI mass spectrometry.[14] Adduct masses to the B-chain were ~63 Da greater than the B-chain. The discrepancy was narrowed to the adduction of Zn ion, which, with the displacement of two protons for Zn^{2+}, is consistent with the atomic mass for zinc, 65.38 Da. After addition of EDTA to the protein, chelation was no longer observed. The binding site for zinc was narrowed to a cysteine residue after CID was performed on the protein. The neutral loss of zinc sulfide provides evidence that a cysteine residue is involved in chelation of zinc ion.

The structures of cytochrome *c* variants were studied using sustained off-resonance irradiation with collision-induced dissociation (SORI-CID) to obtain primary sequence information for each.[68] It was found that after fragmentation in the gas phase, the iron-containing heme group was in its reduced state, with a charge of 2^+. The result implies that the reduced form of the heme group for cytochrome *c* is more stable after the fragmentation event in the gas phase than the oxidized form. A study comparing the CID patterns for myoglobin, hemoglobin and cytochrome *c* by Henion and coworkers produced a similar result for the dissociated heme group for cytochrome *c*. However, the heme groups for myoglobin and hemoglobin remained in their oxidized forms in the gas phase.[26] The reduced and oxidized forms of cytochrome *c* have also been investigated indirectly by ESI-FTICR mass spectrometry. Wang and co-workers reported the use of capillary electrophoresis-mass spectrometry.[11] They reported the separation of the two forms of cytochrome *c* by capillary electrophoresis before detection, however, the resolution of the mass spectrometer was not capable of distinguishing the mass difference between the oxidized and reduced forms, so it is

not possible to conclude that the reduced sample did not reoxidize prior to mass spectrometric detection. Additional studies of the oxidized forms of metalloproteins are outlined in Chapters 2 and 3 of this work, and further studies of the reduced forms of metalloproteins are covered in Chapters 6 and 7.

VI High Resolution Mass Spectrometry

Fourier transform ion cyclotron resonance (FTICR) mass spectrometry is used for the study of metalloproteins because of its high resolution and mass accuracy.[6, 16, 18, 19, 24, 25] The fundamentals of FTICR mass spectrometry have been covered in several papers.[69-73] A typical experimental sequence is shown in Figure 3. Since ESI is a continuous ion source, the sequence begins with quench of the analyzer cell and hexapole region of the source. This removes ions from these regions and prepares the ionization-detection sequence for a scan. Ions are then pulsed from the hexapole to the analyzer cell where they are first excited and then detected. An illustration of the excitation and detection processes is shown in Figure 4 (adaptation from reference 73). Metalloprotein ions are captured at the center of the ion cyclotron resonance (ICR) cell by trapping voltages that are maintained on the from and back trap plates of the cell. Although the trapped ions have a small amount of kinetic energy, their orbital radius is small compared to the dimensions of the ICR cell. To be detected, they must be excited radially so they approach the edges of the analyzer. This excitation occurs by imparting kinetic energy to the trapped ions by applying an r.f. electric field to the excitation plates of the ICR cell. Chirp excitation, a rapid sweep of a range of frequencies, is often used to excite ions of all mass-to-charge ranges in the analyzer cell. This allows all of the trapped ions to be excited and detected simultaneously. When the cyclotron resonance of an ion of a particular mass-to-charge becomes resonant with the applied field, it spirals away from the center of the trap as shown at the top of Figure 4. If the electric field is maintained, ions will continue their spiral until they collide with the trap itself, becoming neutralized. If the electric field is controlled so that the ions are only excited to a large radius, the cyclotron orbit is

Figure 1.3 The experimental sequence during ESI consists of a cell quench, ionization pulse, excitation of trapped ions and detection. The raised boxes indicate changes in voltage to move ions through the system.

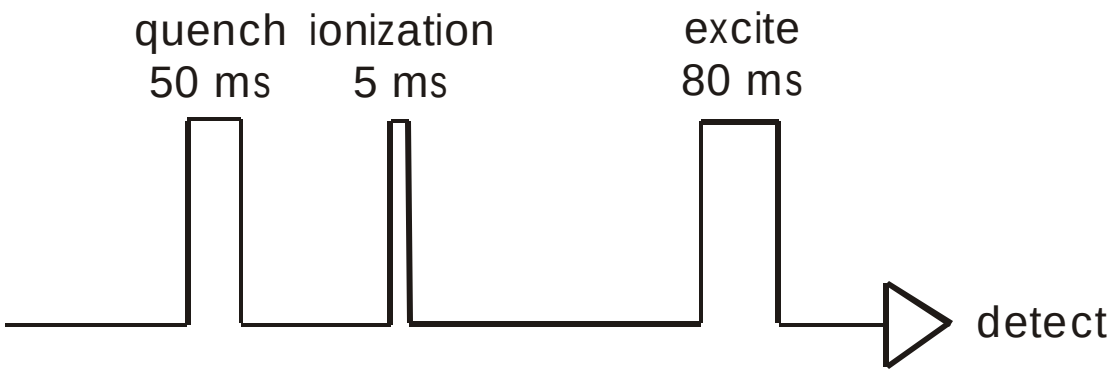
quench
50 ms
ionization
5 ms
excite
80 ms
detect

Figure 1. 4 Excitation of trapped ions is accomplished by imparting kinetic energy to the ions. The magnetic field (field lines point into the page) serves to maintain the orbit of the ions as they spiral away from the center of the cell. The stable orbit of the ions (shown in lower figure) is detected by the cell plates. An image current is induced, and the frequency of the orbiting ions are obtained. The frequency information is transformed into a mass-to-charge scale.

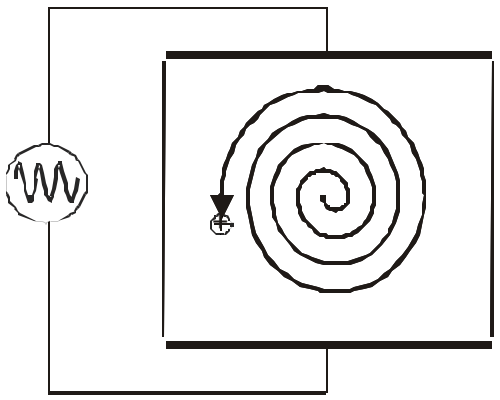

B⊗

$$f = \frac{qB}{2\pi m}$$

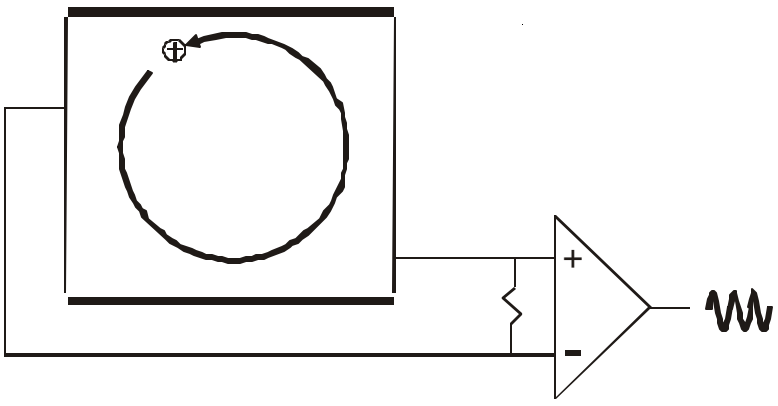

Figure 1.5 The forces acting on a charged particle in a magnetic field include the Lorentz (magnetic field) force and the centrifugal force. The magnetic field lines are oriented into the page.

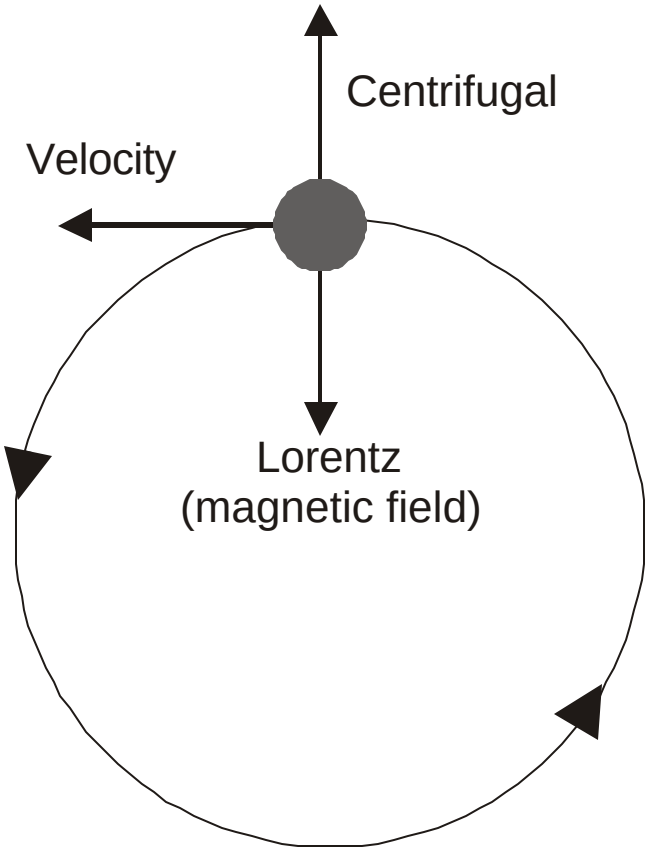
Centrifugal
Velocity
Lorentz
(magnetic field)

preserved as shown at the bottom of Figure 4. The packet of ions of a given mass-to-charge attracts electrons to each detection electrode as it passes by in its orbit. This sinusoidal current, also know as image current, is induced by the orbiting packet of ions. The signal is amplified, digitized, and stored for processing by a computer.[73]

The high accuracy obtained in FTICR mass spectrometry results from the measurement of the frequency of the orbiting ions in the cell. The forces that describe the motion of the ions in the cell can be derived from Figure 5. A charged particle in motion is constrained to its orbit by the magnetic field or Lorentz force. This force is defined by the first half of equation 1, where *q* is the charge on the particle, B is the magnetic field

$$qvB = \frac{mv^2}{r} \qquad (1)$$

strength, and *v* is the velocity of the orbiting particle. The second force affecting the particle is the centrifugal force, which is defined by the second half of equation 1. The mass of the particle is defined as *m*, and the centripetal acceleration is defined by v^2/r. Rearrangement of equation 1 yields equation 2, the cyclotron frequency, *w*.

$$w = \frac{v^2}{r} = \frac{qB}{m} \qquad (2)$$

Although high resolution can be obtained by measurements of an ions cyclotron frequency, there are still limitations to the method. The maximum resolution that can be obtained from a given data set can be calculated from equation 3, where R is resolving power, *w* is the cyclotron frequency, and T is the duration of the transient.

$$R = \frac{wT}{2} \qquad (3)$$

Figure 1.6 Transients for insulin (A, C) and their transformation into the mass-to-charge scale (B, D) are shown. Resolution increases as the duration of the transient increases. The resolution for spectrum obtained from the 0.47 s transient (A, B) is ~27,000. The resolution for the longer 0.83 s transient (C, D) is ~47,000.

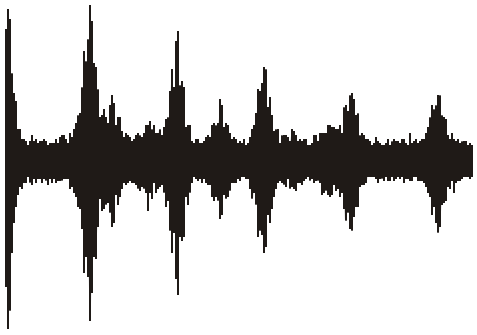

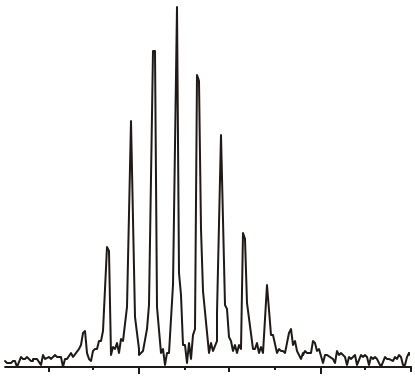

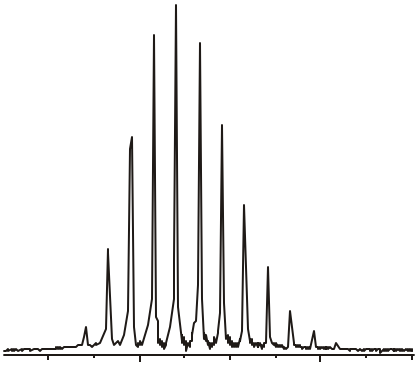

This equation emphasizes the need for long transients in obtaining high resolution data. This requires ions to be constrained in their cyclotron orbits during the time the transient signal is collected. Ultra-high vacuum and the number of trapped ions in the cell are two factors that limit the duration of the transient. An example of the image signal or transient and the mass spectrum that accompanies the data are shown in Figure 6. Both spectra were obtained for bovine insulin and illustrate the application of the Fourier transform to the frequency spectra to yield the mass spectra. Figures 6A and 6C show transients obtained for bovine insulin in two separate experiments. The transient in Figure 6A has a duration of 0.47 s and the transient in Figure 6C has a duration of 0.83 s. Figure 6B is obtained after applying the Fourier transform to the shorter transient signal, and a resolution of ~27,000 is obtained. For the longer transient, Figure 6D was derived. The resolution obtained for the transformed signal is 47,000. From these data and equation 3, one can see that higher resolution is obtained from longer transients.

The mass accuracy of FTICR mass spectrometry also aids in the analysis of the small changes in mass that are associated with metalloproteins depending on their structure and function. Other mass spectrometric methods, such as time-of-flight (TOF) and Quadrupole mass spectrometry are helpful in discerning changes in mass associated with the loss of metal from a metalloprotein,[22] or the identity of metal substitution into a metalloproteins,[21,74] but FTICR mass spectrometry is capable of providing additional information about metalloproteins that can only be acquired through its highly accurate measurements.[18, 25] The one to two mass unit shifts that are associated with disulfide bond

formation or oxidation state determination can be easily investigated over a wide mass range by FTICR mass spectrometry since it is capable of providing mass accuracies of the order of a few ppm over a fairly wide mass-to-charge range.[73] The combination of ESI with FTICR mass spectrometry results in the production of the high resolution data shown if Figure 7, from which charge state information and ultimately molecular weight data can be extracted. The figure consists of three spectra: ampicillin, ubiquitin, and high potential iron-sulfur protein. The proteins are shown in order of increasing molecular weight. The monoisotopic peak in the

Figure 1.7 The theoretically derived spectra for the 1+ charge state of ampicillin dimer and the 7+ charge state of ubiquitin are shown with the experimentally derived spectrum for the 5+ charge state for high-potential iron-sulfur protein. The monoisotopic peak in each spectrum decreases with increasing molecular weight.

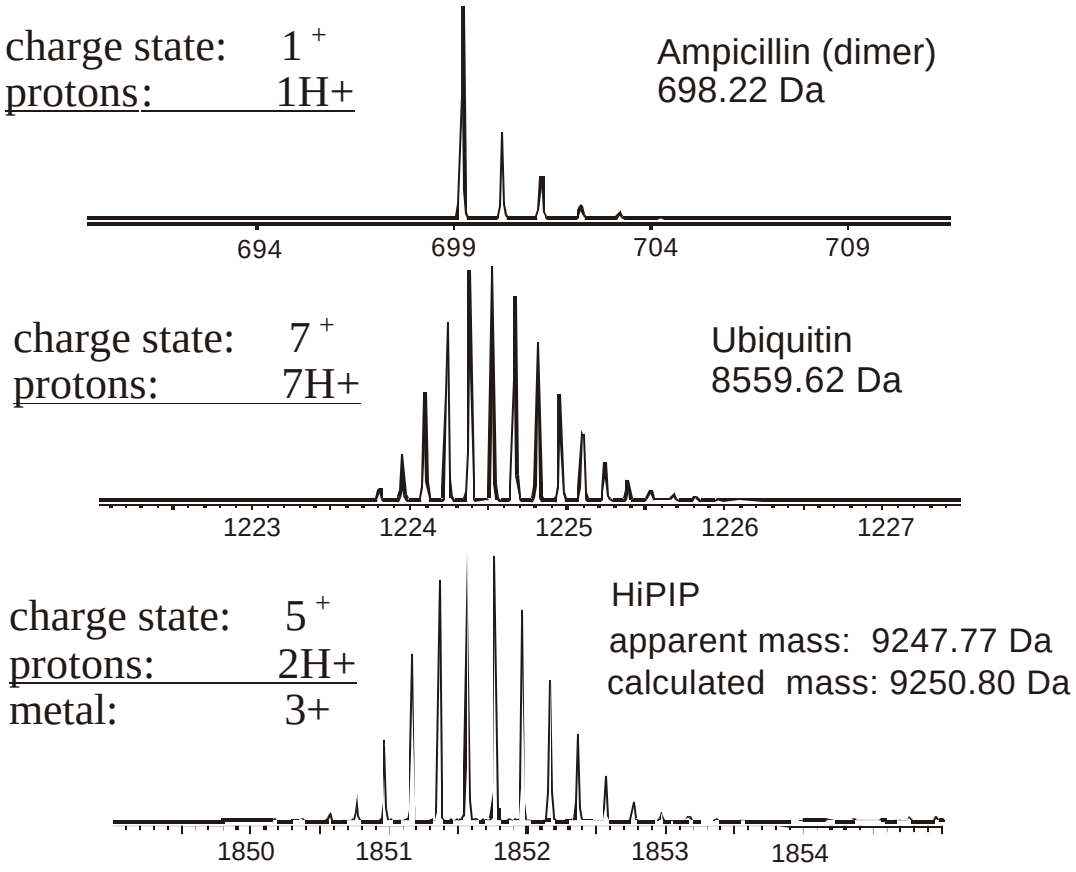
charge state: 1+
protons: 1H+
Ampicillin (dimer)
698.22 Da
694
699
704
709
charge state: 7+
protons: 7H+
Ubiquitin
8559.62 Da
1223
1224
1225
1226
1227
charge state: 5+
protons: 2H+
metal: 3+
HiPIP
apparent mass: 9247.77 Da
calculated mass: 9250.80 Da
1850
1851
1852
1853
1854

distribution obtained for ampicillin is the lowest mass-to-charge peak in the distribution and consists of the sum of all of the lowest mass isotopes of the elements that make up the molecular formula. The monoisotopic species include ^{12}C, ^{1}H, ^{14}N, ^{16}O and ^{32}S. The other peaks in the distribution consist of variations in the molecular formula. The second largest peak in this distribution, for example, is composed of all of the lowest mass isotopes in the molecular formula with the exception that one of the ^{12}C isotopes has been replaced by ^{13}C, which results in an increase of ~ 1Da. The remaining peaks in this distribution are composed of varying contributions of additional ^{13}C isotopes in the molecular formula, as well as variations of the other isotopes, although the abundance of ^{13}C greatly outweighs all other possibilities.

The appearance in the mass spectrum and consistency in the molecular weight increase for ^{13}C isotopes is fortuitous, since the spacing of the isotope peaks depends on the charge present on a given ion. For the *m/z* values in the ampicillin distribution, we can conclude that since the spacing between the isotope peaks is ~1 *m/z* unit, the charge on the ion is also 1+. Alternatively, since the mass difference between ^{12}C and ^{13}C is ~1 Da, the isotope spacing for a singly-charged ion must be ~1 *m/z* unit. For a doubly-charged ion, the spacing between isotope peaks drops to ~0.5 Da. The rule applies to proteins of all molecular weight and to all charge states. The second spectrum in the figure is of the higher molecular weight protein, ubiquitin. The decrease in *m/z* spacing between the isotope peaks suggests that the charge state for this protein is greater than one. In fact, the difference between the spacing is 1/7 the spacing of the 1+ charge state of ampicillin. This 7+ charge state for ubiquitin differs from the ampicillin spectrum in that the monoisotopic peak for ampicillin is the most abundant isotope peak in the

$$M = (m/z)z - zM_{H+} \qquad (4)$$

distribution, whereas for ubiquitin, it is one of the lowest peaks in the distribution. The monoisotopic peak is easily discernible in the mass spectrum for proteins and peptides whose molecular weights are under 5000 Da, however, the increased probability for multiple heavy

isotopes decreases the relative abundance of the monoisotopic peak.[75, 76] After 20000 Da, the monoisotopic peak is no longer visible in the mass spectrum for our current instrument conditions and must be inferred from the data after applying the χ^2 test.[18, 76] The mass of each of these proteins can be obtained using equation 4, where M is apparent mass, M_{H^+} is the mass of a proton, z is the charge present on the ion, and m/z is the measured mass-to-charge ratio. So for ubiquitin of 7+ charge, assuming that all of the charge is in the form of protons, the molecular weight of the monoisotopic species is 8559.62 Da.

The treatment of the data for metalloproteins is the same for all other proteins. In this case, some of the charge on the metal center is in the form of the oxidation state for the metal center, rather than solely in the form of protons. This makes the comparison of the measured monoisotopic mass and the calculated mass unequal. The calculated mass assumes that there are no disulfide bonds in the protein and uses the most abundant form of the metal, not the monoisotopic form, in the calculation of the molecular weight. This corresponds, for example, to ^{56}Fe instead of ^{54}Fe, which is only 6% abundant compared to ^{56}Fe, and produces very weak signals in the mass spectrum. The [4Fe-4S]-containing metalloprotein from high-potential iron-sulfur protein from *Chromatium vinosum* is shown at the bottom of the figure. The molecular weight calculated from the data is 9247.77 Da and is compared to the theoretical molecular weight, 9250.80 Da. Since some of the charge on a metalloprotein ion is in the form of the oxidation state of the metal, eq 4 overestimates (for positive ions) the number of protons that make up a given charge state. In this case, the apparent mass will be lower than the calculated molecular weight (monoisotopic mass) by the mass of protons that are equal to the charge on the metal center. The charge state calculated from the spacing between the isotope peaks is 5+, and we assume that all of the charge is present in the form of protons, we have overestimated the number of protons by an amount equal to the charge on the metal center of the protein, $[4Fe\text{-}4S]^{3+}$. This treatment is described in more detail in the following chapters. Although the charge state information can be derived from both high resolution and low resolution ESI mass spectra, the small changes in mass described here, in addition to other

circumstances encountered during later chapters, illustrate the necessity for having FTICR aid in the determination of mass from a variety of metalloproteins.

As the molecular weight of metalloproteins increases, the charge state distribution for the ions approaches higher mass-to-charge. The higher charge states, and the probability of having a greater number of isotopes for a given mass decreases the isotope spacing for an ion. The isotope statistics, or the relative abundances of the isotopes, which aid in the assignment of the monoisotopic peak in the distribution, also become less certain. For this reason, many of the measurements that require high resolution can only be achieved for metalloproteins with molecular weights less than ~20,000 Da, although stoichiometry and substrate binding can still be analyzed for large metalloproteins. The effective mass range of any analyzer is increased by a factor equal to the number of charges on an ion.[77] Many enzymes and metalloproteins fall into the high molecular weight category where this is advantageous. Hemoglobin, for example is a tetrameric metalloprotein that binds a variety of ligands. ESI-FTICR mass spectrometry is used in Chapter 7 to observe ligand binding to hemoglobin and myoglobin in their reduced and oxidized forms.

The studies included in this dissertation expand on literature that has been conducted by other groups and it also provides new information in the study of metalloproteins. We have examined the small changes in mass that are associated with metalloprotein structure and function and in doing so have developed a variety of methods for future investigations. The details of these methods are included and a synopsis of the potential future direction of this research is also outlined (Chapter 8).

References

1 Zaia, J.; Jiang, L. C.; Han, M. S.; Tabb, J. R.; Wu, Z. C.; Fabris, D.; Fenselau, C. *Biochemistry.* **1996,** *35*, 2830-2835.

2 Nemirovskiy, O. V.; Ramanathan, R.; Gross, M. L. *J. Am. Soc. Mass Spectrom.* **1997,** *8*, 809-812.

3 Otsuka, S.; Yamanaka, T. In *Bioactive Molecules*; Elsevier: Tokyo, 1988; Vol. 8.

4 Veenstra, T. D.; Johnson, K. L.; Tomlinson, A. J.; Craig, T. A.; Kumar, R.; Naylor, S. *J. Am. Soc. Mass Spectrom.* **1998,** *9*, 8-14.

5 Chowdhury, S. K.; Katta, V.; Chait, B. T. *J. Am. Chem. Soc.* **1990,** *112*, 9012-9013.

6 Wang, F.; Li, W. Q.; Emmett, M. R.; Marshall, A. G.; Corson, D.; Sykes, B. D. *J. Am. Soc. Mass Spectrom.* **1999,** *10*, 703-710.

7 Cowan, J. *J. Am. Chem. Soc.* **1997,** *119*, 4080-4083.

8 Lippincott, J.; Fattor, T. J.; Lemon, D. D.; Apostol, I. *Anal. Biochem.* **2000,** *284*, 247-255.

9 Eyles, S. J.; Speir, J. P.; Kruppa, G. H.; Gierasch, L. M.; Kaltashov, I. A. *J. Am. Chem. Soc.* **2000,** *122*, 495-500.

10 McLafferty, F. *J. Am. Chem. Soc.* **1998,** *120*, 4732-4740.

11 He, T.; Chandramouli, N.; Fu, E.; Wu, A.; Wang, K. *Anal. Biochem.* **1999,** *271*, 189-192.

12 Konermann, L.; Douglas, D. J. *Biochemistry.* **1997,** *36*, 12296-12302.

13 Konermann, L.; Rosell, F. I.; Mauk, A. G.; Douglas, D. J. *Biochemistry.* **1997,** *36*, 6448-6454.

14 Lei, Q. P.; Cui, X. Y.; Kurtz, D. M.; Amster, I. J.; Chernushevich, I. V.; Standing, K. G. *Anal. Chem.* **1998,** *70*, 1838-1846.

15 Ens, W.; Standing, K.; Chernushevich, I. In *NATO ASI series. Series C, Mathematical and physical sciences*; Dordrecht, Boston, 1998; Vol. 510, pp 149-156.

16 Nemirovskiy, O.; Giblin, D. E.; Gross, M. L. *J. Am. Soc. Mass Spectrom.* **1999,** *10*, 711-718.

17 Neubert, T. A.; Walsh, K. A.; Hurley, J. B.; Johnson, R. S. *Protein Sci.* **1997,** *6*, 843-850.

18 Johnson, K. A.; Verhagen, M.; Adams, M. W. W.; Amster, I. J. *Anal. Chem.* **2000,** *72*, 1410-1418.

19 Johnson, K. A.; Amster, I. J. *J. Am. Soc. Mass Spectrom.* **2000**, Submitted.

20 Remigy, H.; Jaquinod, M.; Petillot, Y.; Gagnon, J.; Cheng, H.; Xia, B.; Markley, J. L.; Hurley, J. K.; Tollin, G.; Forest, E. *J. Protein Chem.* **1997,** *16*, 527-532.

21 Hay, M. T.; Milberg, R. M.; Lu, Y. *J. Am. Chem. Soc.* **1996,** *118*, 11976-11977.

22 Petillot, Y.; Forest, E.; Mathieu, I.; Meyer, J.; Moulis, J. M. *Biochemistry. J.* **1993,** *296*, 657-661.

23 MichaudSoret, I.; Adrait, A.; Jaquinod, M.; Forest, E.; Touati, D.; Latour, J. M. *FEBS Lett.* **1997,** *413*, 473-476.

24 Johnson, K. A.; Shira, B. A.; Anderson, J. A.; Amster, I. J. *Anal. Chem.* **2000**, Submitted.

25 He, F.; Hendrickson, C. L.; Marshall, A. G. *J. Am. Soc. Mass Spectrom.* **2000,** *11*, 120-126.

26 Li, Y. T.; Hsieh, Y. L.; Henion, J. D.; Ganem, B. *J. Am. Soc. Mass Spectrom.* **1993,** *4*, 631-637.

27 Zubarev, R. A.; Horn, D. M.; Fridriksson, E. K.; Kelleher, N. L.; Kruger, N. A.; Lewis, M. A.; Carpenter, B. K.; McLafferty, F. W. *Anal. Chem.* **2000,** *72*, 563-573.

28 Dole, M.; Mack, L. L.; Hines, R. L.; Mobley, R. C.; Ferguson, L. D.; Alice, M. B. *J. Chem. Phys.* **1968,** *52*, 4977.

29 Rayleigh, L. *Philos. Mag.* **1882,** *14*, 184.

30 Konermann, L. *Science Progress* **1998,** *81*, 123-140.

31 Petillot, Y.; Golinelli, M. P.; Forest, E.; Meyer, J. *Biochem. Biophys. Res. Commun.* **1995,** *210*, 686-694.

32 Feng, R.; Castelhano, A. L.; Billedeau, R.; Yuan, Z. Y. *J. Am. Soc. Mass Spectrom.* **1995,** *6*, 1105-1111.

33 Stillman, M. J.; Thomas, D.; Trevithick, C.; Guo, X.; Siu, M. *J. of Inorg. Biochem.* **2000,** *79*, 11-19.

34 Fabris, D.; Hathout, Y.; Fenselau, C. *Inorg. Biochem.* **1999,** *38*, 1322-1325.

35 He, F.; Hendrickson, C. L.; Marshall, A. G. *J. Am. Soc. Mass Spectrom.* **2000**, 120-126.

36 Bakhtiar, R.; Stearns, R. A. *Rapid Commun. Mass Spectrom.* **1995,** *9*, 240-244.

37 Hsieh, F. Y. L.; Tong, X.; Wachs, T.; Ganem, B.; Henion, J. *Anal. Biochem.* **1995,** *229*, 20-25.

38 Schneider, R. P.; Lynch, M. J.; Ericson, J. F.; Fouda, H. G. *Anal. Chem.* **1991,** *63*, 1789-1794.

39 Chassaigne, H.; Lobinski, R. *Analyst* **1998,** *123*, 2125-2130.

40 Wilm, M.; Mann, M. *Int. J. Mass Spectrom. Ion Process.* **1994,** *136*, 167-180.

41 Wilm, M.; Mann, M. *Anal. Chem.* **1996,** *68*, 1-8.

42 Loo, J. A. *Mass Spectrom. Rev.* **1997,** *16*, 1-23.

43 Hay, M. T.; Lu, Y. *J. Biol. Inorg. Chem.* **2000,** *5*, 699-712.

44 Veenstra, T. D. *Biophys. Chem.* **1999,** *79*, 63-79.

45 Meyer, J. *Biochem. Biophys. Res. Commun.* **1995,** *210*, 686-694.

46 Douglas, D.; Konerman, L. *J. Am. Soc. Mass Spectrom.* **1998,** *9*, 1248-1254.

47 Katta, V.; Chait, B. T. *J. Am. Chem. Soc.* **1991,** *113*, 8534-8535.

48 Kochendoerfer, G. G.; Kent, S. B. H. *Curr. Opin. Chem. Biol.* **1999,** *3*, 665-671.

49 Jensen, C.; Andersen, S. O.; Roepstorff, P. *Biochem. Biophys. Res. Commun. M.* **1998,** *1429*, 151-162.

50 Fitzgerald, M. C.; Siuzdak, G. *Chemistry & Biology* **1996,** *3*, 707-715.

51 Pramanik, B. N.; Bartner, P. L.; Mirza, U. A.; Liu, Y. H.; Ganguly, A. K. *J. Mass Spectrom.* **1998,** *33*, 911-920.

52 Glocker, M. O.; Bauer, S. H. J.; Kast, J.; Volz, J.; Przybylski, M. *J. Mass Spectrom.* **1996,** *31*, 1221-1227.

53 Nelson, R. W.; Hutchens, T. W. *Rapid Commun. Mass Spectrom.* **1992,** *6*, 4-8.

54 Hornshaw, M. P.; McDermott, J. R.; Candy, J. M. *Biochemistry. Biophys. Res. Commun.* **1995,** *207*, 621-629.

55 Woods, A. S.; Buchsbaum, J. C.; Worrall, T. A.; Berg, J. M.; Cotter, R. J. *Anal. Chem.* **1995,** *67*, 4462-4465.

56 Salih, B.; Masselon, C.; Zenobi, R. *J. Mass Spectrom.* **1998,** *33*, 994-1002.

57 Natarajan, K.; Cowan, J. A. *J. Am. Chem. Soc.* **1997,** *119*, 4082-4083.

58 Wattenberg, A.; Sobott, F.; Brutschy, B. *Rapid Commun. Mass Spectrom.* **2000,** *14*, 859-861.

59 Wattenberg, A.; Sobott, F.; Barth, H. D.; Brutschy, B. *Int. J. Mass Spectrom.* **2000,** *203*, 49-57.

60 Wilkins, M. R.; Gasteiger, E.; Gooley, A. A.; Herbert, B. R.; Molloy, M. P.; Binz, P. A.; Ou, K. L.; Sanchez, J. C.; Bairoch, A.; Williams, K. L.; Hochstrasser, D. F. *J. Mol. Biol.* **1999,** *289*, 645-657.

61 Smith, R. D.; Loo, J. A.; Loo, R. R. O.; Busman, M. *Mass Spectrom. Rev.* **1991,** *10*, 359-451.

62 Kelly, M. A.; Vestling, M. M.; Fenselau, C. C.; Smith, P. B. *Org. Mass Spectrom.* **1992,** *27*, 1143-1147.

63 Noguchi, T.; Ono, T.; Inoue, Y. *Biochem. Biophys. Res. Commun.* **1995,** *1228*, 189-200.

64 Petillot, Y.; Forest, E.; Meyer, J.; Moulis, J. M. *Anal. Biochem.* **1995,** *228*, 56-63.

65 Veenstra, T. D.; Johnson, K. L.; Tomlinson, A. J.; Naylor, S.; Kumar, R. *Biochemistry.* **1997,** *36*, 3535-3542.

66 Armengaud, J.; Gaillard, J.; Forest, E.; Jouanneau, Y. *Eur. J. Biochem.* **1995,** *231*, 396-404.

67 Fabris, D.; Zaia, J.; Hathout, Y.; Fenselau, C. *J. Am. Chem. Soc.* **1996,** *118*, 12242-12243.

68 Wu, Q. Y.; Vanorden, S.; Cheng, X. H.; Bakhtiar, R.; Smith, R. D. *Anal. Chem.* **1995,** *67*, 2498-2509.

69 Easterling, M. L.; Mize, T. H.; Amster, I. J. *Anal. Chem.* **1999,** *71*, 624-632.

70 Marshall, A. G. *Int. J. Mass Spectrom.* **2000,** *200*, 331-356.

71 Comisarow, M. B.; Marshall, A. G. *J. Mass Spectrom.* **1996,** *31*, 581-585.

72 Comisarow, M. B.; Marshall, A. G. *J. Mass Spectrom.* **1996,** *31*, 586-587.

73 Amster, I. J. *J. Mass Spectrom.* **1996,** *31*, 1325-1337.

74 Hay, M. T.; Ang, M. C.; Gamelin, D. R.; Solomon, E. I.; Antholine, W. E.; Ralle, M.; Blackburn, N. J.; Massey, P. D.; Wang, X. T.; Kwon, A. H.; Lu, Y. *Inorg. Chem.* **1998,** *37*, 191-198.

75 Shi, S. D. H.; Hendrickson, C. L.; Marshall, A. G. *Proc. Natl. Acad. Sci. U.S.A.* **1998,** *95*, 11532-11537.

76 Senko, M. W.; Beu, S. C.; McLafferty, F. W. *J. Am. Soc. Mass Spectrom.* **1995,** *6*, 229-233.

77 Fenn, J. B.; Mann, M.; Meng, C. K.; Wong, S. F.; Whitehouse, C. M. *Science* **1989,** *246*, 64-70.

CHAPTER 2

PROBING THE STOICHIOMETRY AND OXIDATION STATES OF METAL-SULFUR CENTERS IN IRON-SULFUR PROTEINS USING ELECTROSPRAY FTICR MASS SPECTROMETRY[1]

[1]Keith A. Johnson, Marc F.J.M. Verhagen, Phillip S. Brereton , Michael W.W. Adams and I. Jonathan Amster. Anal. Chem. 2000, *72*, 1410-1418.

Abstract

Electrospray ionization (ESI) Fourier transform ion cyclotron resonance mass spectrometry is used to determine the stoichiometry and oxidation states of the metal centers in several iron-sulfur proteins. Samples are introduced into the ESI source under nondenaturing conditions in order to observe intact metal-containing protein ions. The stoichiometry and oxidation state of the metal or metal-sulfur cluster in the protein ion can be derived from the mass spectrum. Mononuclear metal-containing proteins and [4Fe-4S] centers are very stable and yield the molecular ion with little or no fragmentation. Proteins that contain [2Fe-2S] clusters are less stable, and yield loss of one or two sulfur atoms from the molecular species, although the molecular ion is more abundant than the fragment peaks. [3Fe-4S]-containing proteins are the least stable of the species investigated, yielding abundant peaks corresponding to the loss of one to four sulfur atoms in addition to a peak representing the molecular ion. Isotope labeling experiments show that the sulfur loss originates from the [3Fe-4S] center. Negative ion mode mass spectra were obtained and found to produce much more stable [3Fe-4S]-containing ions than obtained in positive ion mode. ESI analysis of the same proteins under denaturing conditions yields mass spectra of the apo form of the proteins. Disulfide bonds are observed in the apoprotein mass spectra that are not present in the holoprotein. These result from oxidative coupling of the cysteinyl sulfur atoms that are responsible for binding the metal center. In addition, inorganic sulfide is found to incorporate itself into the apoprotein by forming sulfur bridges between cysteine residues.

Introduction

Metal ions are essential to the catalytic function and structural stability of many metalloproteins.[1, 2] In this role, metal ions serve as a means to orient and stabilize the conformation of a protein. Metals also mediate chemical reactions, most commonly redox reactions that are accompanied by a change in the oxidation state of the metal or metal cluster. A wide variety of spectroscopic methods have been used to examine metalloproteins.[3, 4]

Recently, mass spectrometry has been used to characterize metal-containing proteins and their metal centers. Electrospray ionization mass spectrometry has been applied to metal-containing proteins because the tightly folded, compact structure of the protein's native conformation can be retained under appropriate sample conditions, permitting the retention of the metal center.[5-7] This biologically active conformation is usually denatured by exposure to heat or organic solvents, which can weaken or disrupt interactions between a protein and a metal or metal-containing complex, resulting in the loss of the metal from the protein. Thus electrospray ionization is generally more useful for examining intact metalloproteins than is matrix-assisted laser desorption/ionization (MALDI), as the sample preparation conditions for the latter tend to be highly denaturing. Chait and co-workers have described the ESI conditions necessary for the detection of holomyoglobin,[8] and some more recent publications have presented the application of electrospray ionization to noncovalent complexes including metal-protein interactions.[2, 9-11]

In electrospray ionization mass spectrometry, the molecular weight of a protein is assigned from the mass-to-charge values that are measured for multiply-charged ions. Such assignments are trivial to make if it can be assumed that all of the charge that is present on an ion results from an excess of protons for positive ions or a deficit of protons for negative ions. Metalloproteins offer an additional consideration, as the metals that are present can carry charge as well, and they can exhibit more than one oxidation state. The oxidation state of the metal must be taken into account in order to properly assign a molecular weight from the mass spectral data. Henion and co-workers described the effect of the oxidation state of iron in heme-containing proteins, and studied ferric heme associated with myoglobin and ferrous heme associated with cytochrome *c*, in which only a 1 mass unit difference distinguished the two oxidation states of heme.[12] The influence of the oxidation state of the metal centers on ions in electrospray has also been described for iron-containing rubrerythrin and hemerythrin,[13] as well as for Cd^{2+} and Zn^{2+} metallothioneins.[14]

The high resolving power and mass accuracy of Fourier transform ion cyclotron resonance (FTICR) mass spectrometry combined with electrospray ionization make the method useful in determining the small mass changes that signal subtle but significant structural details for metalloproteins. In this paper we present the application of FTICR mass spectrometry to iron-sulfur proteins, which are defined as proteins that contain iron with at least partial coordination to sulfur. This includes both proteins with a mononuclear iron center, such as that present in rubredoxin, which coordinates iron to the protein through cysteinyl sulfur, as well as proteins with more complex metal centers that contain clusters of iron and inorganic sulfide ranging from [2Fe-2S] to [4Fe-4S] and even multiple iron-sulfur clusters.[15] The redox activity of these proteins allows them to exhibit more than one oxidation state, which makes the interpretation of the mass spectra data more challenging.

The stability of *Anabaena* ferredoxin has been previously examined using electrospray mass spectrometry to examine mutant versions of the protein,[16] and the stoichiometry and identity of iron-sulfur clusters in *Sulfolobus acidocaldarius*[17] and *Rhodobacter capsulatus*[18] ferredoxins have also been determined using mass spectrometry. More recently, an intermediate cluster structure from the high-potential iron-sulfur protein (HiPIP) from *Chromatium vinosum* has been investigated by mass spectrometry as a possible model for characterizing the assembly of metal-sulfur clusters in ferredoxin.[19] The iron and zinc forms of *Clostridium pasteurianum* (*Cp*) rubredoxin and its recombinant counterpart purified from *Escherichia coli* have also been investigated using electrospray ionization mass spectrometry to determine conditions that prevent the loss of the metal centers.[20]

Iron-sulfur proteins are good candidates for study by FTICR mass spectrometry because of the small changes in mass that are predicted to occur with the changes in the metal center's oxidation state and stoichiometry. The high resolving power of FTICR mass spectrometry can be used to distinguish small mass differences associated with changes such as oxidized versus reduced disulfide bonds, changes in a metalloprotein's oxidation state, and

changes in metal substitution. Such small, but significant changes can be measured more accurately by FTICR than by any other mass spectrometric method.

Experimental

All proteins examined here were produced by overexpression in *E. coli*. The preparation and purification of recombinant wild-type (WT) and D14C *Pyrococcus furiosus* (*Pf*) ferredoxin has been described previously.[21] The same procedures were used to generate and purify the C21A mutant. The [4Fe-4S] cluster was converted to the 3Fe form by treating the ferredoxin with 5-fold excess of ferricyanide for 15 min and removing excess oxidant by gel filtration.[22] *Pf* ferredoxin with a ^{34}S-enriched metal center was prepared by reconstitution of the apoprotein using $Na_2{}^{34}S$ and $FeCl_3$ to form the [4Fe-4^{34}S] cluster. The 3Fe form of this protein was generated using ferricyanide as described above. The δ subunit of *Pf* pyruvate oxidoreductase (POR-δ) was obtained as the apoprotein through separate expression in *E. coli*. In vitro reconstitution of the purified apoprotein using $FeCl_3$ and Na_2S resulted in the incorporation of two [4Fe-4S] clusters/δ subunit.[23] The [2Fe-2S]-containing γ-subunit of *Thermotoga maritima* (*Tm*) hydrogenase was obtained as the recombinant form expressed in *E. coli*. The protein was purified using Q-sepharose ion-exchange and Superdex 75 gel filtration chromatography. Prior to analysis, protein solutions were desalted by concentration in a microcentrifuge tube with integral dialysis membrane (Millipore Corp., Bedford, MA). After concentration in the microcentrifuge tube, the protein was resuspended in 15 mM ammonium acetate solution to yield a final protein concentration of 15 μM. Apoprotein mass spectra were obtained for most of the samples by electrospraying a solution of the holoprotein dissolved in 49% methanol, 49% water, and 2% acetic acid. WT and D14C apoproteins were denatured in 1 M hydrochloric acid, which removed the cluster and precipitated the protein. The protein was resolubilized by adjusting the pH to 8.0 by adding concentrated buffer. The reduction of D14C mutant from *Pf* was conducted in both sodium dithionite (J. T. Baker, Phillipsburg, NJ) and 3,10-dimethyl-5-deazaisoalloxazine (5-deazaflavin) (provided by Dr. Vincent Massey,

Department of Biological Chemistry, University of Michigan, Ann Arbor). The reduction of ferredoxin using sodium dithionite has been described previously.[21] The reduction of D14C mutant with deazaflavin was carried out using 50 μM protein in a solution of 15 mM EDTA/diammonium salt hydrate (Milwaukee, WI) to produce a final volume of 1 mL. 5-Deazaflavin was prepared as a 1 mM solution in water and was isolated from light and purged with nitrogen for 15 min to remove oxygen. Exactly 1 μL of this solution was added to the protein solution, and the solution was exposed to light until reduced. Reduction was monitored using a UV-visible spectrophotometer.

All mass spectra were acquired with a Bruker BioApex 7-T FTICR mass spectrometer equipped with an electrospray ionization source by Analytica. The glass capillary in the Analytica source was replaced by a heated metal capillary. All samples were ionized by nanoelectrospray. Capillary tips for nanoelectrospray were produced in our lab from 100 μm i.d. fused-silica capillary (Polymicro Technologies, Phoenix, AZ). The capillary was pulled to a fine tip by pulling with a constant force while heating with a microtorch (Microflame, Inc., Minnetonka, MN). The average flow rate for sample introduction to the mass spectrometry was 8 μL/h. A liquid electrical junction was formed by applying 1.2 kV to the syringe needle that infused the sample into the spray capillary.[24] The heated metal capillary was maintained at a temperature between 100 and 140 °C for the experiments. Ions were stored in the source region in a hexapole ion guide for 0.5-0.75 s and were pulsed through a series of electrostatic lenses into the detection cell where trapping potentials of 0.90 V and 0.95 V were used on the front and back trapping plates of the cell to isolate ions for excitation and detection. The time domain signal (transient) was collected by averaging approximately 50 scans. The summed transient was apodized prior to application of the Fourier transform, followed by calibration to yield a mass spectrum. Negative ion mass spectra used the same magnitude voltages for electrospray, external injection ion optics, and trapping potentials, but the polarities were reversed.

Calculations of isotope distributions for the proteins were made by using IsoPro software (http://www.members.aol/msmssoft). The χ^2 test was used to match experimentally obtained isotope distributions with calculated distributions, as described by McLafferty and co-workers.[25] After assigning the isotope composition of each of the peaks in the experimentally observed distribution, an estimate of the monoisotopic mass was derived from each peak by subtracting the ^{12}C-^{13}C mass difference times the integer number of heavy isotope atoms assigned to the peak. This analysis makes the reasonable assumption that the principal heavy isotope composition of each peak is ^{13}C. The monoisotopic masses that are reported are the average of the values derived from the five to eight most abundant isotope peaks in an isotope distribution of the most abundant charge state present in the mass spectrum.

Results and Discussion

The metalloproteins described below are challenging targets for mass spectrometric analysis, as the details that are sought must be discerned by measuring a relatively small change in the molecular weight of the protein. The oxidized versus reduced metal produces a change in the observed mass of the ion as small as 1 Da, and the reduction of a disulfide linkage shifts the molecular weight by 2 mass units per bond. To discern these small changes against the relatively large molecular weight of the protein, we obtain isotopically resolved mass spectra from which we can deduce the monoisotopic molecular weight of the protein. Monoisotopic mass is defined as the sum of the lowest molecular weight isotopes in the molecular formula. For most proteins, this corresponds to ^{12}C, ^{1}H, ^{14}N, ^{16}O and ^{32}S. This measurement is more accurate than that of average molecular weight, which corresponds to the centroid of the isotope distribution of the molecular peak and which requires accuracy in the measurement of both mass-to-charge and abundance of each ion. McLafferty and co-workers have described the measurement of the monoisotopic mass of proteins by comparing calculated and experimentally observed isotope distributions for the protein, using the χ^2 test to match the two and to assign the correct number of heavy isotopes to each peak in a distribution.[25] Measuring

the monoisotopic mass removes the error associated with an average mass for a distribution of isotopes, because the monoisotopic mass is not affected by the natural variability in isotope abundances in a sample or the statistical variation in measured isotope distributions.

For most proteins, a molecular weight is calculated based on an elemental composition of a neutral protein molecule, i.e. all ionizable sites in the protein are assumed to be neutral. There are no similar conventions to guide the calculation of the molecular weight of a metalloprotein. Since the metal center can carry charge, the assumption of neutrality for the protein would require that one subtract (or add) protons from the elemental composition to achieve a charge of zero. This is unsatisfactory, because one would calculate a different molecular weight for each oxidation state of the metal. For the purpose of discussion, we have adopted the convention that molecular weight is calculated as if the metal center has an oxidation state of zero. The monoisotopic mass that is calculated in this manner for a metalloprotein corresponds to the mass of the apoprotein plus the atomic masses of the components of the metal center. For these calculations, we use the nuclidic mass of the most abundant isotope of the metal, rather than the lowest atomic mass isotope. For iron, this corresponds to ^{56}Fe rather than ^{54}Fe, which has a relative abundance of 6% compared to ^{56}Fe and which produces very weak signals in the mass spectrum. More importantly, the mass difference between the most abundant isotope peak of an iron-containing protein and that of its apoprotein corresponds to the loss of ^{56}Fe. This is true for all proteins described below, even those that contain eight iron atoms. Note that, for this manner of calculating a molecular weight, it is assumed that no disulfide bonds are present. If thiol linkages are present, they will exhibit themselves as a deviation of two masses per disulfide bond between the calculated and experimentally determined molecular weights.

For the purpose of discussion, we also define a term, “apparent mass”. The apparent mass is the molecular weight that we derive directly from experimental data using the common algorithm for converting mass-to-charge for a multiply charged ion to the mass of the zero-charge molecule, shown in eq 1 below, where M_a is apparent mass, M_{H^+} is the mass of a

proton, *z* is the charge present on the ion, and *m/z* is the measured mass-to-charge ratio. This algorithm assumes that all charge is due to excess protons. While this is true for an apoprotein, for a metalloprotein some of the charge that is present results from a nonzero oxidation state of the metal atom or metal-containing prosthetic group. Thus, for metalloproteins, eq 1 overestimates the number of protons that provide charge to the molecule. The apparent mass derived from eq 1 will be lower than the calculated molecular weight by the mass of the protons equal in number to the oxidation state of the metal. For example, if one Fe(III) atom is present in a protein, then the apparent mass derived from the mass spectrum will be lower than the calculated molecular weight by the mass of three protons.

$$M_a = (m/z)z - zM_{H+} \qquad (1)$$

The apparent mass is an experimentally measured monoisotopic mass. Where the monoisotopic peak cannot discerned by inspection, it is derived by comparing experimental and calculated isotope distributions with the χ^2 test.[25] As stated above, the apparent mass will differ from the calculated mass both as a result of the oxidation state of the metal, and, if present, from disulfide bonds. The mass difference allows one to assign these features. Once these have been determined, the apparent mass can be corrected to yield the actual molecular weight of the metalloprotein.

Mononuclear Metal Centers. The smallest iron-sulfur protein investigated here is rubredoxin from (*Cp*), which contains a single iron atom coordinated to the protein by four cysteinyl sulfur atoms. Figure 1 shows the electrospray mass spectrum obtained for rubredoxin, showing the +3, +4 and +5 charge states for the protein. The most abundant peak corresponds to the holoprotein ion in the +4 charge state. Figure 1 shows an expansion of the +3 charge state of the spectrum, and compares this to the isotope distribution expected for this molecule. The χ^2 test is used to compare the calculated isotope distribution with the

Figure 2.1 The ESI-FTICR mass spectrum of iron rubredoxin from *Clostridium pasteurianum* containing apoprotein and holoprotein. The observed signal corresponds principally to the metal-containing holoprotein. A small signal is also observed for the apoprotein. Small adduct signals appear at higher mass-to-charge, and represent the addition of oxygen and sodium to the holoprotein. The inset illustrated the calculated (top) and measured (bottom) isotope distributions for the 3+ charge state of iron rubredoxin from *Cp*. The monoisotopic peak is calculated from the sum of all of the lowest molecular weight isotopes in the molecular formula, ^{12}C, ^{1}H, ^{14}N, ^{16}O, ^{32}S and the most abundant isotope of the metal, ^{56}Fe, and is labeled as ^{56}Fe in the top panel.

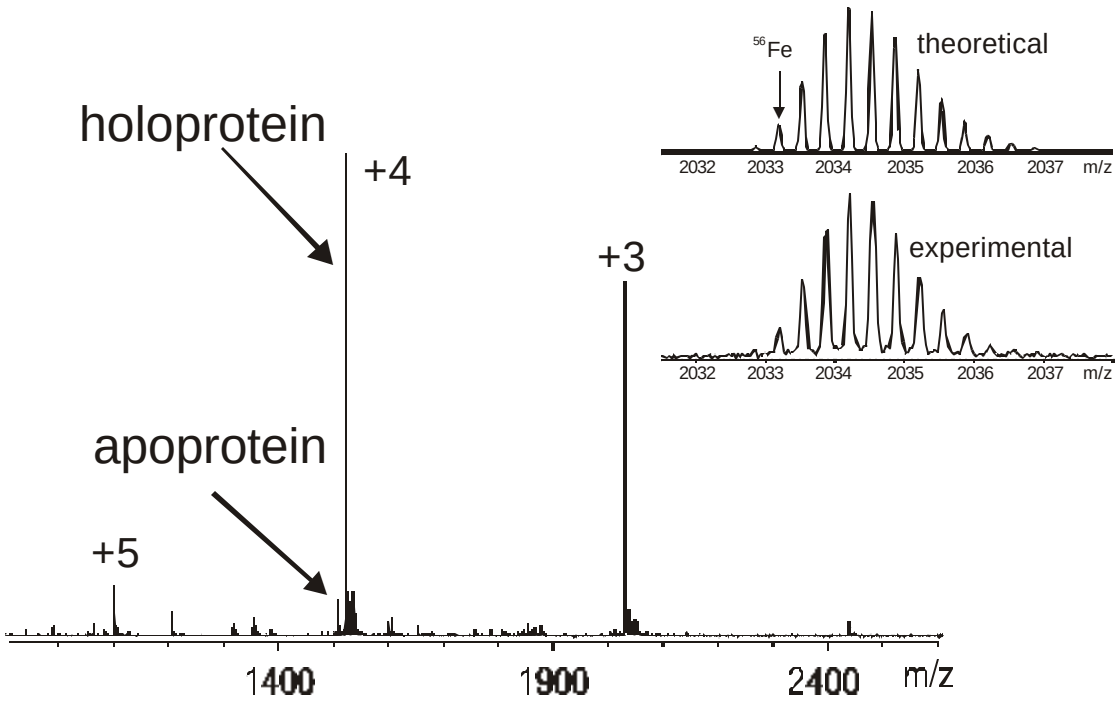
holoprotein
+4
+3
apoprotein
+5
1400
1900
2400
m/z
^{56}Fe
theoretical
2032
2033
2034
2035
2036
2037
m/z
experimental
2032
2033
2034
2035
2036
2037
m/z

experimentally observed distribution. The number of heavy isotopes present in each peak in the experimental data is assigned, and the monoisotope peak is identified. This peak consists of isotopes ^{12}C, ^{1}H, ^{14}N, ^{16}O, ^{32}S in addition to ^{56}Fe, which has a natural abundance of 91.8%. The "monoisotopic" peak is not the lowest mass-to-charge peak in the isotope distribution, but refers here to a composite of the masses of all monoisotopic elements in the molecular formula of the apoprotein plus the mass of the most abundant isotope of the metal contained in the active site. The apparent mass derived from these data is 6096.58 Da compared to the calculated mass of 6099.55 Da, a difference of 3 Da. The oxidation state of iron in this protein is 3+; thus, it contributes three charges to the ion. Correcting for the charge on the metal results in an assignment of the monoisotopic mass of 6099.59 Da, which agrees with the calculated value within 6.23 ppm. The 3+ oxidation state of iron in rubredoxin is the highest oxidation state that is possible for this metalloprotein biologically

Also observed in the mass spectrum is a signal corresponding to the apoprotein, at *m/z* 1511. The derived monoisotopic mass is 6039.65 Da, which is four mass units lower than the calculated molecular weight of 6043.61 Da. In this case, the mass difference is the result of the formation of two disulfide bonds. Upon loss of the metal from rubredoxin, the four cysteine residues that coordinated iron are available to form two disulfide bonds. It is important to recognize that the number of disulfide bonds can vary between a metalloprotein and its apoprotein, particularly if one wishes to use the apoprotein peaks as an internal mass calibrant for the metalloprotein.[27-29]

[4Fe-4S] Clusters. Cuboidal [4Fe-4S] clusters are frequently found in iron-sulfur proteins, and a number of these were investigated in this study. The mass spectrum of *Pyrococcus furiosus* ferredoxin (*Pf* Fd) containing a [4Fe-4S] cluster, and that of its mutant, D14C (aspartic acid replaced by cysteine at position 14), are shown in Figure 2. The mass spectrum of the wild type protein exhibits the +3, +4 and +5 charge states of the protein, although the +4

Figure 2.2 Wild-type [4Fe-4S] ferredoxin (top) and D14C [4Fe-4S] ferredoxin (bottom) from *Pf* are shown. The cuboidal [4Fe-4S] cluster, shown in the inset, is ligated to the protein through three cysteine residues and an aspartic acid residue in the wild-type protein. The addition of oxygen to the protein produces a less abundant ion that is observed at higher mass-to-charge ratios in each of the mass spectra. The monoisotopic peak in the isotope distributions for both WT and D14C are labeled 4 ^{56}Fe. The * denotes a noise peak in the mass spectrum.

charge state dominates the mass spectrum. From these data an apparent mass of 7509.83 Da is derived, which is 4 mass units less than the calculated mass of 7513.87 Da. The highest oxidation state for the protein in its biological environment is 2+,[21] although it is possible for the [4Fe-4S] cluster to have an oxidation state of 4+ (4 Fe^{3+} and 4 S^{2-}). The 4+ oxidation state is not observed under biological conditions,[30] and we do not interpret the data as corresponding to this high oxidation state. The native ferredoxin from *Pf* is also known to contain a disulfide bond that is remote from the iron-sulfur cluster,[22] and this bond together with a 2+ oxidation state for the metal center would be consistent with the 4 Da difference that we observe. Likewise, the mass difference between the calculated mass and the apparent mass (7501.85 Da vs. 7497.72 Da, respectively) of the D14C mutant is 4 Da, also consistent with the assignment of a 2+ oxidation state and a disulfide bond. However, these data do not allow us to distinguish the possibility of a metal center with a 4+ oxidation state in a protein with no disulfide bond. To verify our assignment of the oxidation state of the metal center, the C21A mutant (alanine replaces cysteine at position 21) was examined. By replacing cysteine with alanine, the formation of the remote disulfide bond between amino acid positions 21 and 48 is no longer possible. The apparent mass for C21A calculated from the spectrum shown in Figure 3 is 7479.89 Da and the calculated mass is 7481.90 Da. The difference in mass between the apparent and theoretical masses is 2 Da and corresponds directly to the charge on the metal cluster. These data suggest that the 4 mass unit difference between the apparent mass and the calculated mass in both the wild-type ferredoxin and the D14C mutant can be attributed to an oxidation state of 2+ for the metal cluster and the presence of a disulfide bond between residues 21 and 48. The mass spectra of wild-type ferredoxin and the D14C mutant also show peaks 16 Da higher in mass than the protein with the [4Fe-4S] cluster that we assign as the addition of oxygen. This satellite peak 16 mass units above the molecular peak is seen in most of the ferredoxin mass spectra presented here, although the abundance of this ion in the mass spectra varies greatly. Sodium adducts and combination sodium and oxygen adducts are also observed at low abundance in the D14C spectrum at higher mass-to-charge values.

Figure 2.3 ESI-FTICR mass spectrum of ferredoxin mutant C21A (cysteine at position 21 replaced by alanine). The elimination of the disulfide bond between positions 21 and 48 in this ferredoxin allows the unequivocal assignment of the oxidation state of the iron-sulfur cluster as 2+. The monoisotopic peak in the isotope distribution is labeled as 4 ^{56}Fe.

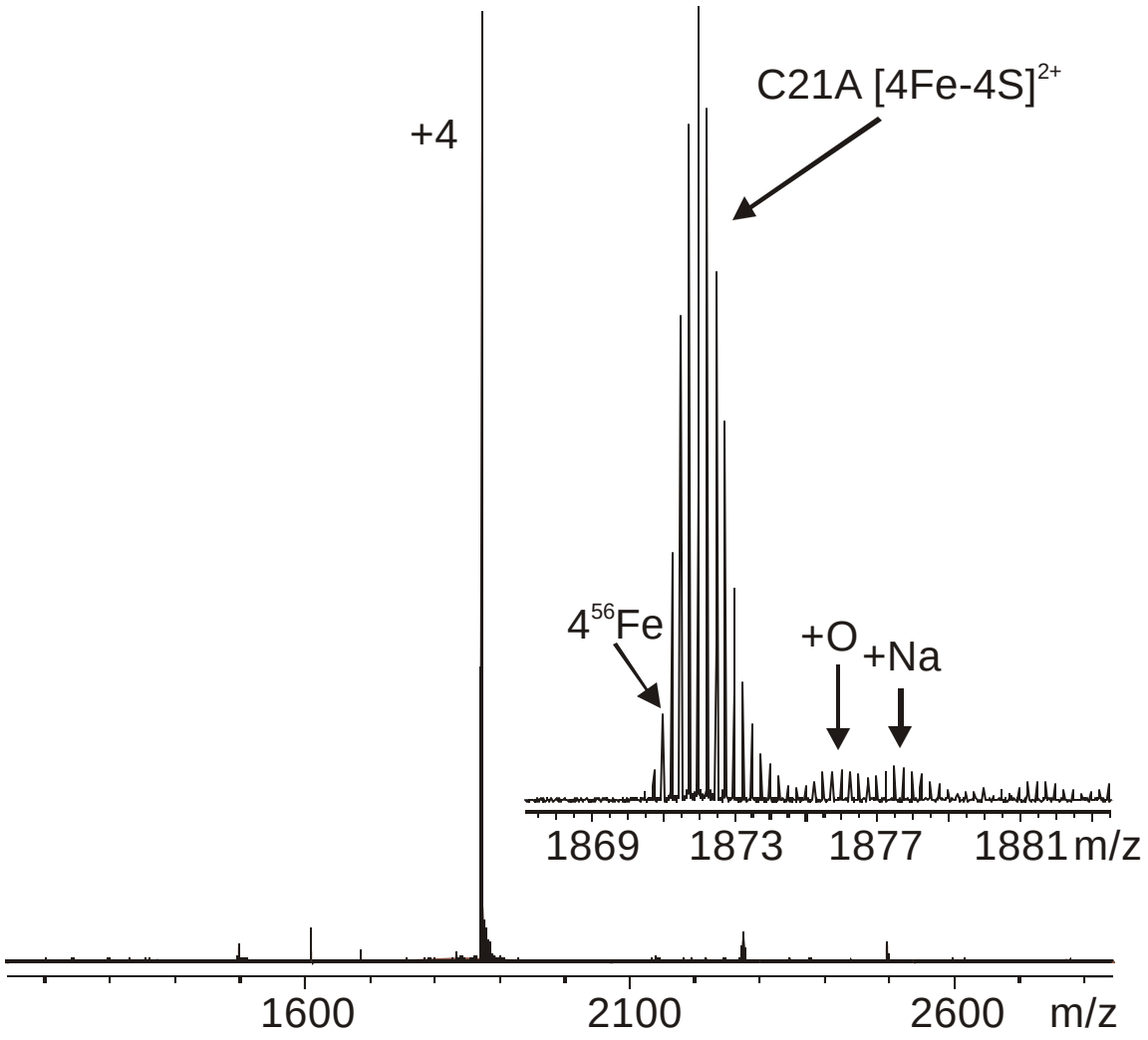
C21A [4Fe-4S]2+
+4
4 56Fe
+O
+Na
1869
1873
1877
1881 m/z
1600
2100
2600 m/z

Lower oxidation states of the metal center are observed under biological conditions, but we have never observed these in the mass spectra. We have attempted to reduce the D14C ferredoxin by using deazaflavin as a reducing agent,[31] but have so far been unable to obtain a mass spectrum for the reduced form of the protein. Deazaflavin was chosen to reduce the protein because of its low reduction potential and because only a small amount of the reducing agent is needed to reduce a much larger amount of protein due to its catalytic behavior.[32] Sodium dithionite was also used to reduce the metal center in the protein, but this reducing agent is incompatible with electrospray ionization. Sodium dithionite is the reducing agent normally chosen for ferredoxins, which themselves have low reduction potentials.[21] Unfortunately, sodium creates a plethora of adduct peaks which dominate the mass spectrum, and greatly diminishes the signal intensity to a point where interpretable data can not be acquired. Removal of sodium from the sample after reduction of the metal center by buffer exchange with ammonium acetate has been performed; however, the protein ions observed in the mass spectra appear in the higher oxidation state (2+) once again. The use of deazaflavin as a reducing agent allowed us to reduce the ferredoxin with only a small amount of reducing agent. This provided a means of electrospraying our sample without a rinsing step to remove the buffer and was compatible with a stable spray during ionization. Although the D14C sample was reduced as evident from UV spectroscopy data (not shown), only the oxidized (2+) protein was detected using FTICR. Thus, it appears that the electrospray process itself leads to the oxidation of the metal center. Our results are in agreement with those of Van Berkel and Zhou, who have described the redox behavior of the elctrospray ion source and have shown that the nickel (II) octaethylporphyrin is oxidized to its nickel (III) form during the electrospray process.[33]

The formation of new disulfide bonds in the apoprotein between the cysteine residues that serve as ligands for the metal centers of the holoprotein has been observed in ferredoxin as well as in rubredoxin. The mass spectra of the apo forms of wild-type ferredoxin from *Pf* and the D14C mutant of ferredoxin are shown in Figure 4.

Figure 2.4 ESI-FTICR mass spectra of the apoprotein of wild-type ferredoxin (top) and D14C ferredoxin (bottom). Wild-type ferredoxin contains five cysteine residues and exhibits two disulfide bonds upon removal of the iron-sulfur cluster. D14C contains six cysteine residues and exhibits three disulfide bonds after the iron-sulfur cluster is removed. Adducts of oxygen and sodium are seen in both spectra. Peaks representing sulfur addition are observed in the mass spectrum of the D14C mutant.

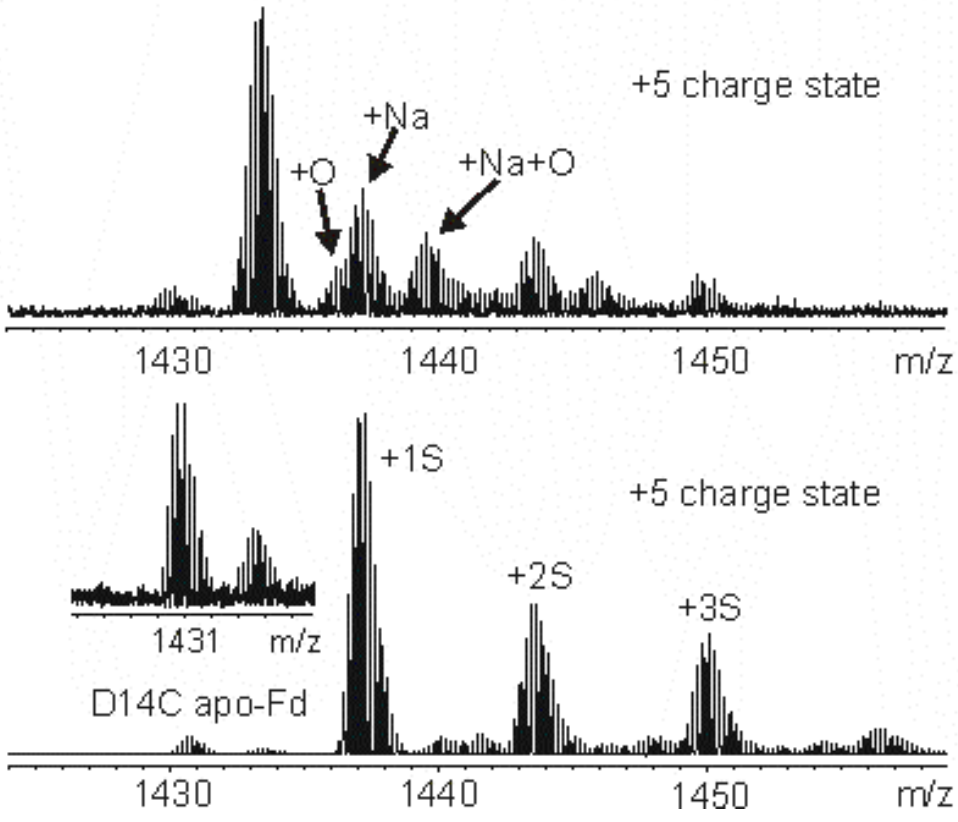
+5 charge state
+Na
+O
+Na+O
1430
1440
1450
m/z
+1S
+5 charge state
+2S
+3S
1431
m/z
D14C apo-Fd
1430
1440
1450
m/z

The number of cysteine residues in the wild-type protein is five, two of which (C21 and C48) do not participate in metal binding, and which are known to form a disulfide bond.[34] The three remaining cysteine residues are involved in binding the metal cluster with the participation of an aspartate residue.[22] In the apoprotein, a maximum of four of the cysteine residues can form disulfide bonds. The calculated mass for the wild-type ferredoxin with all cysteine residues reduced is 7162.24 Da, while the mass that is measured is 7158.18 Da. The difference of 4 Da suggests that two disulfide bonds are present. Most likely, one is between C21 and C48, as well as one between two of the

three cysteine groups that bind the metal center in the holoprotein. To verify that disulfide bond formation is possible at the cluster site after the cluster is removed, a mutant with six cysteine residues, D14C, was examined. In this protein, the aspartic acid that participates in cluster binding is replaced by cysteine. The calculated mass for the reduced form of the mutant is 7150.23 Da and the measured mass was found to be 7144.22 Da. The 6 Da difference is consistent with formation of three disulfide bonds. The holoprotein only exhibits one disulfide bond (Figure 2). Both of the mass spectra in Figure 4 also include a series of adducts separated in mass by 32 Da. These adduct peaks suggest the addition of inorganic sulfide to the protein. These measurements suggest that sulfur has inserted itself into the disulfide bonds to form *Cys*-*S*-**S**-*S*-*Cys* or larger chains rather than breaking internal disulfide bonds to form Cys-S-**SH**. In the latter case, the mass corresponding to the addition of two hydrogen atoms (by reduction of a disulfide bond) would have caused a mass separation of 34 Da between the peaks, rather than the 32 Da spacing that is observed.

There are also a group of ferredoxins that contain [4Fe-4S] clusters which are capable of existing in oxidation states higher than 2+ in their biological environments. These ferredoxin proteins, which can cycle between 2+ and 3+ in their reduced and oxidized forms, are called high-potential iron-sulfur proteins.[30,19] The mass spectrum of HiPIP from *Chromatium vinosum* (*Cv*) is shown in Figure 5. The +5 and +6 charge states of the HiPIP containing intact [4Fe-4S] clusters are shown. Each charge state contains a peak corresponding to

Figure 2.5 ESI-FTICR mass spectrum of apoprotein and holoprotein of the high potential iron-sulfur protein from *Cv*. Mass differences between apparent and calculated values are consistent with an oxidation state of 3+ for the [4Fe-4S] cluster. The protein dimer (+8 and +9 charge states) is also observed in the mass spectrum at higher mass-to-charge values. The inset shows the isotope distribution from the +5 charge state and the monoisotopic peak is labeled 4 ^{56}Fe. Adduct peaks are observed for both oxygen and sodium attachment.

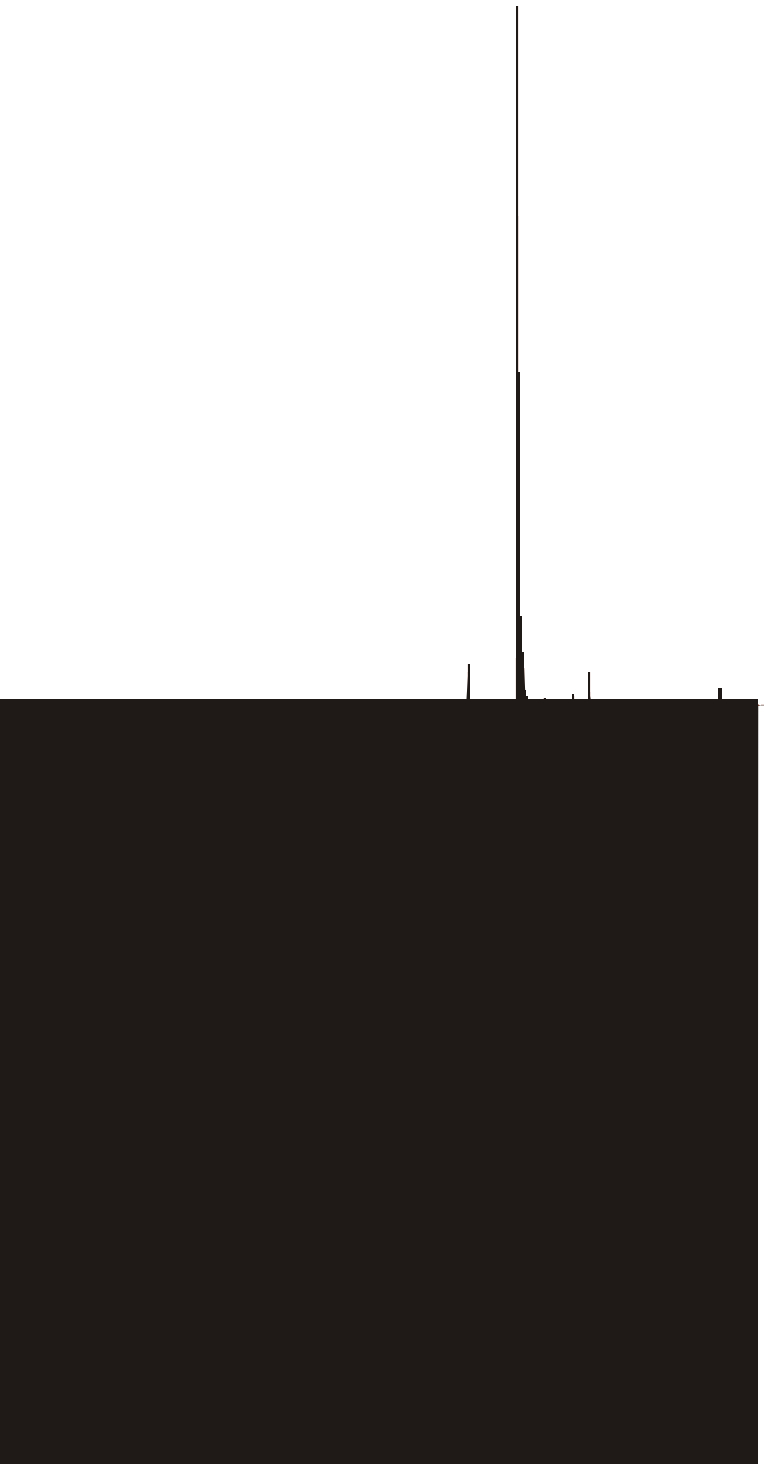

apoprotein. These peaks are located in the spectrum at m/z 1484 and m/z 1781 and were used as an internal calibrant in obtaining an apparent mass for the holoprotein. The calibration on the apoprotein peak was made assuming that the cysteine residues involved in cluster coordination form disulfide bonds upon cluster removal like all of the proteins that have been discussed. The calculated mass for apoprotein with 2 disulfide bonds is 8896.20 Da. The apparent mass for the holoprotein is 9248.88 Da and the calculated mass is 9251.86 Da. Since the protein contains only four cysteine residues, and each is involved in cluster ligation, no disulfide bonds are present in the holoprotein. The difference between the apparent and calculated masses signifies a 3+ oxidation state for the iron-sulfur cluster, which is in agreement with values measured for the oxidized form of the cluster in its biological environment.[22] Also shown in the mass spectrum in Figure 5 are peaks corresponding to a noncovalent dimer of HiPIP containing intact [4Fe-4S] clusters. Dimerization of HiPIP from *Cv* has been reported previously in condensed phase studies.[35] The nondenaturing conditions used in these studies allow the detection of this noncovalent complex in the gas phase. Peaks at higher mass-to-charge than the holoprotein represent oxygen and sodium adducts.

Multiple [4Fe-4S] Clusters. Other types of ferredoxins are known to contain multiple iron-sulfur clusters, such as the δ subunit of pyruvate oxidoreductase (POR-δ) from *Pf*, which contains two [4Fe-4S] clusters.[23] The mass spectrum for this protein (N-terminal methionine cleaved) is shown in Figure 6. The most abundant peak corresponds to a molecular weight of 12603.85 Da, which equals the mass of the protein with two intact clusters plus an additional 31.93 Da. This extra mass could be caused by the addition of a sulfur atom to the molecule as is seen in the wild-type and D14C apoprotein mass spectra, or could be the result of the addition of two oxygen atoms to the protein. The [4Fe-4S] ferredoxins that we have observed exhibit an oxygen adduct as a small peak. If the peak shown in Figure 6 is due to oxygen, this would suggest the metal center as the site of attachment, since proteins with one cluster add one oxygen and this protein with two clusters adds two oxygen atoms. Both clusters are bound by

Figure 2.6 ESI-FTICR mass spectrum of an expansion of the +9 charge state of POR-δ from *Pf*, which contains two [4Fe-4S] clusters. The principal peak of the mass spectrum corresponds to the mass of the holoprotein with an addition of 31.93 Da, most likely from the addition of one sulfur or two oxygen atoms. The distribution of peaks at lower mass-to-charge ratios corresponds to the apoprotein with four disulfide bonds and from intercalation of zero to seven sulfur atoms into the disulfide linkages.

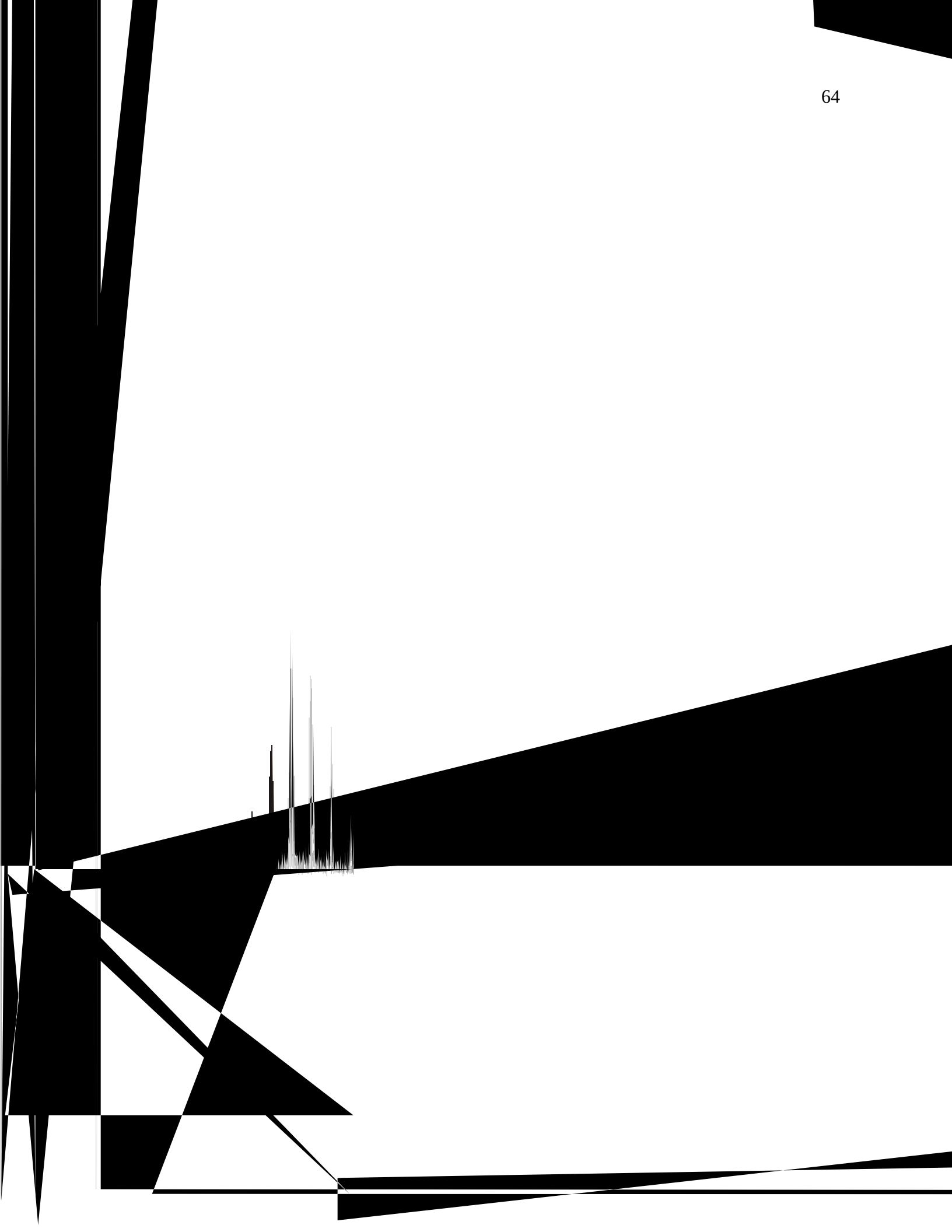

4 cysteine residues each and together have an oxidation state of 4+, or 2+ for each of the clusters. Peaks at higher mass-to-charge ratios than the base peak represent sodium adducts. Interestingly, there is a distribution of ions at lower mass-to-charge than the peak representing holoprotein. The peak at *m/z* 1320 represents the apoprotein, and each additional peak represents the addition of sulfur to the molecule. The apparent mass for the apoprotein is 11864.60 Da and the calculated mass for the protein is 11872.69 Da. The difference between the values is 8 Da, which suggests the formation of four disulfide bonds between the eight free cysteine residues which no longer coordinate the two iron-sulfur clusters. Peaks with one to seven additional atoms of inorganic sulfide are observed in the mass spectrum.. The sulfur atoms appear to insert themselves into the disulfide bonds rather than forming a dithiol, based on the mass difference. This behavior is analogous to the additional sulfur atoms that are seen in the apo forms of *Pf* ferredoxin, Figure 4.

[2Fe-2S] Clusters. Other metal-sulfur stoichiometries in Fe-S proteins have been investigated, such as the α-subunit of hydrogenase from *Tm*, which is known to contain a [2Fe-2S] cluster.[35] The electrospray mass spectrum for the protein is shown in Figure 7. The average apparent molecular weight for the protein with an intact [2Fe-2S] cluster is 18189.12 Da. The calculated mass for the γ subunit is 18191.10 Da. The 2 mass unit difference suggests an oxidation state of 2+ for the cluster, which is the highest state that has been reported for the under biological conditions. Higher mass-to-charge ions show almost no losses of inorganic sulfide from the cluster, while lower mass-to-charge ions show a small peak and a larger peak representing losses of one and two sulfur atoms per cluster. The higher charge states of the protein most likely corresponds to less folded conformations, for which degradation of the metal center can occur. The lowest peak in each charge state represents the degraded protein with two iron atoms bound by the protein, but missing the inorganic sulfide atoms of the cluster. The apparent mass for the protein containing [2Fe], but no inorganic sulfide is 18123.06 Da, 4

Figure 2.7 ESI-FTICR mass spectrum of the [2Fe-2S]-containing γ-subunit of iron hydrogenase from *Tm*. The [2Fe-2S] center exhibits an oxidation state of 2+. Ions of high charge state (low mass-to-charge ratio) exhibit losses of sulfur from the iron-sulfur cluster and may be a result of the unfolding of the protein, while ions of low charge state appear to be more stable toward decomposition of the metal center. The peak labeled * corresponds to noise in the mass spectrum. Removal of both of the sulfur atoms from the active site results in a collective oxidation state of 4+ for the two remaining iron atoms.

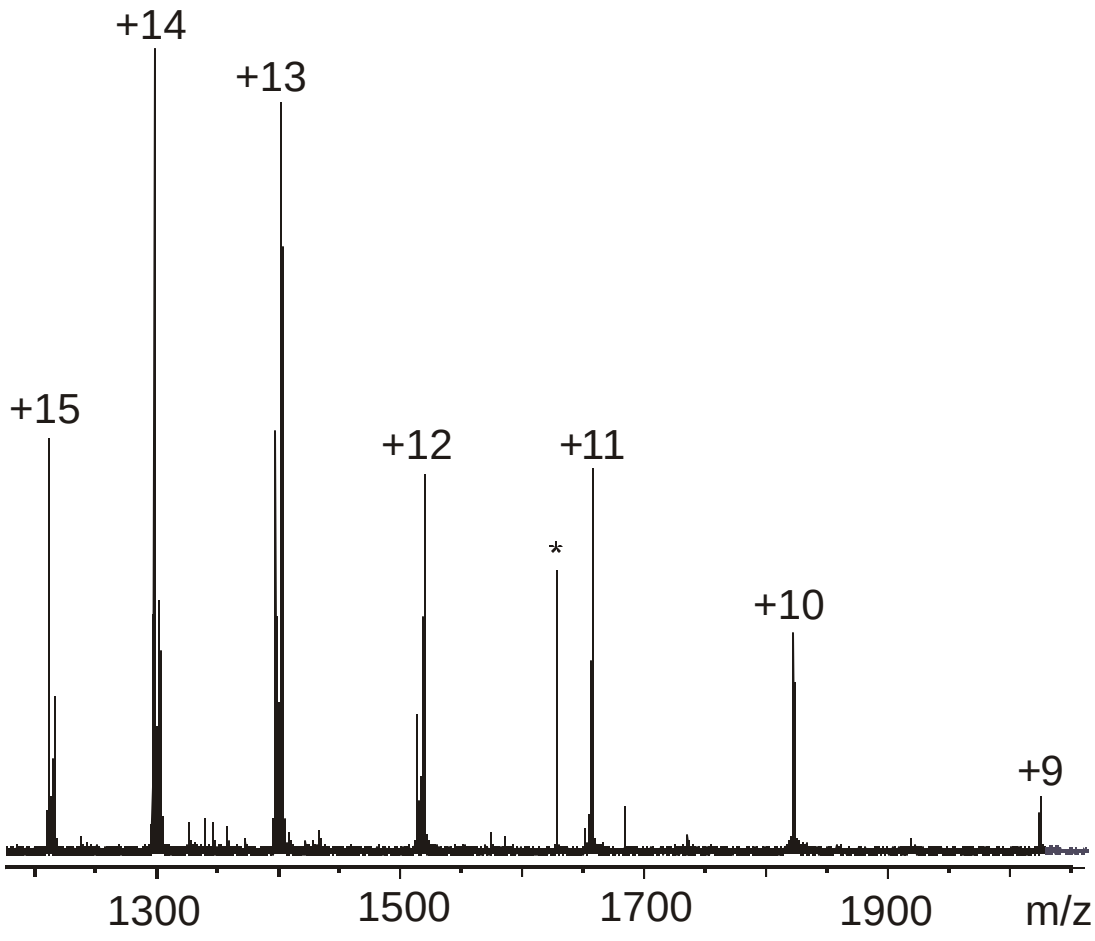
+14
+13
+15
+12
+11
*
+10
+9
1300
1500
1700
1900
m/z

mass units less than the calculated mass of 18127.16 Da. The difference suggests an oxidation state of 2+ for each metal in the cluster after removal of inorganic sulfide.

[3Fe-4S] Clusters. The mass spectrum for *Pf* ferredoxin containing a [3Fe-4S] cluster is shown in Figure 8. The [3Fe-4S] cluster for this ferredoxin is much more labile during electrospray than the [4Fe-4S] ferredoxin forms as is apparent from the various degradation products that are detected. The top spectrum is Figure 8 shows the wild-type protein. The +4 charge state shows the presence of the intact cluster in the protein at *m/z* 1866. The apparent mass of this protein is 7454.92 Da and the calculated mass for the protein is 7457.93 Da. The disulfide bond, as before, was not assumed in calculating the molecular weight. The highest oxidation state for the cluster in the protein under biological conditions is 1+.[22] The electrospray ionization data suggests that the metal center exhibits a charge of 1+, and that the remote disulfide bond accounts for the rest of the difference in mass between apparent and calculated masses. Also observed in this mass spectrum are less abundant peaks corresponding to the addition of oxygen and adducts of sodium. The major peaks at lower mass-to-charge values represent losses of approximately 32 mass units, which corresponds to the loss of inorganic sulfide from the cluster in the protein. These losses moving to lower mass-to-charge are losses of 1S, 2S, 3S and 4S, respectively, which leaves only iron remaining in the core. The loss of inorganic sulfide has been confirmed using isotope labeling of the sulfur in the [3Fe-4S] cluster. For this, the metal center was reconstituted using ^{34}S to form a [3Fe-4^{34}S] cluster. The mass spectrum of the isotopically labeled protein is shown in Figure 8 (bottom). The apparent mass for the intact species is 7462.80 Da, 3 mass units less than the calculated value of 7465.90 Da. The difference, as in the case of the unlabeled protein is interpreted as resulting from one disulfide bond and the 1+ oxidation state of the metal cluster. The protein with the cluster intact is observed at *m/z* 1868. Peaks corresponding to the addition of oxygen and the losses of ^{34}S from the cluster are also observed. The mass difference between each set of peaks is 33.98 Da and the peak at the lowest mass-to-charge represents the protein with

Figure 2.8 ESI-FTICR mass spectrum of [3Fe-4S] ferredoxin from *Pf* (top) in which the intact cluster can be seen at *m/z* 1866. Peaks at higher mass-to-charge ratios represent oxygen, sodium, and sulfur adducts, whereas more intense peaks at lower mass-to-charge ratios represent losses of inorganic sulfide from the cluster. The mass spectrum of ^{34}S labeled [3Fe-4^{34}S] protein from *Pf* is also shown (bottom). The degradation of the protein is similar to the wild-type [3Fe-4S] protein. The loss of inorganic sulfide from the iron-sulfur cluster is confirmed by this example, as the mass difference between the sulfur-loss peaks is 34 Da, whereas in the unlabeled form the difference is 32 Da.

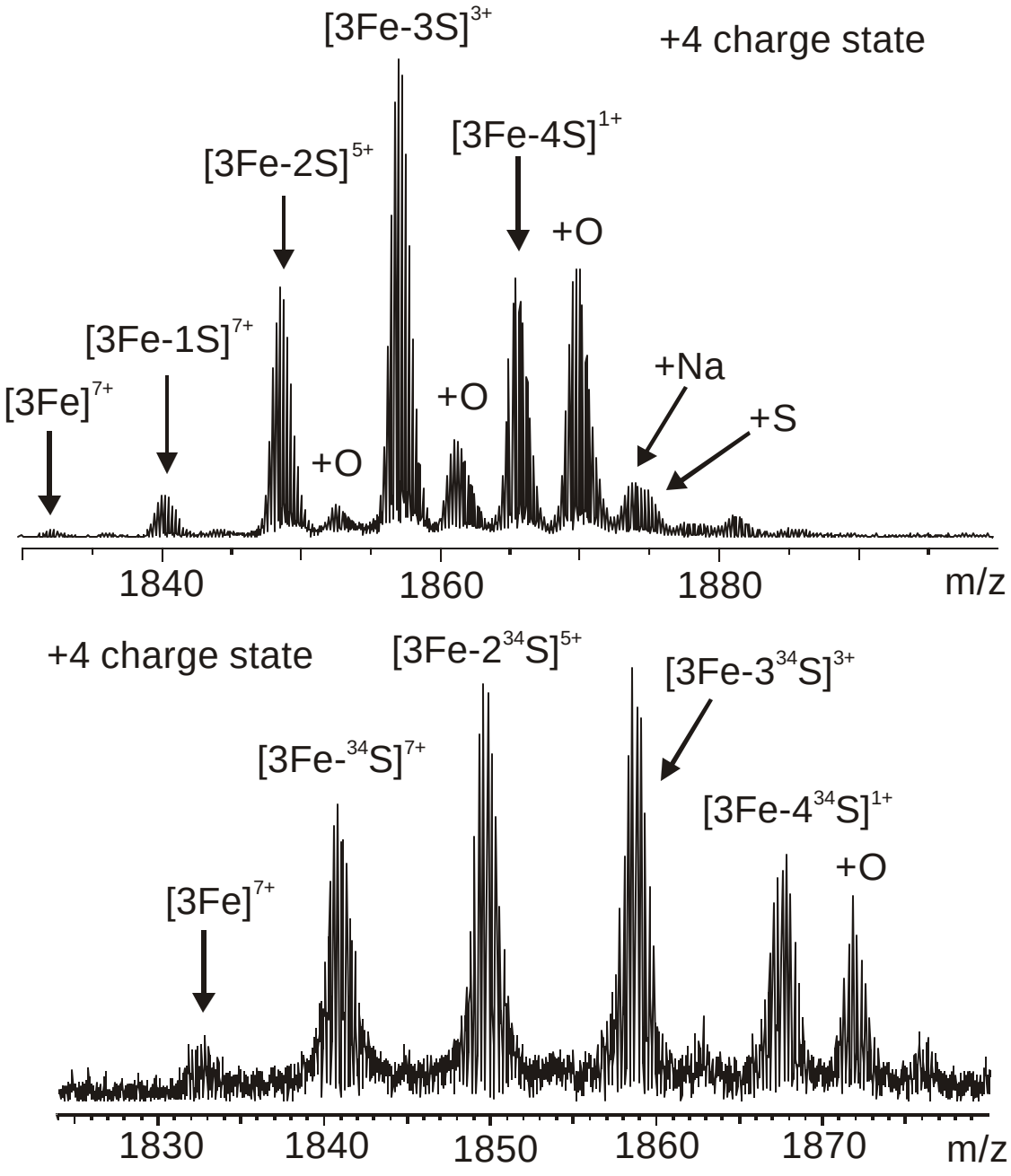
[3Fe-3S]3+
+4 charge state
[3Fe-4S]1+
[3Fe-2S]5+
+O
[3Fe-1S]7+
+Na
[3Fe]7+
+O
+O
+S
1840
1860
1880
m/z
+4 charge state
[3Fe-234S]5+
[3Fe-334S]3+
[3Fe-34S]7+
[3Fe-434S]1+
+O
[3Fe]7+
1830
1840
1850
1860
1870
m/z

only [3Fe] left in the core. The metal clusters formed during the decomposition of the [3Fe-4S]$^{1+}$ cluster are [3Fe-3S]$^{3+}$, [3Fe-2S]$^{5+}$, [3Fe-1S]$^{7+}$, and [3Fe]$^{7+}$. Peaks corresponding to adducts of oxygen and sodium are found between the peaks of these products.

Ferredoxin containing a [3Fe-4S] cluster was also electrosprayed in negative ion mode. The mass spectra for both positive and negative mode are compared in Figure 9. More charge states are observed in the case of the negative mode mass spectrum. The apparent mass obtained from the negative mode data is 7454.99 Da, identical to that from the positive mode data. The difference of 3 mass units between apparent and calculated molecular weight for both modes of ionization corresponds to one disulfide bond in the protein and an oxidation state of 1+ for the [3Fe-4S] cluster. The insets show the expansion of the +5 and -5 charge states in the mass spectrum. The +5 charge state in the positive mode electrospray mass spectrum of the [3Fe-4S] ferredoxin and is very different from the -5 charge state of the same protein electrosprayed in negative mode ionization. The negative mode mass spectrum shows a large peak corresponding to the intact [3Fe-4S] cluster with almost no degradation products. A very small peak corresponding to the loss of 1S from the cluster is observed. These spectra illustrate that the mode of ionization does not influence the oxidation state of the cluster. Labile clusters that are electrosprayed in negative mode may allow the observation of the intact cluster; however, information regarding intermediate clusters can be obtained through ionization in the positive mode. Both ferredoxin and rubredoxin have been investigated in positive and negative ionization modes by other researchers, and negative ions in both cases have proven to be more stable.[16,20]

Conclusion

Electrospray FTICR mass spectrometry can be used to determine the stoichiometry and oxidation states of metal clusters in iron-sulfur proteins ranging from a simple mononuclear iron to more complex clusters such as [2Fe-2S], [3Fe-4S] and [4Fe-4S]. The oxidation states

Figure 2.9 Comparison of the ESI-FTICR mass spectra of [3Fe-4S] ferredoxin from *Pf* electrosprayed in the positive ion (top) and negative *Pf* ion (bottom) modes. Positive ions show a narrower distribution of charge states but a larger degree of fragmentation (* indicates a noise peak in the mass spectrum). Negative ions show a wider distribution of ions, principally containing the intact cluster. Expansion of the +5 and -5 charge-state regions of the mass spectra are also shown. One observes substantial fragmentation of the iron-sulfur clusters in the positive ion mode but very little degradation of the metal center in the negative ion mode.

that have been observed to date correspond to the highest states that have observed by other methods under biological conditions, but not necessarily the highest possible oxidation state for such clusters. The results for the [4Fe-4S] proteins show an oxidation state of 2+ for *Pf* ferredoxin, and 3+ for the HiPIP ferredoxin, in agreement with observations under biological conditions. An oxidation state of 4+ is possible, for [4Fe-4S] but has never been observed under biological conditions. These results suggest that the higher-order structure of the proteins has not changed significantly during the ionization process, as the maximum oxidation state that is achieved is known to be sensitive to the local environment of the metal center. These data suggest that mass spectrometry to provides a biologically relevant measurement of the maximum oxidation states of metal centers in proteins. It is fortuitous that we observe only one oxidation state of the protein in all of the mass spectra, as the presence of multiple oxidation states would lead to additional complexity in the isotope distributions that are observed. The oxidation state that is observed appears to be independent of the redox form that exists in the solution being sprayed, as conditions that produce the reduced form of the iron-sulfur protein in solution still yield the biologically relevant oxidized form in the gas phase.

Degradation products of the metal centers of some iron-sulfur proteins are also observed, particularly in the case of the [3Fe-4S] proteins. Although these products have not been observed in solution, it is feasible that they are intermediates in the construction of clusters within the proteins and may even be closely associated with the folding of these peptides.[1,19] Further investigations of the intermediates in iron-sulfur cluster assembly and disassembly are underway.

Acknowledgment

We gratefully acknowledge funding provided by the National Science Foundation, Grants CHE-9412334 and 9974579 (IJA) and MCB 9809060 (MWA). We thank Professor John R. Eyler at the University of Florida for providing the heated metal capillary interface used in these experiments. We thank Michael Johnson of the University of Georgia for discussions

and insights regarding iron-sulfur proteins, as well as for providing several of the samples used for these studies.

References

(1) Hellinga, H. W. *Fold. Des.* **1998,** *3*, R1-R8.

(2) Loo, J. A. *Mass Spectrom. Rev.* **1997,** *16*, 1-23.

(3) Kyritsis, P.; Kummerle, R.; Huber, J. G.; Gaillard, J.; Guigliarelli, B.; Popescu, C.; Munck, E.; Moulis, J. M. *Biochemistry.* **1999,** *38*, 6335-6345.

(4) Telser, J.; Davydov, R.; Kim, C. H.; Adams, M. W. W.; Hoffman, B. M. *Inorg. Chem.* **1999,** *38*, 3550-3553.

(5) Troxler, H.; Kuster, T.; Rhyner, J. A.; Gehrig, P.; Heizmann, C. W. *Anal. Biochem.* **1999,** *268*, 64-71.

(6) Hay, M. T.; Milberg, R. M.; Lu, Y. *J. Am. Chem. Soc.* **1996,** *118*, 11976-11977.

(7) Veenstra, T. D.; Johnson, K. L.; Tomlinson, A. J.; Craig, T. A.; Kumar, R.; Naylor, S. *J. Am. Soc. Mass Spectrom.* **1998,** *9*, 8-14.

(8) Katta, V.; Chait, B. T. *J. Am. Chem. Soc.* **1991,** *113*, 8534-8535.

(9) Veenstra, T. D. *Biophys. Chem.* **1999,** *79*, 63-79.

(10) Pramanik, B. N.; Bartner, P. L.; Mirza, U. A.; Liu, Y. H.; Ganguly, A. K. *J. Mass Spectrom.* **1998,** *33*, 911-920.

(11) Ens, W.; Standing, K.; Chernushevich, I. In *NATO ASI series. Series C, Mathematical and physical sciences*; Dordrecht, Boston, 1998; Vol. 510, pp 149-156.

(12) Li, Y. T.; Hsieh, Y. L.; Henion, J. D.; Ganem, B. *J. Am. Soc. Mass Spectrom.* **1993,** *4*, 631-637.

(13) Lei, Q. P.; Cui, X. Y.; Kurtz, D. M.; Amster, I. J.; Chernushevich, I. V.; Standing, K. G. *Anal. Chem.* **1998,** *70*, 1838-1846.

(14) Yu, X. L.; Wojciechowski, M.; Fenselau, C. *Anal. Chem.* **1993,** *65*, 1355-1359.

(15) Johnson, M. K. Iron-Sulfur Clusters. In *Encyclopedia of Inorganic Chemistry*. King, R. B. Ed; John Wiley and Sons: New York. **1994,** Vol 4, pp 1896-1913.

(16) Remigy, H.; Jaquinod, M.; Petillot, Y.; Gagnon, J.; Cheng, H.; Xia, B.; Markley, J. L.; Hurley, J. K.; Tollin, G.; Forest, E. *J. Protein. Chem.* **1997,** *16*, 527-532.

(17) Breton, J. L.; Duff, J. L. C.; Butt, J. N.; Armstrong, F. A.; George, S. J.; Petillot, Y.; Forest, E.; Schafer, G.; Thomson, A. J. *Eur. J. Biochem.* **1995,** *233*, 937-946.

(18) Armengaud, J.; Gaillard, J.; Forest, E.; Jouanneau, Y. *Eur. J. Biochem.* **1995,** *231*, 396-404.

(19) Natarajan, K.; Cowan, J. A. *J. Am. Chem. Soc.* **1997,** *119*, 4082-4083.

(20) Petillot, Y.; Forest, E.; Mathieu, I.; Meyer, J.; Moulis, J. M. *Biochem. J.* **1993,** *296*, 657-661.

(21) Brereton, P. S.; Verhagen, M. F. J. M.; Zhou, Z. H.; Adams, M., W.W. *Biochemistry.* **1998,** *37*, 7351-7362.

(22) Conover, R. C.; Kowal, A. T.; Fu, W.; Park, J. B.; Aono, S.; Adams, M. W. W.; Johnson, M. K. *J. Biol. Chem.* **1990,** *265*, 8533-8541.

(23) Menon, A. L.; Hendrix, H.; Hutchins, A.; Verhagen, M.; Adams, M. W. W. *Biochemistry.* **1998,** *37*, 12838-12846.

(24) Koenig, S.; Haegele, K.; Fales, H. *Anal. Chem.* **1998,** *70*, 4453-4455.

(25) Senko, M. W.; Beu, S. C.; McLafferty, F. W. *J. Am. Soc. Mass Spectrom.* **1995,** *6*, 229-233.

(26) Volkman, B. F.; Wilkins, S. J.; Lee, A. L.; Westler, W. M.; Beger, R.; Markley, J. L. *J. Am. Chem. Soc.* **1999**. 121, 4677-4683.

(27) Mortz, E.; Vorm, O.; Mann, M.; Roepstorff, P. *Biol. Mass Spectrom.* **1994,** *23*, 249-261.

(28) Bahr, U.; Karas, M. *Rapid Commun. Mass Spectrom.* **1999,** *13*, 1052-1058.

(29) Easterling, M. L.; Mize, T. H.; Amster, I. J. *Anal. Chem.* **1999,** *71*, 624-632.

(30) Cheng, H.; Markley, J. L. *Annu. Rev. Biophys. Biomol. Struct.* **1995,** *24*, 209-237.

(31) Ollagnier, S.; Meier, C.; Mulliez, E.; Gaillard, J.; Schuenemann, V.; Trautwein, A.; Mattioli, T.; Lutz, M.; Fontecave, M. *J. Am. Chem. Soc.* **1999,** *121*, 6344-6350.

(32) Bianchi, V.; Eliasson, R.; Fontecave, M.; Mulliez, E.; Hoover, D. M.; Matthews, R. G.; Reichard, P. *Biochemistry. Biophys. Res. Commun.* **1993,** *197*, 792-797.

(33) Van Berkel, G. J.; Zhou, F. *Anal. Chem.* **1995**, 67, 2916-2923.

(34) Bruschi, M.; Guerlesquin, F. *FEMS Microbiol. Rev.* **1988**, 155-176.

(35) Dunham, W.; Hagen, W.; Fee, J.; Sands, R.; Dunbar, J.; Humblet, C. *Biochim. Biophys. Acta* **1991,** *1079*, 253-262.

(36) Verhagen, M.; O'Rourke, T.; Adams, M. W. W. *Biochem. Biophys. Res. Commun.* **1999,** *1412*, 212-229.

CHAPTER 3

FIRST OBSERVATION BY MASS SPECTROMETRY OF A 3+ OXIDATION STATE FOR A [4FE-4S] METALLOPROTEIN: AN ESI-FTICR MASS SPECTROMETRY STUDY OF THE HIGH POTENTIAL IRON-SULFUR PROTEIN FROM *CHROMATIUM VINOSUM*[1]

[1]Johnson, K.A. and I. J. Amster. 2001. Submitted to the Journal of the American Society for Mass Spectrometry.

Abstract

Electrospray ionization (ESI) Fourier transform ion cyclotron resonance mass spectrometry (FTICR) is used to measure the molecular weight of the high potential iron-sulfur protein (HiPIP) from *Chromatium vinosum* (*C. vinosum*) and its corresponding apoprotein. By accurate mass measurement of the metalloprotein, the oxidation state of the [4Fe-4S] metal center is assigned as 3+. This is the highest oxidation state yet observed by mass spectrometry for a [4Fe-4S] cluster, which usually appear in the 2+ oxidation state. In order to make this assignment correctly, the mass spectrum of the apoprotein was acquired, and a 1 Dalton difference was found between the molecular mass of the apoprotein and its published amino acid sequence. The mass spectra of the trypsin and cyanogen bromide digests of the alkylated apoprotein were obtained, and the data suggests that the C-terminal glycine residue is amidated.

Introduction

Iron-sulfur clusters constitute the active sites of a number of soluble and membrane-bound proteins [1]. Mass spectrometry has been used to characterize several iron-sulfur proteins, and provides and accurate method to determine the stoichiometry of the inorganic portion of these and other metalloproteins [2-5]. Mass spectrometry also provides a means to measure the oxidation state of metal centers in proteins [2,6-12]. We have recently examined several iron-sulfur proteins with stoichiometries of Fe_nS_m (n=1-8, m=2-8) by electrospray ionization Fourier transform ion cyclotron resonance mass spectrometry [2,6]. Interestingly, the highest biologically relevant oxidation state is the one observed in most of the mass spectra of metalloproteins that have been published. For most [4Fe-4S] proteins, the highest oxidation state reported under biological conditions is 2+, and is the one that has been observed by mass spectrometry, even though oxidation states ranging from 0 to 4+ are possible [2]. Under reducing, anaerobic conditions, we have recently been able to observe the lowest biologically relevant oxidation state for a number of metalloproteins [13]. Such observations support the

contention that the gas-phase properties of protein ions closely resemble their known solution properties. To test this assertion, we have chosen to examine the high potential iron-sulfur protein (HiPIP) from *Chromatium vinosum* [14-24]. This [4Fe-4S] protein can achieve an oxidation state as high as 3+ under biological conditions [14]. The higher oxidation state of this protein results from an interaction of the iron-sulfur cluster with the surrounding amino acids, i.e. the oxidation state is sensitive to the three dimensional structure of the protein, particularly in the region surrounding the metal center. This the observation of a 3+ oxidation state for [4Fe-4S] in the mass spectrum of this protein would provide significant evidence that the structure of the protein ion closely resembles that of the solvated molecule.

In order to assign the oxidation state of a metal center in a metalloprotein, the mass of the holoprotein must be measured with an accuracy of at least 1 Da, which is easily achieved with isotopically resolved data such as can be obtained by FTICR mass spectrometry [2,25,7]. The difference in mass between the holoprotein and the apoprotein can be assigned to the inorganic portion of the metalloprotein, from which the stoichiometry of the metal center can be derived. The oxidation state of the metal center is determined from the difference between the charge present on an ion and the number of excess proteins that are present, i.e. the charge of a metalloprotein ion is determined by the number of excess proteins and the oxidation state of the metal center. The number of excess protons present on a protein ion can be determined by comparing the accurate mass measurement of the ion with the mass calculated for the known elemental composition of the ion. However, post-translational modifications of the protein sequence can interfere with this calculation. For example, amidation of carboxyl groups or deamidation of an amide changes the molecular weight of a protein by 1 Da. As will be illustrated by the data presented below, the potential for errors introduced by such modifications require that both the apoprotein and holoprotein are accurately measured in order to properly assign the oxidation state of a metal center.

In this paper, we report the analysis of high potential iron-sulfur protein (HiPIP) from *Chromatium vinosum* by ESI-FTICR mass spectrometry, and the identification of a post-

translational modification of its C-terminal glycine residue. The original amino acid sequence for this HiPIP was reported in 1973 [23]. The protein was found to contain a single 85 amino acid peptide chain with four cysteine residues that coordinate the metal. The molecular weight of the holoprotein was found to be 9.2 kDa, and the N-terminal and C-terminal ends of the protein were found to be readily accessible to exopeptidases for degradation. The secondary structure of the protein was found by crystallography to contain and antiparallel β-sheet near the C-terminal end of the protein [26]. The N-terminal portion of the protein contains two short helical segments. The protein contains five lysine residues, two arginine residues, and one methionine residue, resulting in eight peptides by tryptic digestion and two peptides by cyanogen bromide cleavage. The tertiary solution structure of the protein has recently been solved for the oxidized form of the HiPIP from *C. vinosum* by NMR [16]. Electrospray ionization mass spectrometry has been used to observe HiPIP holoprotein in both negative and positive ionization modes [27]. HiPIP from *C. vinosum* binds four iron atoms that are coordinated to the protein through cysteine residues 43, 46, 63 and 77. The iron atoms are bridged by inorganic sulfide atoms to form the [4Fe-4S] cluster. The [4Fe-4S] clusters from iron-sulfur proteins can cycle between oxidation states of 1+ to 3+, but no single iron-sulfur center is known to cycle between all three states. The common forms of the clusters cycle between 1+ and 2+, while 2+ and 3+ are the active redox states for the high potential iron-sulfur cluster proteins [14]. HiPIP is of interest to us because it provides an opportunity to observe a higher oxidation for the [4Fe-4S] cluster, and to provide further evidence that mass spectrometry measures a biologically relevant value for the oxidation state of the metal. Since the oxidation states of metals exhibit themselves as integer changes in mass, it is important that the mass of the apoprotein, and any post-translational modifications be fully characterized.

Experimental

All mass spectra were acquired with a Bruker BioApex 7 Tesla FTICR mass spectrometer equipped with an electrospray ionization source by Analytica. The glass capillary

in the Analytica source was replaced by a heated metal capillary. All samples were ionized by nanoelectrospray. Capillary tips for nanospray were produced in our lab from 100 μm inner diameter fused silica capillary (Polymicro Technologies, Phoenix, AZ). The capillary was pulled to a fine tip by pulling with a constant force while heating with a micro-torch (Microflame, Inc., Minnetonka, MN). The average flow rate for sample introduction to the mass spectrometry was 8 μL/hour. The heated metal capillary was maintained at a temperature between 100-140 °C for the experiments. Ions were stored in the source region in a hexapole ion guide for 0.5-0.75 s and were pulsed through a series of electrostatic lenses into the detection cell where trapping potentials of 0.90 V and 0.95 V were used on the front and back trapping plates of the cell to isolate ions for excitation and detection. The time domain signal (transient) was collected by averaging approximately 50 scans. The summed transient was apodized prior to application of the Fourier transform, followed by calibration to yield a mass spectrum.

The high potential iron-sulfur protein was isolated from *Chromatium vinosum,* and was purified using the procedure outlined by Knaff and co-workers [20]. Apoprotein for the HiPIP was generated by heating the holoprotein at 90 °C for 15 minutes. Disulfide bonds in the denatured HiPIP were reduced before alkylation by incubating the apoprotein (15 μM) with dithiothreitol (4.5 mM) at 45 °C for 15 minutes [23]. The reduced protein sample was alkylated using iodoacetamide at a concentration of 10 mM. The sample was mixed with a vortex shaker for 30 seconds and then allowed to rest at room temperature for 5 minutes. Excess reducing agent was removed by concentrating the sample in a microcentrifuge tube with a 5 kDa cutoff integral dialysis membrane (Millipore Corporation, Bedford, MA) and washed with 200 μL of 15 mM ammonium acetate solution. The alkylated protein was resuspended in water, yielding a final concentration of 15 μM.

Trypsin digestion was performed on both the denatured HiPIP and the alkylated apoprotein. The protein solutions were desalted by buffer exchange with 15 mM ammonium acetate using a microcentrifuge tube with a 5 kDa cutoff integral dialysis membrane. A solution

of modified trypsin (Promega, Madison, WI) at a concentration of 2 μg/100 μL in 100 mM ammonium bicarbonate solution was mixed with an equal volume of the 15 μM protein solutions and incubated for 24 hours at 45 °C.

For chemical digestion of HiPIP, cyanogen bromide was dissolved in a solution of 70% formic acid to yield a concentration of 5 mg/mL [28]. 15 μL of the resulting cyanogen bromide solution was added to the lyophilized protein to yield a final concentration of 1 mg/mL of protein. The digest solution was vortexed for 30 seconds and then wrapped in aluminum foil to protect the sample from visible radiation. The sample was allowed to react for 22 hours. The solution was then lyophilized and the resulting peptides were resuspended in a solution of 49% methanol, 49% water and 2% acetic acid.

The FTICR data produces isotopically-resolved mass spectra from which the monoisotopic molecular weight of the protein is determined. Monoisotopic molecular weight is defined as the sum of the lowest molecular weight isotopes in the molecular formula, and for most proteins, this corresponds to ^{12}C, ^{1}H, ^{14}N, ^{16}O and ^{32}S. A comparison of theoretically derived isotope distribution with experimental data, allows identification of the monoisotopic peak in the experimental data from which the molecular weight may be calculated [29]. For metalloproteins, the definition of monoisotopic peak is slightly different than for other proteins. The monoisotopic peak for a metalloprotein is defined here as the sum of all of the lowest molecular weight isotopes in the molecular formula of the protein plus the mass of the most abundant isotope of the metal or metals that make up the metalloprotein. This corresponds to ^{56}Fe instead of ^{54}Fe, since the natural abundance of ^{54}Fe is 5.82%, and produces a peak that is usually too small to be identified.

Molecular weights for most proteins are calculated assuming all of the ionizable sites in the protein are neutral, but metalloproteins provide an additional challenge for mass spectrometry since the metal or metal cluster can also carry charge [7,2,6]. We use “apparent mass” to refer to the molecular weight that is derived assuming all of the charge present on an ion is due to excess protons. “Calculated mass” is the mass derived from the sum of all of the

lowest molecular weight isotopes in a given molecular formula (with the exception of iron, as described above). This is identical to the monoisotopic mass except when disulfide bonds are present in the molecule of interest. The calculated mass makes no assumptions about the formation of disulfide bonds in a protein. The difference in mass between the calculated mass and the apparent mass allows one to assign the oxidation state of the metal center and the number of disulfide bonds in the molecule. The apparent and calculated masses can differ by as little as one Dalton in the case of oxidized versus reduced metal or two Daltons per disulfide bond within the molecule. This procedure has been described in detail in an earlier publication [2].

Results and Discussion

Figure 1 shows the mass spectrum of a typical [4Fe-4S] protein, ferredoxin from *Pyrococcus furiosus (Pf).* The [4Fe-4S] cluster is coordinated to the protein through three cysteine residues and one aspartic acid residue [30]. The apparent mass calculated for the protein is 7509.83 Da and the calculated mass for the protein is 7513.87 Da. The difference of 4 Da supports the assignment of a 2+ oxidation state for the metal center and a single disulfide bond between two cysteines in the protein (C21 and C48). The oxidation state of the metal was confirmed in previous work in which mutation of one of the cysteine residues to alanine (C21A) eliminated the disulfide bond [2]. The highest oxidation state observed by other methods for *Pf* ferredoxin is 2+ [30]. Several similar examples of iron-sulfur proteins have been recently published that establish the mass spectral data provide a way to determine the highest biologically relevant oxidation state of the metal center of a metalloprotein [2,6].

HiPIP from *C. vinosum* is similar to *Pf* ferredoxin in that it contains a [4Fe-4S] metal center. The ESI-FTICR mass spectrum for HiPIP from *C. vinosum* is shown in Figure 2. The 4+, 5+ and 6+ charge states are observed, corresponding to protein with an intact [4Fe-4S] cluster is observed. In addition, the 9+ charge state of HiPIP dimer containing 2 intact [4Fe-

Figure 3.1 The ESI-FTICR mass spectrum of ferredoxin from *Pyrococcus furiosus* containing a [4Fe-4S] cluster. The measured molecular weight for the protein is consistent with the presence of a single disulfide bond (C21-C48) and an oxidation state for the metal cluster of 2+.

86

Figure 3.2 (Top) The ESI-FTICR mass spectrum of high potential iron-sulfur protein (HiPIP) holoprotein from *C. vinosum* under nondenaturing conditions. The small peak at mass-to-charge 2027 representing HiPIP dimer. (Bottom) The ESI-FTICR mass spectrum of HiPIP to which apoprotein was added as an internal calibrant. The inset compares theoretical (circles) and experimentally-observed isotope abundances for the 5+ charge state.

4S] clusters is observed in the mass spectrum obtained under nondenaturing conditions (top). The spectrum was calibrated externally using ubiquitin, and the apparent mass for the holoprotein is 9247.77 Da, while the mass calculated from the reported amino acid sequence is 9251.86 Da. Since the protein only contains 4 cysteine residues and all of them are involved in cluster ligation to the protein, the mass difference cannot be a result of disulfide bond formation. Rather, the difference of 4 mass units suggests a 4+ charge state on the metal cluster. Since the inorganic sulfide ions have a formal oxidation state of 2-, and iron could conceivable be present as Fe^{3+}, an overall charge on the cluster may seem reasonable. However, prior solution studies suggest that the highest oxidation state for this cluster is 3+ in this protein [16]. To verify the 4 Da difference between apparent and calculated masses, apoprotein was added as an internal calibrant to the holoprotein solution and a mass spectrum was obtained. The resulting spectrum is shown at the bottom of Figure 2. Apoprotein in the 5+ and 6+ charge states were used for the internal calibration assuming that the free cysteine residues that normally ligate the iron-sulfur cluster were oxidatively coupled after cluster removal. This assumption is consistent with previous measurements of ferredoxin apoprotein and other denatured metalloproteins [2]. The molecular weight of the apoprotein was derived from the published amino acid sequence [23]. After internal calibration with the apoprotein peaks (using the published amino acid sequence for this protein), the apparent mass that was derived from the 6+ charge state of the holoprotein was 9248.88 Da, one mass unit higher than by external calibration. From this value, one derives a 3+ oxidation state for, which agrees with literature values for the oxidized form of the cluster [14], and provides further support for our contention that the highest biologically relevant oxidation state is the one produced by non-denaturing electrospray ionization.

The mass difference of 1 Da between the molecular weights determined by internal calibration with the apoprotein versus external calibration with a well characterized peptide standard suggests that the HiPIP structure reported in the literature, which was used to calculate the mass for internal calibration, is incorrect, and the protein weighs one mass unit less that the molecular weight calculated from the published sequence [23].

Our assignment of 2 disulfide bonds in the HiPIP apoprotein was confirmed by alkylating the apoprotein to prevent the formation of disulfide bonds before detection. The resulting mass spectrum is shown in Figure 3. The apparent mass that is derived from the data obtained from the mass spectrum is 9127.29 Da, 1 amu less that the value calculated from the literature sequence, 9128.32 Da. This difference suggests a difference between the published sequence and the isolated protein, such as a post-translational modification of one of the amino acids.

The location of the modification was first examined by conducting a cyanogen bromide digestion of the alkylated protein, which is expected to cleave on the C-terminal side of the single methionine residue at position 49, near the middle of the protein. The mass spectrum obtained after digestion is shown in Figure 4. The expected and measured masses of the resulting peptides are shown in Table 1. Two charge states of the N-terminal fragment were detected from which an apparent mass of 5177.44 Da was derived, in excellent agreement with the calculated mass for this fragment, 5177.43 Da. The measured mass for the C-terminal fragment is 3919.97 Da, one mass unit less than the value calculated from the published sequence, 3920.86 Da. This confirms that a modification has occurred in one of the amino acids of the C-terminal half of the protein that reduces the mass by 1 Dalton. Peaks in the mass spectrum represent fragments containing homoserine and homoserine lactone as well as formylation of amino groups in the peptides. The masses of these peaks are in agreement with a 1 mass unit shift in the C-terminal fragment. Low intensity peaks from undigested apoprotein were also detected.

To more precisely locate the modification to the published sequence, we examined a tryptic digest of the protein for which cysteines were alkylated by iodoacetamine. Table 2 compares predicted and measured masses for the tryptic fragments of the alkylated protein. Of the eight fragments that are expected, six were detected in the ESI-FTICR mass spectrum, shown in Figure 5. Undetected fragments were fragment T_3, which consists of amino acids SER and fragment T_8, which consists of amino acids AG. Since SER resides in the N-terminal half of the protein, the results of the cyanogen bromide digest eliminate T_3 as a modified

Figure 3.3 The ESI-FTICR mass spectrum of the HiPIP apoprotein from *C. vinosum*, in which the cysteines have been alkylated by iodoacetamide. (Top) An expansion of the 8+ charge state. (Bottom) The entire mass spectrum with charge state distribution from 4+ to 9+.

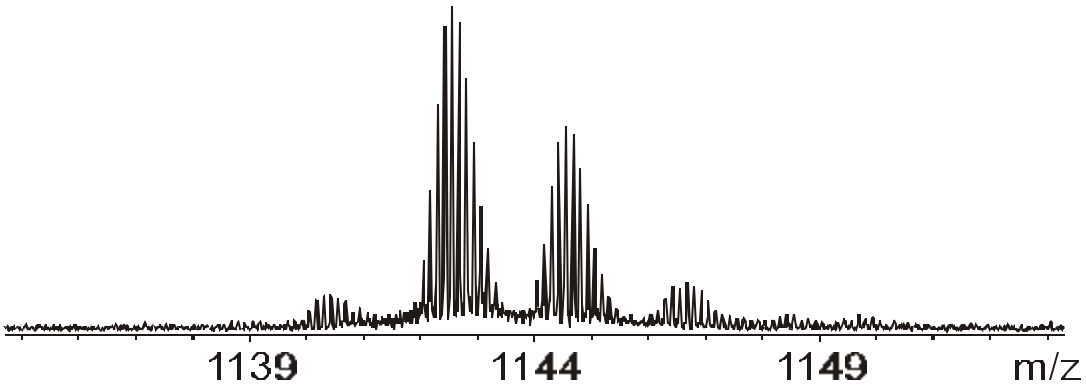
1139
1144
1149
m/z

Figure 3.4 The ESI-FTICR mass spectrum of the cyanogen bromide digest of the alkylated apoprotein of HiPIP. The C-terminal fragment mass is found to be 1 Da less than its predicted mass. A small amount of undigested apoprotein is also observed in the mass spectrum. Peaks labeled "P" result from polyethylene glycol from the containers used for the chemical digestion. (Inset) An expansion of the region of the spectrum showing peptide 50-85 (T_2) and additional adduct peaks.

Table 3.1 Peptide Fragment Masses Resulting from Cyanogen Bromide Digestion of HiPIP.

CNBr Fragment	Peptide Sequence	predicted mass (Daltons)	measured mass (Daltons)
F_1	SAPANAVAADDATAIALKYNQ DATKSERVAAARPGLPPEEQ HCANCQFM	5177.44	5177.35
F_2	QADAAGATDEWKGCQLFPGK LINVDGWCASWTLKAG	3920.86	3919.80

Table 3.2 Tryptic Fragment Calculated and Measured Masses for Cysteine-Alkylated HiPIP. [a]Fragement T_5 is unexpected because of the proline residue at its N-terminus, but is nevertheless observed.

Tryptic Fragment	Peptide Sequence	predicted mass (Daltons)	measured mass (Daltons)
T_1	SAPANAVAADDATAIALK	1668.87	1668.85
T_2	YNQDATK	838.38	838.37
T_3	SER	390.19	Not Detected
T_4	VAAAR	486.29	486.28
T_5[a]	PGLPPEEQH**(C)**AN**(C)**QF MQADAAGATDEWK	3157.33	3157.24
T_6	G**(C)**QLFPGK	905.44	905.43
T_7	LINVDGW**(C)**ASWTLK	1661.82	1661.81
T_8	AG	146.07	Not Detected

Figure 3.5 The ESI-FTICR mass spectrum of the tryptic fragments of the alkylated HiPIP apoprotein. Of eight possible fragments, six are found in the mass spectrum (Table 1). From these data, the 1 Da mass difference for the complete protein can be assigned to a modification in either T_3 (SER) or fragment T_8 (AG).

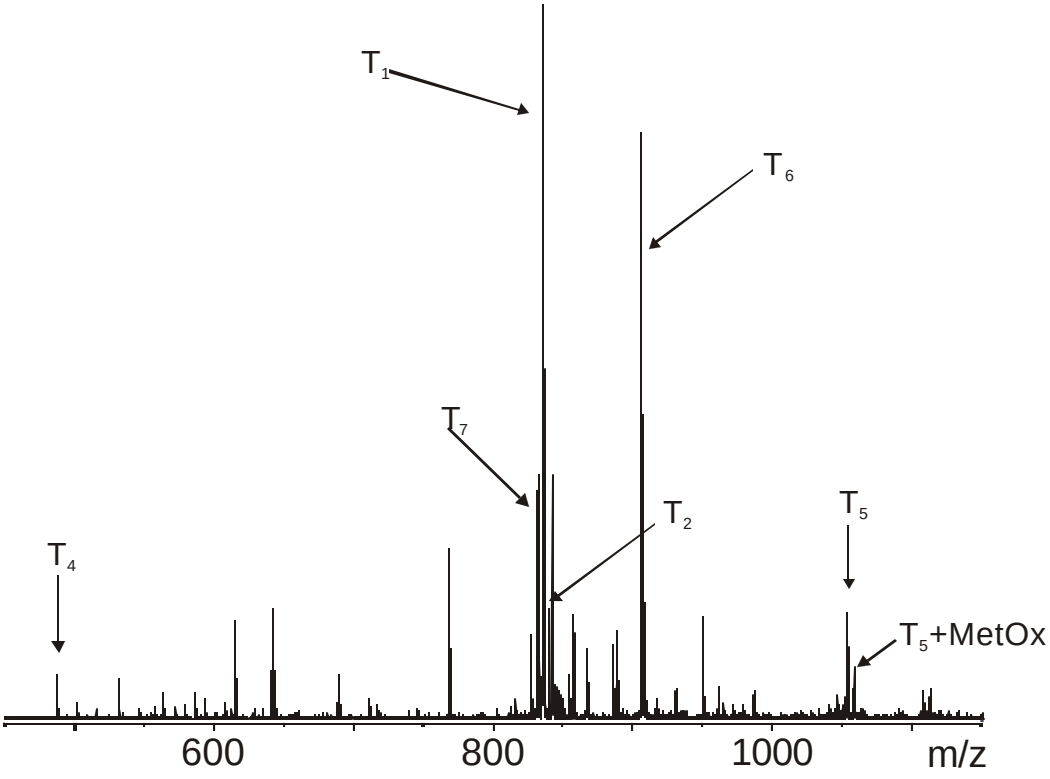
T1
T6
T7
T2
T5
T4
T5+MetOx
600
800
1000
m/z

fragment, and suggests that AG, fragment T_8, is modified. The one mass unit decrease from the expected value suggests amidation, probably by modification of glycine in the AG residue at the C-terminus of the protein.

Since the AG residue was not observed in the trypsin digest of the alkylated protein, further measurements were made to try to directly observe this residue. A trypsin digest was produced for the non-alkylated apoprotein. Some fragments of the protein were found to be linked via dislufide bonds, and peaks due to incomplete digestion of the protein were also observed. Nevertheless, complete coverage of the protein was obtained from the mass spectral data shown in Figure 6. The predicted masses and measured masses are listed in Table 3. Peaks corresponding to fragments T_2+T_3 and T_7+T_8 arise from incomplete digestion of the protein at lysine residues. These data show the preference of trypsin for arginine compared to lysine [20]. The peaks of greatest interest in the mass spectrum are labeled as fragment T_6+T_7 and fragment T_7+T_8. The apparent mass for the peak labeled T_6+T_7 is 2451.10 Da and the calculated mass is 2453.22 Da. Although each of the two fragments has been cleaved at both C-terminal and N-terminal residues by trypsin, they are still linked by a disulfide bond which is consistent with the 2 Da mass difference between the apparent and calculated masses. The C-terminal fragment, T_7+T_8, has an apparent mass of 1731.85 Da and a calculated mass of 1732.85 Da. Since residue T_7 agrees with its predicted mass (from the trypsin digest of the alkylated protein), these data confirm that the C-terminal fragment consisting of amino acids alanine and glycine has been modified to produce a decrease in mass of 1 Da. Side chain modification is unlikely, so amidation of the C-terminal glycine is deduced from these data. This is a fairly common modification in eukaryotes, but can also occur in bacteria [31].

Enzymes of high specificity are of great importance in the analytical applications of proteins [32]. Rules governing amino acid cleavage are important because of their use in te interrogation of database proteins that generate theoretical fragments for comparison to

Figure 3.6 The ESI-FTICR mass spectrum of the tryptic digest of the non-alkylated protein. Complete coverage of the protein is observed in the mass spectrum. The measured mass of T_6-S-S-T_7 agrees with its calculated value, while T_7+T_8 has an apparent mass that is 1 Da less than its calculated value, indicating that the modification is in T_8, the dipeptide, AG.

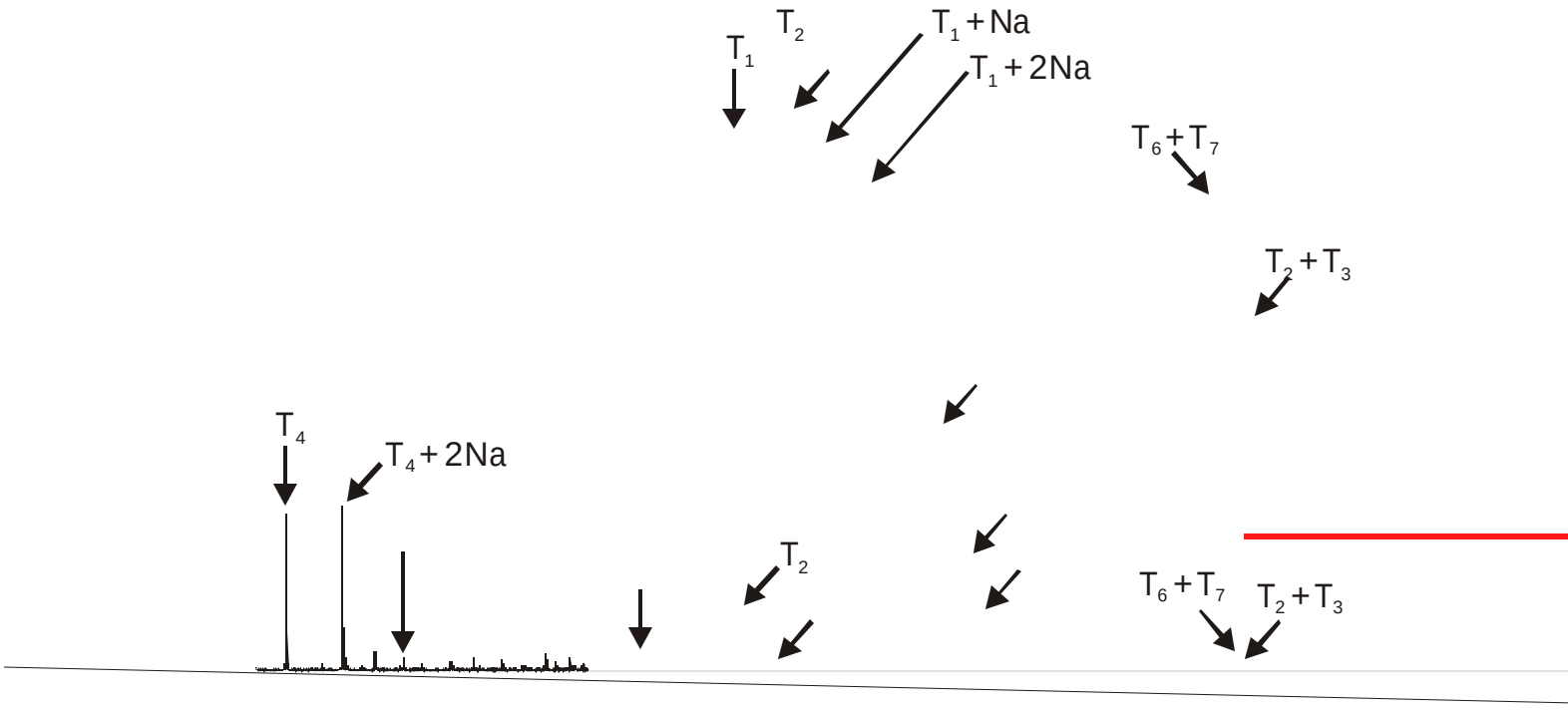
T1
T2
T1 + Na
T1 + 2Na
T6 + T7
T2 + T3
T4
T4 + 2Na
T2
T6 + T7
T2 + T3

Table 3.3 Peptide Fragment Masses for Tryptic Digestion of the Non-Alkylated HiPIP. [a]Predicted masses take into account the two mass unit difference from disulfide bond formation.

Tryptic Fragment	Peptide Sequence	predicted mass (Daltons)	measured mass (Daltons)
T_1	SAPANAVAADDATAIALK	1668.87	1668.79
T_2	YNQDATK	838.38	838.30
T_3	SER	390.186	Not detected
T_4	VAAAR	486.29	486.29
T_5(S-S)[a]	PGLPPEEQH**C**AN**C**QFMQ ADAAGATDEWK	3041.27	3041.20
T_6	GCQLFPGK	848.42	Not detected
T_7	LINVDGWCASWTLK	1604.80	Not detected
T_8	AG	146.07	Not detected
T_2-T_3	YNQDATK-SER	1228.59	1228.57
T_6-S-S-T_7[a]	G**C**QLFPGK + LINVDGW**C**ASWTLK	2051.20	2051.10
T_7-T_8	LINVDGWCASWTLK-AG	1731.86	1732.86

experimentally derived fragment masses. All digestion methods give some heterogeneity in specificity of bond cleavage, so products must be characterized in detail [33]. The difficulties that arise from this heterogeneity are synonymous with the problems that are found in the detection of post-translational modifications in that these occurrences can not be predicted. An example of such an unpredictable cleavage in these data is peptide T5, resulting from cleavage of a R-P bond. Although peptide bonds between basic residues and proline (RP or KP) are usually immune from trypsinolysis, cleavage can occur in rare cases [33], and is observed here.

Conclusion

A 3+ oxidation state is assigned to the [4Fe-4S] center of HiPIP from *C. vinosum*. This is the naturally occurring oxidized state of the metal center under biological conditions, and provides yet another example that metalloproteins exhibit the highest biologically relevant oxidation state when analyzed using electrospray ionization mass spectrometry. The highest oxidation state achieved by the [4Fe-4S] cluster depends in a sensitive manner on the environment of the metal center, specifically, the presence of specific amino acids in the coordination sphere of the metals. These data suggest that the three dimensional structure of the protein is retained to a point late in the ionization process, and perhaps even in the gas phase.

The previously unknown amidation of the C-terminal glycine residue of the high potential iron-sulfur protein from *C.vinosum* has been identified through ESI-FTICR mass spectrometry. Such a modification produces only a 1 Da decrease in the molecular weight of the molecule, but this is readily discerned by FTICR mass spectrometry. The proper assignment of the molecular weight of this protein is required ro determine the oxidation state of the metal center. The identification of such small mass shifts in an ion that weighs approximately 10 kDa demonstrated the utility of FTICR mass spectrometry for bioanalytical measurements.

Acknowledgment

The authors thank Professor David B. Knaff at the Texas Tech University for providing the *C. vinosum* HiPIP, and Marc F.J.M. Verhagen and Mike W.W. Adams from the University of Georgia for providing the *P. furiosus* ferredoxin used in this study. We gratefully acknowledge funding provided by the National Science Foundation (CHE-9974579).

References

1. Johnson, M. K. Iron-Sulfur Clusters. In *Encyclopedia of Inorganic Chemistry*. King, R. B. Ed; John Wiley and Sons: New York. **1994,** Vol 4, pp 1896-1913.
2. Johnson, K. A.; Verhagen, M.; Adams, M. W. W.; Amster, I. J. *Anal. Chem.* **2000,** *72*, 1410-1418.
3. Veenstra, T. D.; Johnson, K. L.; Tomlinson, A. J.; Craig, T. A.; Kumar, R.; Naylor, S. *J. Am. Soc. Mass Spectrom.* **1998,** *9*, 8-14.
4. Henin, O.; Barbier, B.; Boillot, F.; Brack, A. *Chem.-Eur. J.* **1999,** *5*, 218-226.
5. Vo, E.; Wang, H. C.; Germanas, J. P. *J. Am. Chem. Soc.* **1997,** *119*, 1934-1940.
6. McLafferty, F. W.; Guan, Z. Q. Haupts, U.; Wood, T. D.; Kelleher, N. L. *J. Am. Chem. Soc.* **1998**, 120, 4732-4740.
7. Johnson, K. A.; Verhagen, M.; Adams, M. W. W.; Amster, I. J. *Int. J. Mass Spectrom.* **2001**, 204, 77-85.
8. He, F.; Hendrickson, C. L.; Marshall, A. G. *J. Am. Soc. Mass Spectrom.* **2000**, 120-126.
9. Fabris, D.; Zaia, J.; Hathout, Y.; Fenselau, C. *J. Am. Chem. Soc.* **1996,** *118*, 12242-12243.
10. Troxler, H.; Kuster, T.; Rhyner, J. A.; Gehrig, P.; Heizmann, C. W. *Anal. Biochem.* **1999,** *268*, 64-71.
11. Li, Y. T.; Hsieh, Y. L.; Henion, J. D.; Ganem, B. *J. Am. Soc. Mass Spectrom.* **1993,** *4*, 631-637.

12. Yu, X. L.; Wojciechowski, M.; Fenselau, C. *Anal. Chem.* **1993,** *65*, 1355-1359.

13. Lei, Q. P.; Cui, X. Y.; Kurtz, D. M.; Amster, I. J.; Chernushevich, I. V.; Standing, K. G. *Anal. Chem.* **1998,** *70*, 1838-1846.

14. Johnson, K. A.; Shira, B. A.; Anderson, J. L.; Amster, I. J. *Anal. Chem.* **2001,** *73*, Submitted.

15. Adman, E. T.; Mather, M. W.; Fee, J. A. *Biochim. Biophys. Acta* **1993,** *1142*, 93-98.

16. Agarwal, A.; Tan, J.; Eren, M.; Tevelev, A.; Lui, S. M.; Cowan, J. A. *Biochem. Biophys. Res. Commun.* **1993,** *197*, 1357-1362.

17. Bertini, I.; Dikiy, A.; Kastrau, D. H. W.; Luchinat, C.; Sompornpisut, P. *Biochemistry.* **1995,** *34*, 9851-9858.

18. Kyritsis, P.; Kummerle, R.; Huber, J. G.; Gaillard, J.; Guigliarelli, B.; Popescu, C.; Munck, E.; Moulis, J. M. *Biochemistry.* **1999,** *38*, 6335-6345.

19. Tan, J.; Corson, G. E.; Chen, Y. L.; Garcia, M. C.; Guner, S.; Knaff, D. B. *Biochim. Biophys. Acta* **1993,** *1144*, 69-76.

20. Bertini, I.; Cowan, J. A.; Luchinat, C.; Natarajan, K.; Piccioli, M. *Biochemistry.* **1997,** *36*, 9332-9339.

21. Cowan, J. A.; Lui, S. M. Structure-function correlations in high-potential iron proteins. In *Advances in Inorganic Chemistry, Vol 45*, 1998; Vol. 45; pp. 313-350.

22. Natarajan, K.; Cowan, J. A. *J. Am. Chem. Soc.* **1997,** *119*, 4082-4083.

23. Wang, P. L.; Donaire, A.; Zhou, Z. H.; Adams, M. W. W.; LaMar, G. N. *Biochemistry.* **1996,** *35*, 11319-11328.

24. Backes, G.; Mino, Y.; Loehr, T. M.; Meyer, T. E.; Cusanovich, M. A.; Sweeney, W. V.; Adman, E. T.; Sandersloehr, J. *J. Am. Chem. Soc.* **1991,** *113*, 2055-2064.

25. Dus, K.; Tedro, S.; Bartsch, R. *J. Biol. Chem.* **1973,** *248*, 644-649.

26. Carter, C. W.; Kraut, J.; Freer, S. T.; Xuong, N. H.; Alden, R. A.; Bartsch, R. G. *J. Biol. Chem.* **1974,** *249*, 4212-4225.

27. Petillot, Y.; Forest, E.; Meyer, J.; Moulis, J. *Anal. Biochem.* **1995,** *228*, 56-63.

28. Coligan, J. E.; Dunn, B. M.; Ploegh, H. L.; Speicher, D. W.; Wingfield, P. T. Protocol for Cyanogen Bromide (CNBr) Cleavage of Proteins. In Current Protocols in Protein Science. Vol 4. **1995,** *2*.

29. Senko, M. W.; Beu, S. C.; McLafferty, F. W. *J. Am. Soc. Mass Spectrom.* **1995,** *6*, 229-233.

30. Conover, R. C.; Kowal, A. T.; Fu, W.; Park, J. B.; Aono, S.; Adams, M. W. W.; Johnson, M. K. *J. Biol. Chem.* **1990,** *265*, 8533-8541.

31. Wilkins, M. R.; Gasteiger, E.; Gooley, A. A.; Herbert, B. R.; Molloy, M. P.; Binz, P. A.; Ou, K. L.; Sanchez, J. C.; Bairoch, A.; Williams, K. L.; Hochstrasser, D. F. *J. Mol. Biol.* **1999,** *289*, 645-657.

32. Cottrell, J. *Peptide Res.* **1994,** *7*, 115-123.

33. Nadler, T.; Blackburn, C.; Mark, J.; Gordon, N.; Regnier, F. E.; Vella, G. *J. Chromatogr. A* **1996,** *743*, 91-98.

CHAPTER 4

DIFFERENCES BETWEEN POSITIVE AND NEGATIVE ION STABILITIES OF METAL-SULFUR CLUSTER PROTEINS: AN ESI-FTICR STUDY[1]

[1]Keith A. Johnson, Marc F.J.M. Verhagen, Michael W.W. Adams and I. Jonathan Amster. International Journal of Mass Spectrometry. **2001**, 204, 77-85.

Abstract

The stability of iron-sulfur proteins during electrospray ionization in both positive ion and negative ion modes was investigated using Fourier transform ion cyclotron resonance mass spectrometry. Positive ion and negative ion mode mass spectra of iron and zinc rubredoxin from *Clostridium pasteurianum* and ferredoxins from *Pyrococcus furiosus* containing [3Fe-4S], [4Fe-4S], [3FeNi-4S] and [3FeMn-4S] clusters are compared. The results demonstrate that all clusters are stable as negative ions, while only the [3FeM-4S], (M=Fe, Mn, Ni) clusters are stable as positive ions. The formal oxidation state of each metal-sulfur cluster is determined by the mass-to-charge measurement, and is found to be the same for both positive and negative ions.

Introduction

Electrospray ionization (ESI) has become a valuable tool in the investigation of protein interactions by mass spectrometry. It is capable of preserving the noncovalent interactions that exist in solution while the complex is transferred to the gas phase. This nondestructive transformation is especially important when analyzing metal-protein interactions. Binding stoichiometry, binding cooperativity, and conformational changes of protein in the presence of metal ions are targets for analysis by ESI mass spectrometry. The use of ESI mass spectrometry for the analysis of noncovalent interactions has recently been reviewed [1-3]. ESI has been used in both positive and negative modes of ionization by generating positive protein ions by the addition of protons during electrospray and by generating negative ions through the extraction of protons. The choice of ionization modes is generally based on the isoelectric point (pI) of a given protein. Normally, positive ion mode is chosen for basic or neutral proteins, whereas negative ion mode is used for the ionization of acidic proteins, however, it has been shown that ESI can generate positive ions from acidic amino acids and negative ions from basic amino acids [4,5]. Questions concerning the differences between these modes of ionization and the information that can be extracted from data collected in each mode have recently been investigated by Konermann and Douglas [6]. One result of the investigation shows that the tertiary structure of proteins can be monitored using

denaturing and nondenturing conditions for positive ions, but the same data is not always available from the mass spectra generated under the same solvent conditions in negative ion mode.

The higher order structure of metalloproteins has also been monitored in both modes of ionization. There have been numerous studies of metal-containing proteins in positive mode ESI, and range from measurements of metal atom stoichiometry of non-heme iron containing rubrerythrin [7] and calcium binding parvalbumin [8] to the investigation of conformational changes associated with the unfolding of cytochrome *c* and myoglobin [9]. Several studies of metal-protein interaction using negative mode electrospray ionization have been published. These include calcium induced noncovalent interactions between proteins as well as measurements of the stoichiometry and cooperativity of metal atom binding to proteins [7,10,11]. A comparison of the two modes of ionization for a single metalloprotein has been published [12]. The iron and zinc forms of *Clostridium pasteurianum* (*Cp*) rubredoxin and its recombinant counterpart purified from *Escherichia coli* (*E. coli*) have been investigated using electrospray ionization mass spectrometry to isolate conditions that prevent the loss of the metal from the two forms of the protein [13]. Iron-sulfur cluster containing ferredoxins have been investigated using both positive and negative modes of electrospray ionization and the clusters are more stable in negative mode than in positive mode [14,15]. The stoichiometry and identification of iron-sulfur clusters from *Sulfolobus acidocaldarius* [16] and *Rhodobacter capsulatus* [17] ferredoxins have been determined using electrospray mass spectrometry. More recently, an intermediate cluster structure from the high potential iron-sulfur protein (HiPIP) from *Chromatium vinosum* (*Cv*) has been investigated by mass spectrometry as a possible model for characterizing the assembly of metal-sulfur clusters in ferredoxin [18]. The effect of the oxidation state of iron in heme-containing proteins was resolved by Henion and co-workers, who investigated ferric heme associated with myoglobin and ferrous heme associated with cytochrome *c*, in which only a 1 mass unit difference distinguished the two oxidation states of heme [19]. The influence of the oxidation state of the metal centers on ions in electrospray have also been described for rubrerythrin and hemerythrin [7], and for Cd^{2+} and Zn^{2+} metallothioneins [20].

Electrospray Fourier transform ion cyclotron resonance (ESI-FTICR) mass spectrometry has become a valuable tool in the arsenal of techniques used to probe the structure of proteins [3]. The soft ionization of electrospray ionization along with the high resolution and high mass accuracy that are possible with the technique facilitate the investigation of the stoichiometry and oxidation states of metalloproteins. Iron-sulfur cluster containing proteins that range from mononuclear metal centers to [4Fe-4S] clusters have been investigated to determine the effect of the oxidation state and the presence or absence of disulfide bonds on the measured mass [15]. The high resolution and high mass accuracy of FTICR mass spectrometry enable the detection of small changes in mass of metalloproteins that are accompanied by the formation or removal of disulfide bonds and mass differences associated with oxidized versus reduced forms of metal centers [15,21]. In this article, we compare the stability of various iron-sulfur cluster proteins by ESI-FTICR mass spectrometry using both positive ion and negative modes of ionization.

Experimental

All proteins examined here were produced by over-expression in *E. coli*. The preparation and purification of recombinant wild-type *Pyrococcus furiosus* (*Pf*) ferredoxin has been described previously [22]. The [4Fe-4S] cluster was converted to the [3Fe-4S] form by treating the ferredoxin with a five fold excess of ferricyanide for 15 minutes. The oxidant was subsequently removed by gel filtration [23]. Prior to analysis, protein solutions were desalted by ultrafiltration in a microcentrifuge tube with 1 mL of 15 mM ammonium acetate solution with a 5 kDa cutoff membrane (Millipore Corporation, Bedford, MA). The protein was then resuspended in water to yield a final protein concentration of 15 μM.

All mass spectra were acquired with a Bruker BioApex 7 Tesla FTICR mass spectrometer equipped with an Analytica electrospray ionization source. The source was modified by replacing the glass capillary with a heated metal capillary which provides gentler desolvation of ions during ESI without using higher voltages that can cause loss of the metal cluster. Capillary tips for electrospray ionization were produced in our laboratory from 100 μm inner diameter fused silica

capillary (Polymicro Technologies, Phoenix, AZ). The capillary was pulled to a fine tip by heating it with a microtorch (Microflame, Inc., Minnetonka, MN) while applying a constant force. The flow rates for sample introduction to the mass spectrometer ranged between 6 and 10 μL/h. A voltage of 1.2 kV (-1.2 kV for negative ions) was applied to the syringe needle that infused the sample into the spray capillary, forming a liquid electrical junction [24]. The ion source parameters varied between positive mode and negative mode electrospray. For negative mode ionization, the ion source parameters (average values) were as follows: skimmer, -4.80 V; hexapole DC offset, 2.35 V; hexapole extract plate, -1.89 V; hexapole trap, -6.74 V For positive mode: skimmer, 5.44 V; hexapole DC offset, -4.74 V; hexapole extract plate, 1.22 V; hexapole trap, 6.78 V. The heated metal capillary was maintained at a temperature between 110 and 130 °C for the experiments. Although the signal intensity was adjusted through the variation in temperature of the metal capillary, no significant improvement or deterioration of the signal was observed for slightly higher temperatures. At temperatures lower than 100 °C, the signal became unstable. Ions were stored in the source region in a hexapole ion guide for 0.5-0.75 s and were pulsed through a series of electrostatic lenses into the detection cell where trapping potentials of 0.90 V and 0.95 V (-0.90 V and -0.95 V for negative ions) were used on the front and back trapping plates of the cell to isolate ions for excitation and detection. The time domain signal (transient) was collected by averaging approximately 50 scans. The summed transient was apodized prior to application of the Fourier transform, followed by calibration to yield a mass spectrum.

Calculations of isotope distributions for the proteins were made by using IsoPro software available from (http://www.members.aol/msmssoft). Experimentally obtained isotope distributions and calculated distributions were matched using the χ^2 test as described by McLafferty and co-workers [25]. The estimation of the monoisotopic mass was made after assigning the isotope composition of each of the peaks in the experimentally observed distribution as described previously [15].

Results and Discussion

ESI-FTICR mass spectrometry is a valuable tool in identifying the small changes in mass associated with a metalloprotein's oxidation state or in counting disulfide bonds within a protein. The isotopically resolved mass spectra that are obtained from the data yield the monoisotopic molecular weight of the protein. Monoisotopic molecular weight is defined as the sum of the lowest atomic weight isotopes in the molecular formula, and for most proteins, this corresponds to ^{12}C, ^{1}H, ^{14}N, ^{16}O and ^{32}S, the lowest mass and most abundant isotopes of these elements. For metals, the lowest mass isotope is often not the most abundant. We define the monoisotopic mass of a metalloprotein as the sum of the monoisotopic molecular weight of the apoprotein plus the atomic mass of the most abundant isotope of the metal or metals that make up the metal center. For example, we use ^{56}Fe instead of ^{54}Fe since their natural abundances are 91.8% and 5.82%, respectively. Since the mass difference between peaks containing different numbers of iron correspond to the mass of ^{56}Fe rather than ^{54}Fe, this arbitrary convention is more practical than the strict definition of monoisotopic molecular weight [15].

The molecular weight for a protein is normally calculated assuming that all of the ionizable sites in the amino acid sequence for the protein are neutral. However, the metals in metalloproteins exist in oxidation states other than zero, which make this rule impractical. Using this rule for metalloproteins would result in molecular weights that vary according to the oxidation state of the metal center, because metalloproteins with metal centers having different oxidation states would require different numbers of protons to achieve charge neutrality. To avoid this problem, we define the "apparent mass" as the mass that is calculated from the data making the assumption that all of the charge present on an ion is due to excess protons (or a deficit of protons, for negative ions). By using this convention, we make no assumptions about the oxidation state of the metalloprotein prior to calculating a molecular weight. We also define the "calculated mass" as the monoisotopic mass that is calculated from the sum of all of the atomic weights of the lowest mass isotopes of the amino acids in the sequence of the protein plus the atomic weight of the most abundant isotope of the metal or the components of the metal-sulfur cluster. Calculation of the molecular weight by this

method requires no assumptions about internal disulfide bonds. This method allows the derivation of the oxidation state or the number of disulfide bonds in the metalloprotein by calculating the difference between the apparent mass and the calculated mass for the protein. A more complete analysis of this procedure has been discussed recently [15].

Positive and negative ion ESI-FTICR mass spectra of iron *Cp* rubredoxin are shown in Figure 1. The 3+ and 4+ charge states are detected for positive ions and charge states 3- through 7- are detected for negative ions for the iron form of rubredoxin. The apparent mass derived from the mass spectral data of iron rubredoxin is 6096.58 Da and the calculated mass is 6099.55 Da. The difference between the masses indicates that the metal is present in the 3+ oxidation state. This result is the same for both the positive and negative mode data. This is the biologically relevant oxidation state of the iron center under oxidizing conditions. Likewise, the zinc-containing form of *Clostridium pasteurianum* rubredoxin, Figure 2, shows the 2+, 3+ and 4+ charge states in positive mode and charge states ranging from 3- to 7- in the negative mode. These data yield an apparent mass of 6105.58 Da and a calculated mass of 6107.55 Da. The difference of 2 Da agrees with the known oxidation state for Zn in rubredoxin, 2+.

Positive and negative mode mass spectra of metalloproteins obtained under nondenaturing conditions show a consistent pattern in their charge state distributions. The negative ion mass spectra always exhibit a broader distribution of ions than the positive mode mass spectra, as can be seen in Figures 1 and 2. In positive mode spectra, one normally observes that denatured proteins have a broader distribution of charge states of lower mass-to-charge (i.e. with more charge) than are observed in the mass spectra of proteins electrosprayed in their native conformation. It has been proposed that this is the case because the unfolded protein exposes more ionizable sites than the folded protein, which results in the formation of higher charge states [26]. The positively and negatively charged protein ions observed for rubredoxin, Figures 1 and 2, however, were obtained using nondentauring solutions and exist in their native conformations

Figure 4.1 Positive mode (top) and negative mode (bottom) ESI-FTICR mass spectra of iron rubredoxin from *Clostridium pasteurianum*. The positive mode spectrum exhibits the 4+ and 3+ charge states, while the negative mode shows a wider range of charge states from 3- to 7-. Using nondenaturing conditions, only holoprotein is detected.

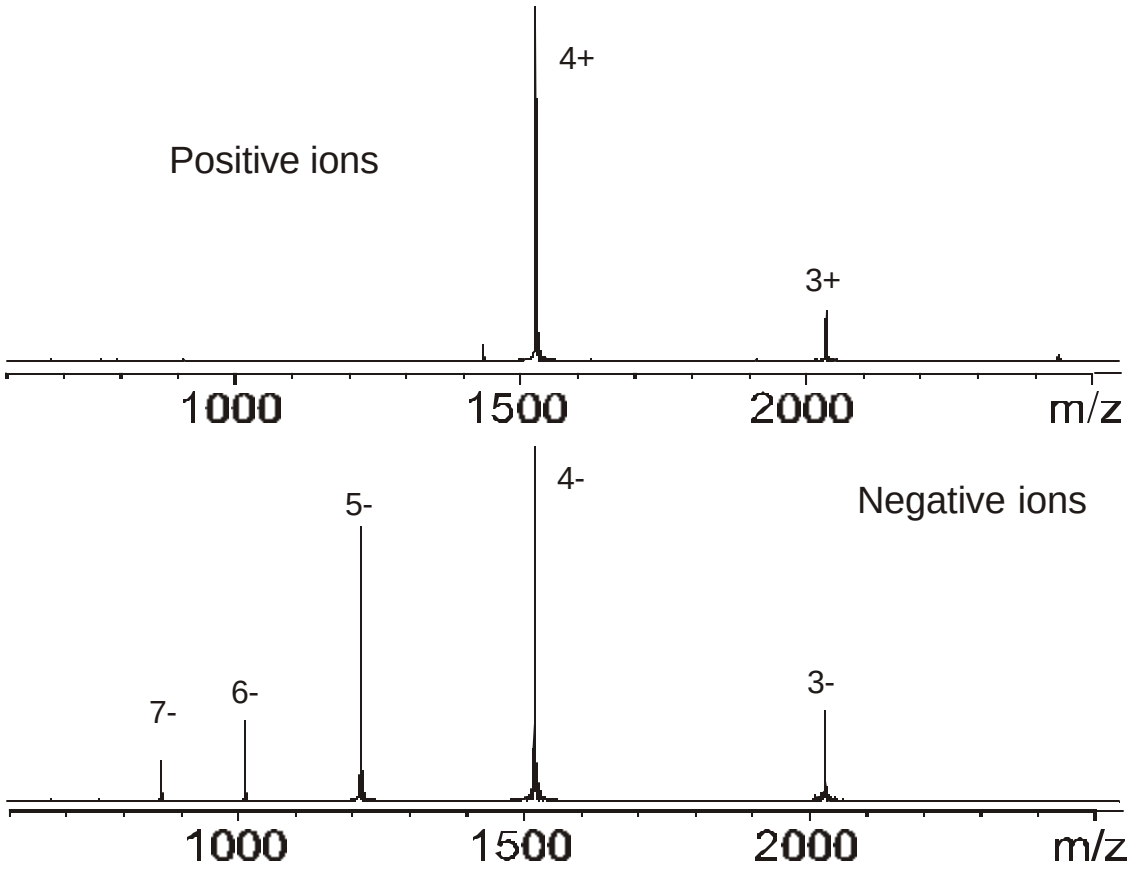
4+
Positive ions
3+
1000
1500
2000
m/z
4-
5-
Negative ions
7-
6-
3-
1000
1500
2000
m/z

Figure 4.2 Positive mode (top) and negative mode (bottom) ESI-FTICR mass spectra of zinc rubredoxin from *Clostridium pasteurianum*. Charge states of 2+, 3+ and 4+ are found in the positive mode spectrum, whereas a wider range of charge states, 3- to 7- are observed in the negative mode mass spectrum. In both mass spectra, only holoprotein is detected.

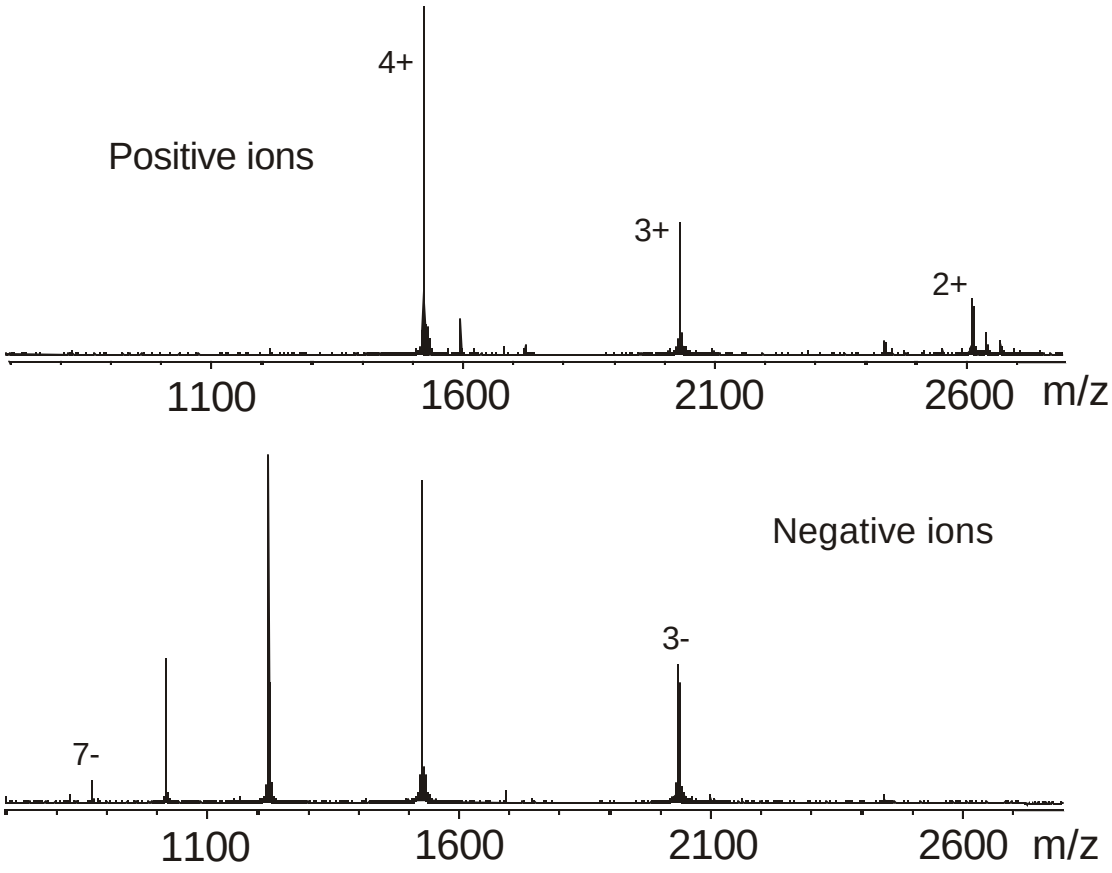
4+
Positive ions
3+
2+
1100
1600
2100
2600
m/z
Negative ions
3-
7-
1100
1600
2100
2600
m/z

with the metal center intact. If the protein ions had unfolded, one would expect the metal to be lost, as is the case for mass spectra obtained under denaturing conditions. This behavior supports the argument that only positive mode ionization can be used to monitor tertiary structure (i.e. conformational changes) in a protein [6]. One might falsely conclude that the abundance of charge states that are formed for negative ions result from the denaturation and exposure of more ionizable sites along the peptide chain. The presence of the intact metal cluster in the negative ion mass spectrum shows that denaturation has not occurred. Figure 3 shows the positive mode mass spectrum of *Pf* ferredoxin, which contains a [4Fe-4S] cluster. The apparent mass, the mass derived assuming all of the excess charge is from protons, is 7509.83 Da. The calculated mass, which is the combined molecular weight of all of the amino acids in the sequence, making no assumptions about disulfide bonds, is 7513.87 Da. The 4 mass unit difference between the two values is attributed to the 2+ oxidation state of the metal cluster and the presence of one disulfide bond that is known to exist distant from the active site of the protein [15,23]. The [4Fe-4S] protein, like the iron and zinc-containing rubredoxins, is stable in positive ion mode and contains only the intact cluster, with no degradation products. The negative mode spectrum, also shown in Figure 3, exhibits a broader distribution of charge states. An oxidation state of 2+ for the [4Fe-4S] cluster is derived from the negative ion data as well.

In solution, the [4Fe-4S] form of this ferredoxin can be converted to a [3Fe-4S] cluster by reaction with ferricyanide, Figure 4 [23]. The [4Fe-4S] cluster exists *in vitro* with a formal oxidation state of 2+ in its most oxidized form, but the [3Fe-4S] cluster exists in a 1+ oxidation state in its oxidized form [23]. Figure 5 shows positive and negative ion mass spectra of the [3Fe-4S] form of ferredoxin. Again, the negative mode mass spectrum contains a wider distribution of charge states than does the positive ion mass spectrum. Moreover, the positive ions show much more complexity for each charge state, corresponding to ions containing various degradation products of the [3Fe-4S] cluster. The apparent mass derived from the holoprotein data containing the intact [3Fe-4S] cluster is 7454.92 Da and the calculated mass is 7457.94 Da, indicating an oxidation state of 1+ as well as one disulfide bond, as expected between C21 and C48. An

Figure 4.3 ESI-FTICR mass spectra of ferredoxin from *P. furiosus.* An intact [4Fe-4S] cluster is observed in the ESI-FTICR mass spectrum in both the positive mode (top) and negative mode (bottom). Dimer is observed at *m/z* 2130 in the negative mode mass spectrum.

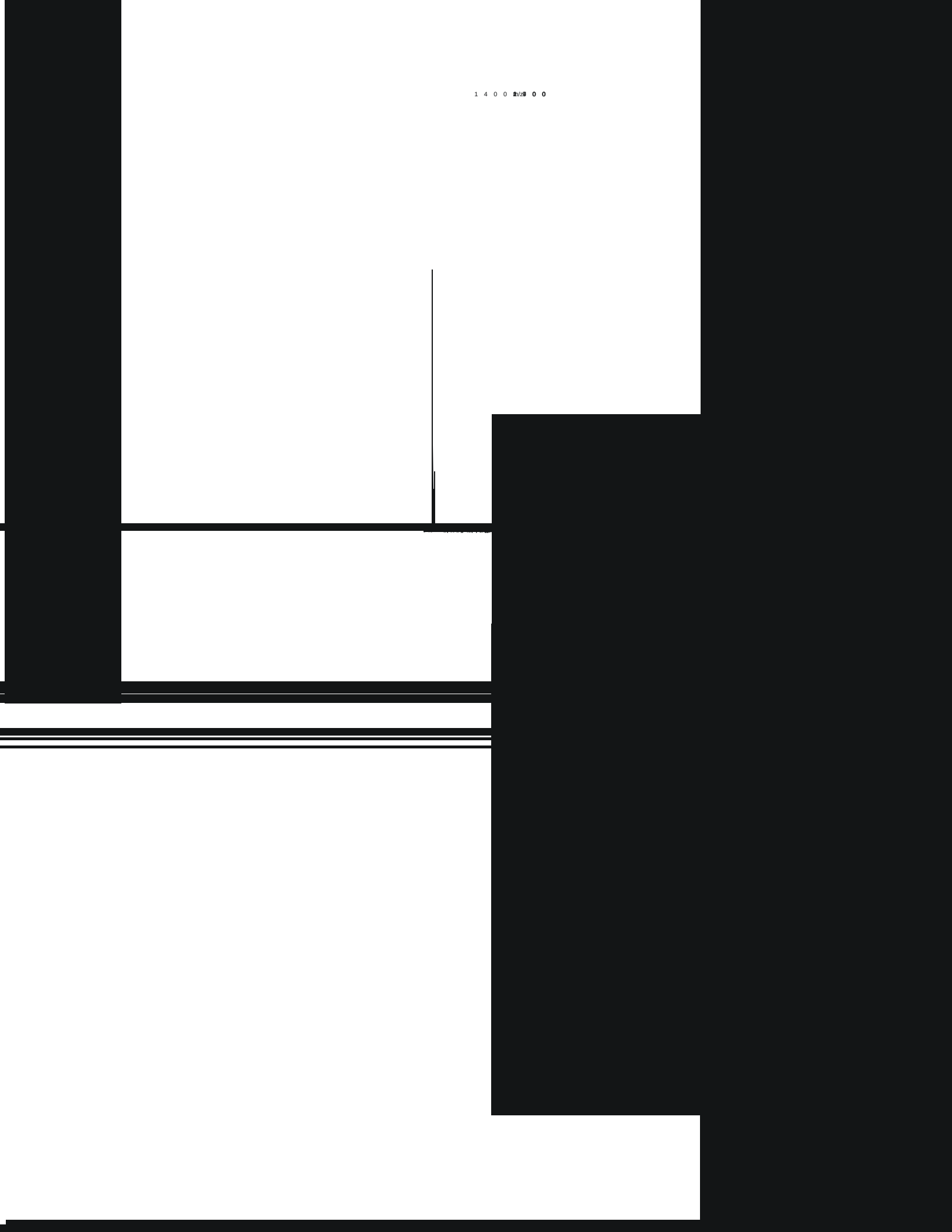
1 4 0 0 m/z

Figure 4.4 Iron-sulfur cluster structures illustrating the reduction of the [4Fe-4S] form to the [3Fe-4S] form. Ligation of the cluster through the aspartic acid residue allows the facile conversion of the [4Fe-4S] form to the [3Fe-4S] form.

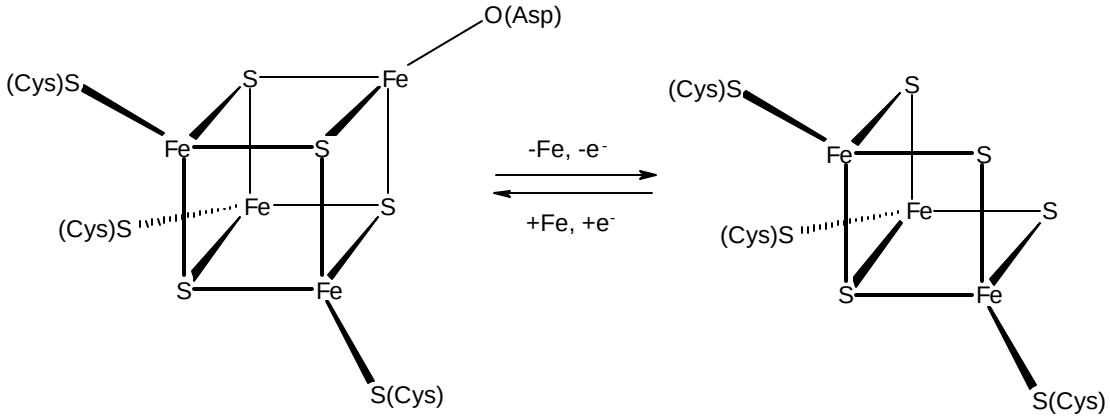
O(Asp)
(Cys)S
S
Fe
Fe
S
Fe
S
(Cys)S
S
Fe
S(Cys)
-Fe, -e-
+Fe, +e-
(Cys)S
S
Fe
S
Fe
(Cys)S
S
Fe
S(Cys)

Figure 4.5 ESI-FTICR mass spectra obtained for [3Fe-4S]-containing ferredoxin in positive ion mode (top) and negative ion mode (bottom). A stable cluster is observed only for the negative mode spectra. The insets show an expansion of the 5+ and 5- charge states. The peaks corresponding to protein with an intact cluster are labeled. Major peaks represent degradation products that consist of [3Fe-3S], [3Fe-2S], [3Fe-1S] and [3Fe] are found only in the positive ion mass spectrum. Additional peaks corresponding to sodium and oxygen adducts are present at lower intensity.

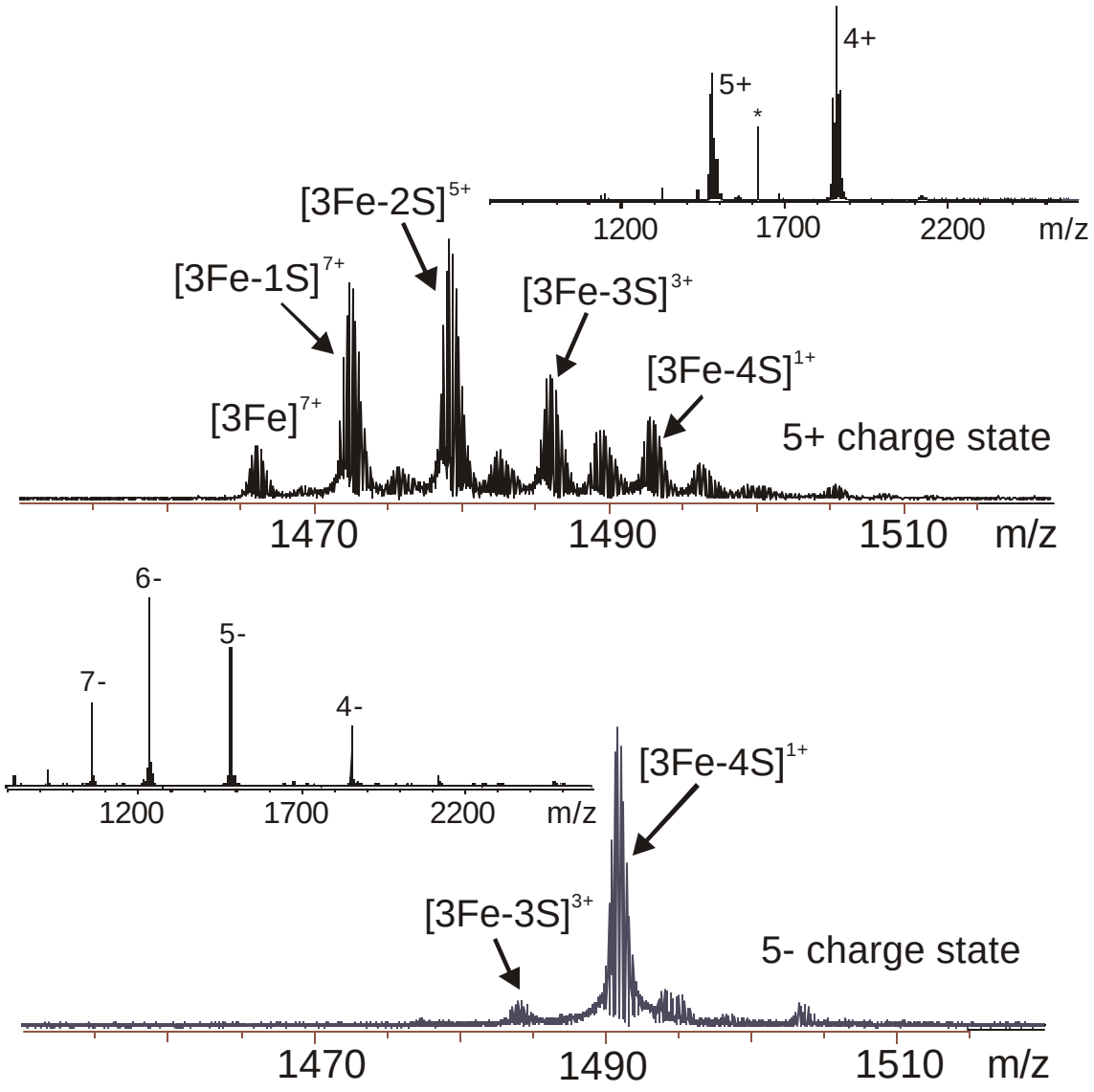
4+
5+
*
1200
1700
2200
m/z
[3Fe-2S]5+
[3Fe-1S]7+
[3Fe-3S]3+
[3Fe-4S]1+
[3Fe]7+
5+ charge state
1470
1490
1510
m/z
6-
5-
7-
4-
1200
1700
2200
m/z
[3Fe-4S]1+
[3Fe-3S]3+
5- charge state
1470
1490
1510
m/z

expansion of the 5+ and 5- charge states for these two mass spectra is also shown in Figure 5. The positive mode mass spectrum is more complex than that of the [4Fe-4S] form, with many degradation products of the intact cluster detected. These products represent losses of inorganic sulfide from the iron-sulfur cluster to yield $[3Fe\text{-}4S]^{1+}$, $[3Fe\text{-}3S]^{3+}$, $[3Fe\text{-}2S]^{5+}$, $[3Fe\text{-}1S]^{7+}$ and $[3Fe]^{7+}$. Additional peaks in this mass spectrum arise from sodium attachment and from oxygen adducts. From these data, the [3Fe-4S] cluster appears much more susceptible to degradation during electrospray ionization in the positive mode. The decrease in the stability of the [3Fe-4S] cluster may result from the lability of the inorganic sulfide in this cluster compared to the [4Fe-4S] form. As can be seen in Figure 4, the [4Fe-4S] cluster contains all trivalent sulfur, while the [3Fe-4S] cluster contains mostly divalent sulfur. Other iron-sulfur proteins with divalent sulfur exhibit similar losses, for example, the [2Fe-2S] cluster of iron hydrogenase γ-subunit [15]. Figure 5 also shows the 5- charge state for [3Fe-4S] ferredoxin that was electrosprayed as a negative ion and shows a large peak corresponding to the intact [3Fe-4S] cluster with almost no degradation products, in strong contrast to the 5+ charge state of the same protein. Although the positive mode spectrum demonstrates the formation of many product ions, the negative mode spectrum contains only one small peak corresponding to the loss of 1 sulfur atom from the cluster. It has been suggested that during negative mode ESI the protein collapses into a highly compact conformation that shelters the cluster from degradation; however, this is not supported by the increased number of lower charge states that are obtained for ubiquitin in prior research [27] or for ferredoxins in negative ion mode as compared to spectra obtained during positive ion mode. Although the mass spectrum obtained in positive ion mode provides information about degradation products and possible intermediates in the formation of iron-sulfur clusters, these data suggest that the protein degrades during ionization rather than degrading by air oxidation while in solution.

Proteins that contain mixed metal clusters provide challenging targets for analysis. The ESI-FTICR mass spectrum of a mixed metal center containing a [3FeNi-4S] cluster from *Thermococcus litoralis* is shown in Figure 6. This cluster is ligated to the protein through four cysteine sulfur-metal bonds. The appearance of the distribution of charge states for the positive

Figure 4.6 Expansion of the peaks corresponding to the 4+ and 4- charge states in the ESI-FTICR mass spectra of ferredoxin from *Thermococcus litoralis* with a nickel-substituted [3FeNi-4S] cluster. The insets show the entire mass range. Adducts of sodium and oxygen are observed at lower abundance.

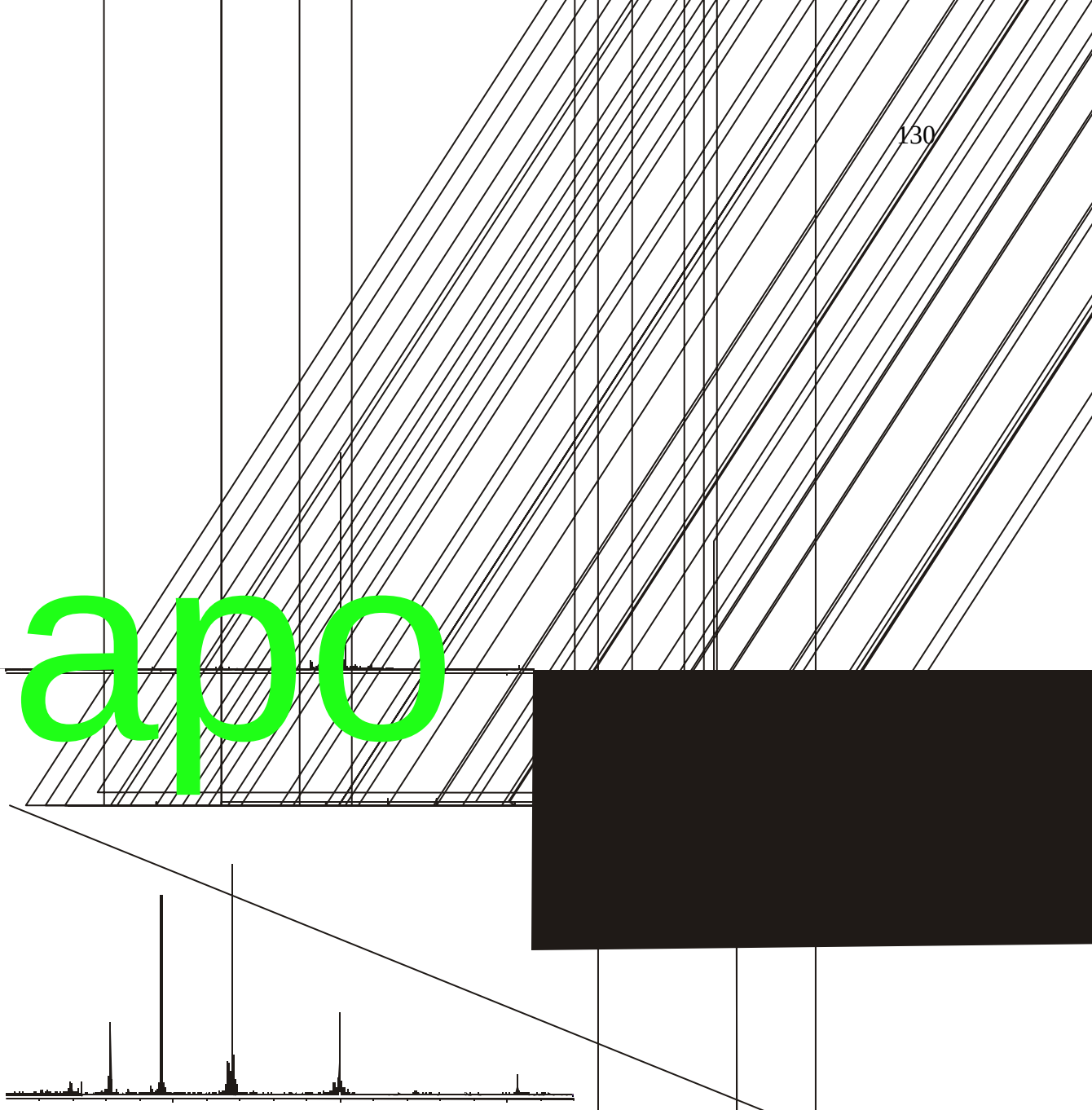

1

and negative mode spectra is similar to that observed for other metalloproteins. The negative mode mass spectrum shows a wider distribution of charge states than for the protein electrosprayed in the positive mode. The metalloprotein is less stable in the positive ion mode, evidenced by the appearance of apoprotein, however, the extent of cluster loss is not significant. The expansion of the 4+ and 4- charge states shows the intact [3FeNi-4S] cluster. The apparent mass for the protein is 6400.40 Da and the calculated mass is 6404.36 Da, which results in a derived oxidation state for the cluster as 2+ and one disulfide bond known to exist between C20 and C43 [28,29]. The observed oxidation state of 2+ corresponds to that measured previously for this metalloprotein under oxidizing conditions in its biological environment. These data for this mixed metal cluster are consistent with our hypothesis that metal-sulfur clusters that contain only trivalent sulfur are stable during ionization in both the positive and negative modes of ionization.

The mass spectrum of [3FeMn-4S] is shown in Figure 7. This mixed metal cluster has been studied by other spectroscopic methods. In prior studies, the presence of this mixed metal center was inferred from the absence of a signal in its magnetic circular dichroism (MCD) spectrum, as this cluster is MCD silent, whereas the [3Fe-4S] center from which it is derived produces a clear signal [30]. Figure 7 shows the positive and negative mode mass spectra for [3FeMn-4S] ferredoxin. Both positive and negative ion mass spectra exhibit a peak corresponding to the [3FeMn-4S]-containing protein. This is the first direct evidence of the existence of this mixed metal cluster in this protein. As is the case for the other iron-sulfur proteins, the negative ions show a wider distribution of charge state, and exhibit higher average charge than the positive ions. Also, the positive ions show greater complexity in their mass spectrum, due to the products [3Fe-nS], (n = 1 to 4). Interestingly, the negative ion mass spectrum also exhibits an intense peak for [3Fe-4S] in addition to the expected [3FeMn-4S] peak. We interpret these results as evidence that some of the protein had degraded to the [3Fe-4S] compound during sample handling. Based on our experience with iron-sulfur protein mass spectra, the data appear to result from a mixture of [3FeMn-4S] and [3Fe-4S]. The sum of the intensities of the [3Fe-nS], (n = 1 to 4) peaks in the positive mode is roughly equal to the intensity of the [3Fe-4S] peak in the negative mode mass

Figure 4.7 Expansion of the most abundant peaks in the ESI-FTICR mass spectra of ferredoxin from *P. furiosus* with a manganese-substituted [3FeMn-4S] cluster in positive mode (4+ charge state, top) and negative mode (7- charge , bottom). The insets show the entire mass range. Adducts of sodium and oxygen are observed at lower abundance.

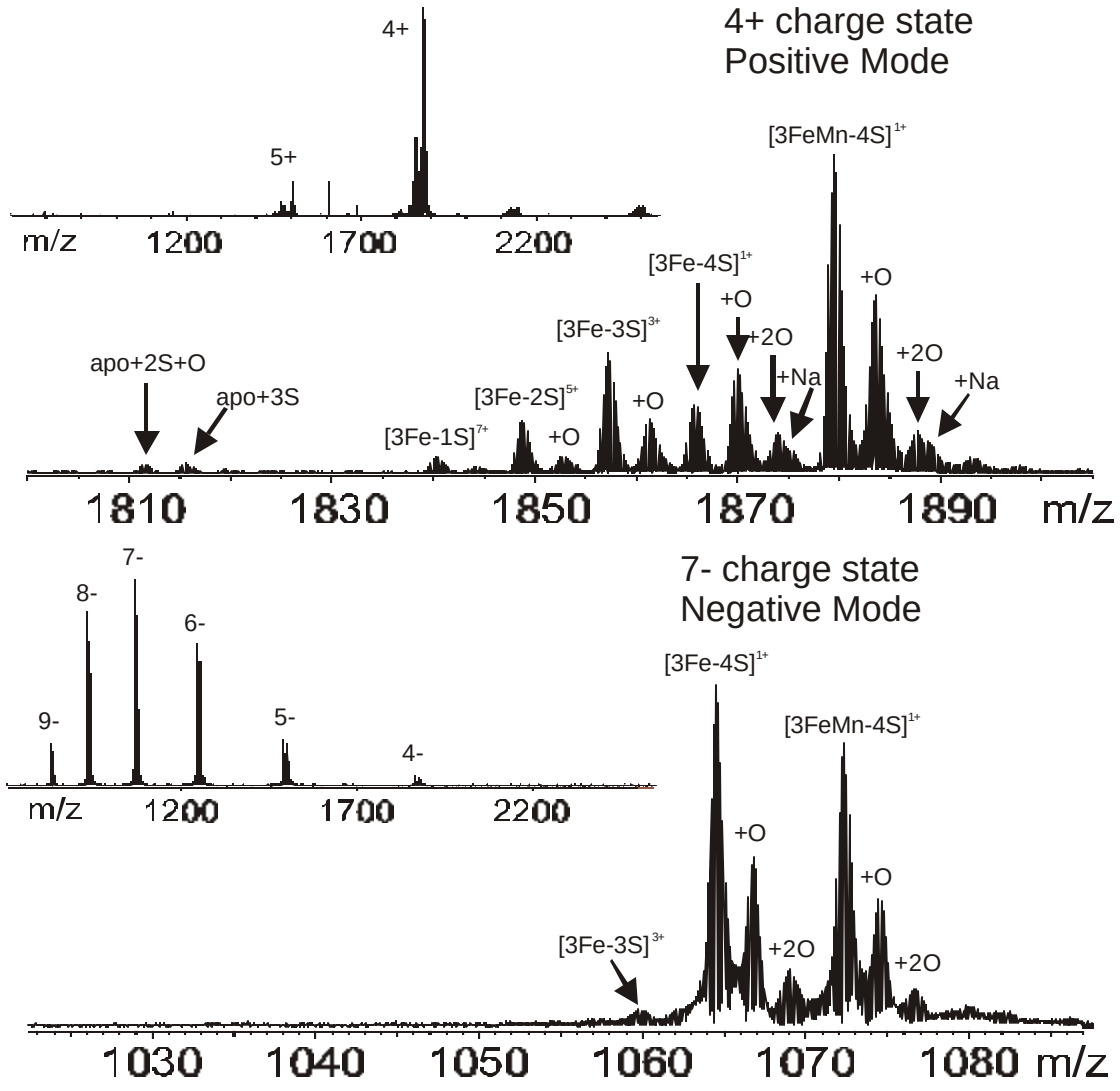
4+ charge state
Positive Mode
4+
5+
m/z
1200
1700
2200
[3FeMn-4S]1+
[3Fe-4S]1+
+O
+2O
+Na
[3Fe-3S]3+
[3Fe-2S]5+
[3Fe-1S]7+
apo+2S+O
apo+3S
1810
1830
1850
1870
1890
m/z
7- charge state
Negative Mode
7-
8-
6-
9-
5-
4-
1030
1040
1050
1060
1070
1080

spectrum. Prior condensed phase studies of the [3FeMn-4S] protein have shown that the cluster readily loses manganese to yield [3Fe-4S] under oxidizing conditions [30]. The [3Fe-4S] cluster is produced upon oxidation of the [3FeMn-4S] center, as manganese is lost from the cluster [30]. The apparent mass for the protein with the manganese cluster is 7509.89 Da and the calculated mass for the protein is 7512.88 Da. The difference of 3 Da between apparent and calculated masses is consistent with one disulfide bond in the protein (C21 and C48) and a 1+ charge on the metal cluster, which is the known oxidation state for the metal cluster in its reduced form [30]. As in the case of the [3Fe-4S] spectra shown in Figure 5, the cluster remains intact as a negative ion, but becomes unstable and degrades during positive mode ionization. Upon loss of manganese from the [3FeMn-4S] cluster as it is oxidized, the [3Fe-4S] cluster is formed and degrades further by losing sulfur. The [3Fe-4S] cluster appears in its oxidized form (1+), and the [3FeMn-4S] cluster is found to be in its reduced form (1+). Prior research has shown that the oxidized form of a metal containing species appears in its highest oxidation state when ionized by ESI [31]. After exposure to air, the oxidized [3FeMn-4S] (oxidation state of 2+) is detected, Figure 8. Both the reduced and the oxidized forms of the manganese-containing cluster are shown in Figure 8. The apparent mass for the protein with the oxidized cluster intact is 7508.86 Da and the calculated mass is 7512.88 Da. The difference is accounted for by having one disulfide bond and an oxidation state of 2+ for the cluster [30]. As the cluster becomes fully oxidized, a manganese adduct peak appears in the mass spectrum, however, the same peak does not appear in the reduced sample. The source of the extra manganese is presumably from protein that has lost this metal during degradation of the mixed metal cluster.

Conclusion

The data presented here for iron-sulfur proteins illustrates the possibilities for analysis using both positive ions and negative ions from electrospray ionization Fourier transform ion cyclotron resonance mass spectrometry (ESI-FTICR-MS). Introducing these metalloproteins to the mass spectrometer leads to considerable fragmentation of the

Figure 4.8 Positive ion ESI-FTICR mass spectra of the reduced (top) and oxidized (bottom) [3FeMn-4S] containing *P. furiosus* ferredoxin. The oxidized form of the protein contains adducts of oxygen and manganese, presumably from other protein molecules that have lost the metal from the cluster during oxidation. The assigned oxidation states are derived from the mass measurement.

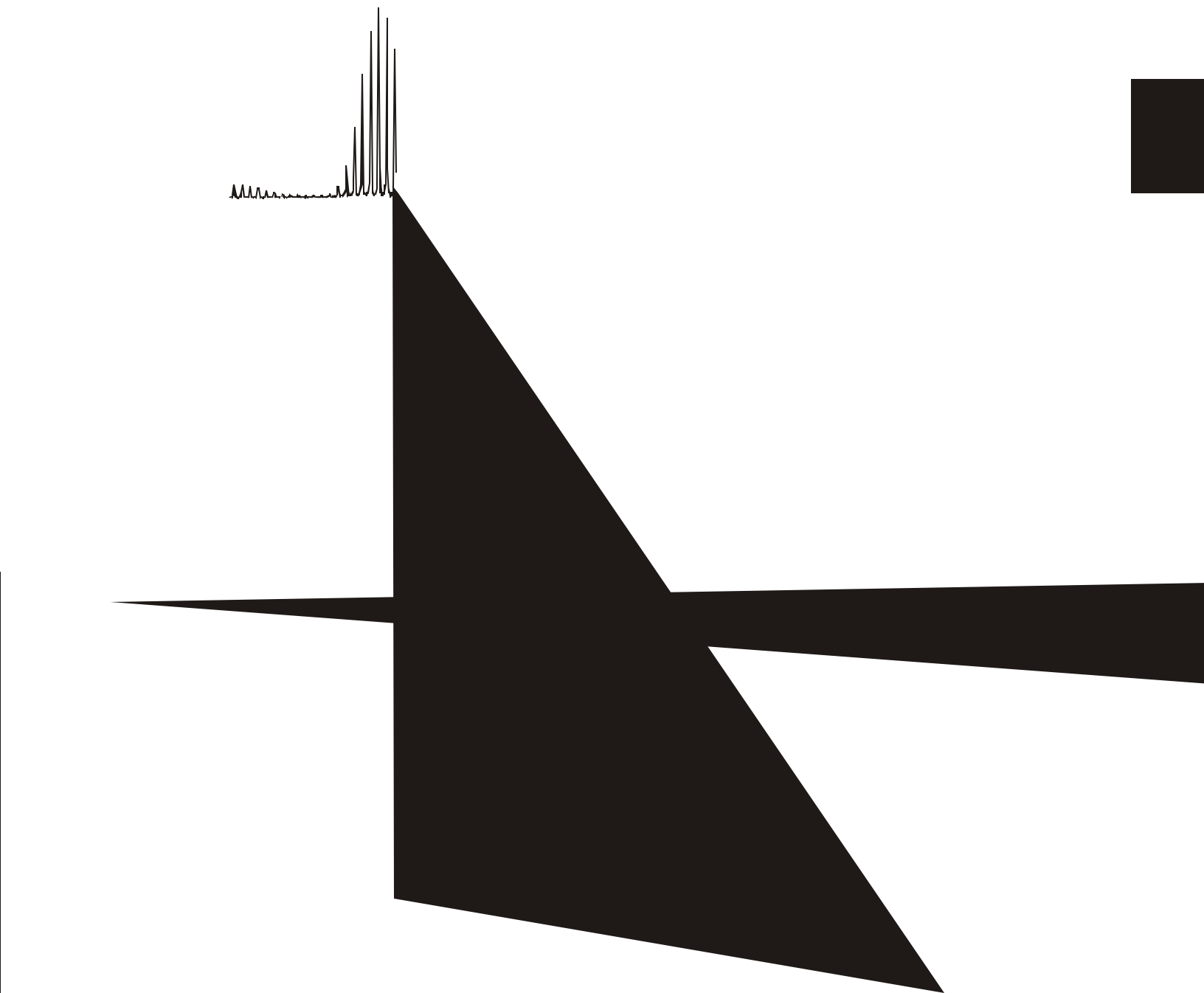

open cuboidal [3Fe-4S] cluster in positive mode, however, these proteins appear more stable when detected as negative ions. Among the metalloproteins studied in this research, generally those metals or metal clusters that are ligated to the protein through four cysteine residues appear the most stable during ESI. These include iron and zinc rubredoxin from *Clostridium pasteurianum* and the [3FeNi-4S] cluster for *Thermococcus litoralis* ferredoxin. The most stable form of wild-type ferredoxin is the [4Fe-4S] cluster, which is as stable as the rubredoxins, even though it is ligated to the protein through only three cysteine ligands and an aspartic acid residue. The [3Fe-4S] version of the same protein is much less stable than its [4Fe-4S] counterpart in positive mode, however, in negative mode, the intact cluster is detected, illustrating an increased stability as a negative ion. The [3FeNi-4S] cluster, as previously discussed, has similar stability in both positive and negative modes of ionization, which may be due to the increase in stability provided by its fourth cysteine ligand. Manganese substitution into the [3Fe-4S] cluster forming a [3FeMn-4S] cluster does increase cluster stability. Degradation of the manganese cluster to the [3Fe-4S] cluster occurs through oxidation of the protein [30] and probably exists in solution prior to ionization in either mode. The intact manganese substituted cluster is detected in both positive and negative mode ionization while the [3Fe-4S] cluster is stable only in the negative ion mode.

Acknowledgment

We gratefully acknowledge funding provided by the National Science Foundation, CHE 9974579 (IJA) and MCB 9809060 (MWA). We thank Professor John R. Eyler at the University of Florida for providing the heated metal capillary interface used in these experiments. We thank Michael Johnson of the University of Georgia for discussions and insights regarding iron-sulfur proteins, as well as for providing several of the samples used for these studies.

References

[1] T. D. Veenstra, Biophys. Chem., 79 (1999) 63.

[2] J. A. Loo, Mass Spectrom. Rev., 16 (1997) 1.

[3] S. A. Lorenz, E. P. Maziarz and T. D. Wood, Appl. Spectrosc., 53 (1999) 18A.

[4] M.A. Kelly, M.M. Vestling, C.C. Fenselau, P.B. Smith, Org. Mass Spectrom. 11 (1997) 1120.

[5] B. A. Mansoori, D. A. Volmer and R. K. Boyd, Rapid Commun. Mass Spectrom., 11 (1997) 1120.

[6] L. Konermann and D. J. Douglas, J. Am. Soc. Mass Spectrom., 9 (1997) 1248.

[7] Q. P. Lei, X. Y. Cui, D. M. Kurtz, I. J. Amster, I. V. Chernushevich and K. G. Standing, Anal. Chem., 70 (1998) 1838.

[8] H. Troxler, T. Kuster, J. A. Rhyner, P. Gehrig and C. W. Heizmann, Anal. Biochem., 268 (1999) 64.

[9] L. Konermann and D. J. Douglas, Biochemistry, 36 (1997) 12296.

[10] P.F. Hu, J.A. Loo, J. Mass Spectrom. 30 (1995) 1076.

[11] O. Henin, B. Barbier, F. Boillot, A. Brack, Chem.-Eur. J. 5 (1999) 218.

[12] O. Nemirovskiy, R. Ramanathan and M. L. Gross, J. Am. Soc. Mass Spectrom., 8 (1997) 809.

[13] Y. Petillot, E. Forest, I. Mathieu, J. Meyer and J. M. Moulis, Biochem. J., 296 (1993) 657.

[14] H. Remigy, M. Jaquinod, Y. Petillot, J. Gagnon, H. Cheng, B. Xia, J. L. Markley, J. K. Hurley, G. Tollin and E. Forest, J. Protein Chem., 16 (1997) 527.

[15] K. A. Johnson and I. J. Amster, J. Am. Soc. Mass Spectrom., 2001. Submitted.

[16] J. L. Breton, J. L. C. Duff, J. N. Butt, F. A. Armstrong, S. J. George, Y. Petillot, E. Forest, G. Schafer and A. J. Thomson, Eur. J. Biochem., 233 (1995) 937.

[17] J. Armengaud, J. Gaillard, E. Forest and Y. Jouanneau, Eur. J. Biochem., 231 (1995) 396.

[18] K. Natarajan and J. A. Cowan, J. Am. Chem. Soc., 119 (1997) 4082.

[19] Y. T. Li, Y. L. Hsieh, J. D. Henion and B. Ganem, J. Am. Soc. Mass Spectrom., 4 (1993) 631.

[20] D. Fabris, J. Zaia, Y. Hathout, C. Fenselau, J. Am. Chem. Soc. 118 (1996) 12242.

[21] F. He, C. L. Hendrickson and A. G. Marshall, J. Am. Soc. Mass Spectrom., (2000) 120.

[22] P. S. Brereton, M. F. J. M. Verhagen, Z. H. Zhou and M. Adams, W.W., Biochemistry, 37 (1998) 7351.

[23] R. C. Conover, A. T. Kowal, W. Fu, J. B. Park, S. Aono, M. W. W. Adams and M. K. Johnson, J. Biol. Chem., 265 (1990) 8533.

[24] S. Koenig, K. Haegele and H. Fales, Anal. Chem., 70 (1998) 4453.

[25] M. W. Senko, S. C. Beu and F. W. McLafferty, J. Am. Soc. Mass Spectrom., 6 (1995) 229.

[26] V. Katta and B. T. Chait, J. Am. Chem. Soc., 113 (1991) 8534.

[27] D. Douglas and L. Konerman, J. Am. Soc. Mass Spectrom., 9 (1998) 1248.

[28] P.L. Wang, A. Donaire, Z.H. Zhou, M.W.W. Adams, G.N. LaMar, Biochemistry 35 (1996) 11319.

[29] R.C. Conover, J.B. Park, M.W.W. Adams, M.K. Johnson, J. Am. Chem. Soc. 112 (1990) 4562.

[30] M. G. Finnegan, R. C. Conover, J. B. Park, Z. H. Zhou, M. W. W. Adams and M. K. Johnson, Inorg. Chem., 34 (1995) 5358.

[31] G. J. Van Berkel, G. E. Giles, J. S. Bullock, L. J. Gray, Anal. Chem. 71 (1999) 5288.

CHAPTER 5

MEASUREMENT OF METAL ATOM STOICHIOMETRY IN THE GALLIUM-SUBSTITUTED CLUSTER FROM *PYROCOCCUS FURIOSUS* FERREDOXIN[1]

[1]Keith A. Johnson, Marc F.J.M. Verhagen, Michael W.W. Adams and I. Jonathan Amster. To be included in a submission to the Journal of the American Chemical Society.

Abstract

The metal atom stoichiometry of gallium-substituted ferredoxin is assigned using electrospray ionization Fourier transform ion cyclotron resonance (FTICR) mass spectrometry. Previous analysis using other spectroscopic methods could not unambiguously assign the metal center stoichiometry. To interpret the mass spectra of the gallium-containing proteins, comparison mass spectra were obtained for the wild-type protein containing [3Fe-4S] cluster and [4Fe-4S] cluster stoichiometries. Positive and negative ionization mass spectra of the iron-sulfur clusters show substantial differences. Both positive and negative ionization produce an abundant molecular ion for the [4Fe-4S] cluster, but only negative mode ionization produces a stable molecular ion for the [3Fe-4S] cluster. Consecutive loss of sulfide from the molecular ion is observed in the positive ion mass spectrum of the [3Fe-4S] protein. The ESI-FTICR mass spectrum of the gallium-substituted ferredoxin exhibits a major peak corresponding to the [3Ga-4S] stoichiometry in the negative ion mode, while positive ionization exhibits a series of sulfur losses from a [3Ga-4S]-containing peak, analogous to those observed for [3Fe-4S] ferredoxin. By comparison to the iron-sulfur protein data, the stoichiometry of the metal center of gallium-substituted protein can be assigned as [3Ga-4S].

Introduction

Electrospray ionization (ESI) mass spectrometry is a useful method for examining metalloproteins because of its speed and accuracy, and because of the gentle ionization that produces intact molecular species [1-4]. Metalloproteins are readily denatured by exposure to heat or organic solvents, disrupting the interactions between a protein and its metal center, so careful control of the sample is required to analyze an intact molecular species. ESI can be applied to metal-containing proteins because the tightly folded, compact structure of the protein's native conformation is retained under appropriate sample conditions, permitting the retention of the metal center [1,5-9]. Recently, we have used ESI mass spectrometry to characterize iron-sulfur proteins. These are defined as proteins that contain iron with at least

partial coordination to sulfur [10]. The sulfur can be in the form of cysteinyl sulfur as in the case of rubredoxin and rubrerythrin, or the iron can be coordinated to inorganic sulfide, as in the cuboidal iron-sulfur clusters found in ferredoxin from *Pyrococcus furiosus* (*Pf*).

A variety of iron-sulfur cluster proteins and their derivatives have been studied by ESI mass spectrometry of both positive and negative ions [1,2,9,11,12]. Rubredoxin from *Clostridium pasteurianum* (*Cp*) was examined by ESI to determine the stability of the metalloprotein under neutral and acidic solvent conditions [13]. The protein was found to be the most stable as a negative ion at neutral pH. A [2Fe-2S] ferredoxin also from *Cp* was found to be more stable as a negative ion [14], presumably because of the low isoelectric point of this ferredoxin. Negative mode ionization has also been used for the detection of ferredoxin from *Rhodobacter capsulatus* [15]. The wild-type protein normally contains one [3Fe-4S] cluster and one [4Fe-4S] cluster, but the reconstituted protein was found by ESI mass spectrometry to have 2[4Fe-4S] clusters. The stability of the [2Fe-2S] cluster from *Anabaena* ferredoxin was investigated by introducing mutations around the active site of the protein before observation by ESI mass spectrometry [16]. Only apoprotein was detected using acidic conditions in positive ionization mode, but the protein containing its intact cluster was detected during negative mode ionization at pH 8. Conformational changes were also monitored by observing variations in charge state distribution after mutations at the active site of the metalloprotein were induced. The wild-type protein showed a tightly folded conformation and was observed by the small envelope of high mass-to-charge ions in the mass spectrum. More unfolded structures were seen, accompanied by a shift to higher charge states and a wider mass-to-charge envelope, although the cluster was not lost from the metalloprotein. This body of work confirms the validity and utility of mass spectrometry for characterizing the stoichiometry of metal clusters in metalloproteins.

In this paper, we report the application of ESI-FTICR mass spectrometry to the characterization of a gallium substituted ferredoxin. The substitution of iron by gallium in metalloproteins has been a useful technique for NMR studies because of the diamagnetic nature

of gallium. The coordination chemistry and the ionic radii of gallium and iron are similar, which allows the substitution to occur without dramatic changes in the geometry of the active site of the protein [17]. There is also no significant differences between the three-dimensional structures of ferredoxin with a [3Fe-4S], cluster and the same protein with a [4Fe-4S] cluster [18], and the same is expected for gallium-substituted proteins. These proteins have been examined by NMR spectroscopy, but NMR is not sensitive to the metal atom stoichiometry. The NMR data suggested that there was restricted motion of the amino acid side chains for three of the four residues that are known to bind the metal-sulfur cluster. One interpretation of the NMR data is that the metal center has [3Ga-4S] stoichiometry, but the evidence is not definitive. The work presented here demonstrates the utility of ESI-FTICR mass spectrometry for determining the stoichiometry of this novel metal cluster.

Experimental

Electrospray ionization mass spectra were acquired using a Bruker BioApex 7 Tesla FTICR mass spectrometer (Billerica, MA) equipped with an Analytica (Branford, CT) ESI source. The glass capillary was replaced with a heated metal capillary that was maintained at 100-140 °C. The metalloproteins were ionized by nanoelectrospray. Capillary tips for nanospray were produced in our lab from 100 μm inner diameter fused silica capillary (Polymicro Technologies, Phoenix, Arizona). The capillary was pulled to a fine tip by pulling with a constant force while heating with a micro-torch (Microflame, Inc., Minnetonka, Minnesota). The sample was infused to the mass spectrometer at a flow rate of approximately 8 μL/hour for each experiment. The voltage applied to the syringe needle was 1.2 kV forming a liquid electrical junction [19]. Negative ion mass spectra used the same magnitude voltages for electrospray, external injection ion optics, and trapping potentials, but the polarities were reversed. Ions were stored in the source region in a RF-only hexapole ion guide for 0.5-0.75 s, and were then transferred by a series of electrostatic lenses into the detection cell where average trapping potentials of 0.90 V and 0.95 V were used on the front and back trapping

plates of the cell during excitation and detection. The time domain signal (transient) was collected by averaging approximately 50 scans. The summed transient was apodized prior to application of the Fourier transform, followed by calibration to yield a mass spectrum.

Ferredoxin from *Pyrococcus furiosus* was produced by overexpression in *E. coli,* and the iron was replaced by gallium using the method that was published previously.(REF) Protein solutions were desalted by concentration in a microcentrifuge tube with an integral dialysis membrane (Millipore Corporation, Bedford, Massachusetts). The protein was suspended in 250 μL of 15 mM ammonium acetate solution and then centrifuged to reconcentrate and remove salts. This process was repeated using a total volume of ammonium acetate of 500 μL. The protein was then resuspended in water to yield a final protein concentration of 15 μM after concentration in the microcentrifuge tube.

Results and Discussion

Ferredoxins from *Pyrococcus furiosus* (*Pf*), *Thermococcus litoralis* (*Tl*), *Chromatium vinosum* (*Cv*M aft-l 12 Tf -0F1]lue [illegible]

Figure 5.1 The [4Fe-4S] cluster from ferredoxin from *Pf* is easily converted to the [3Fe-4S] cluster form during oxidation by ferricyanide. Both clusters have a cuboidal geometry and the clusters are ligated to the protein through three cysteine residues and in the case of the [4Fe-4S] cluster, one aspartic acid residue.

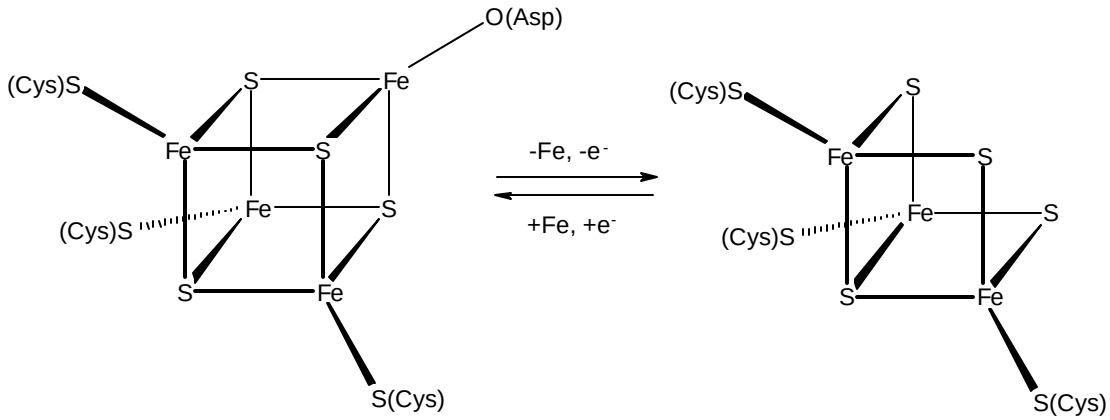
O(Asp)
(Cys)S
S
Fe
Fe
S
Fe
S
(Cys)S
S
Fe
S(Cys)
-Fe, -e-
+Fe, +e-
(Cys)S
S
Fe
S
Fe
S
(Cys)S
S
Fe
S(Cys)

acid at residue 14 replaced by a cysteine residue is substituted in the gallium ferredoxin to improve its stability. This mutant can bind either a [3M-4S] cluster or a [4M-4S] cluster.

The ESI mass spectra for wild-type *Pf* ferredoxin containing intact [3Fe-4S] and [4Fe-4S] clusters are shown in Figure 2, and are compared with the gallium-substituted cluster in both positive and negative ionization modes. Charge state expansions from each mass spectrum are shown in Figure 3. For all of the proteins, the positive mode ESI mass spectra are characterized by one or two charge states, while the negative ion mass spectra exhibit 5-6 charge states. These data are consistent with other work which has shown that the negative ion mode exhibits a wider distribution of charge states, even for nondenatured proteins [21]. From the mass spectrum of the [3Fe-4S] protein cluster obtained in positive mode, (Figure 2d), a monoisotopic mass of 7455.92 Da was derived, which compares favorably to the calculated mass of 7455.93 Da for $[\text{apoprotein} + 3\text{Fe} + 4\text{S} + 3\text{H}]^{4+}$. From Figure 2f, a monoisotopic mass of 7511.84 Da was derived for the [4Fe-4S] containing protein compared to the calculated mass of 7511.87 Da for $[\text{apoprotein} + 4\text{Fe} + 4\text{S} + 2\text{H}]^{4+}$ (disulfide bond between residues C21 and C48). The mass for the major peak in the gallium-substituted spectrum, Figure 2e, is 7447.94 Da and corresponds to $[\text{apoprotein} + 3\text{Ga} + 3\text{S} + 1\text{H}]^{4+}$. The calculated mass for protein containing a [3Ga-3S] cluster with the remote disulfide bond intact is 7452.92 Da. The oxidation state of the [3Ga-3S] center is 3+.

It has been suggested that differences in the charge state distributions of positive and negative ions results from variations in structural sensitivity. For example, ESI in the positive ion mode is an effective way to monitor protein conformational changes based on the accessibility of basic amino acid residues to ionization. The charge state distributions of negative ions are insensitive to the denatured versus nondenatured state of the protein. It has also been suggested that negative mode ionization induces the collapse of the protein into a highly compact conformation [22], which could explain the retention of the intact [3Fe-4S] cluster in negative ion mode, but this does not explain the wider distribution of charge states at lower mass-to-charge in the mass spectrum compared to the positive ions.

Figure 5.2 ESI-FTICR mass spectra comparing the positive and negative mode mass spectra for (a,d) [3Fe-4S]-containing ferredoxin from *Pf*; (b,e) a gallium-substituted cluster from *Pf*; (c,f) [4Fe-4S]-containing ferredoxin from *Pf*. A shift to lower mass-to-charge in each mass spectrum is seen when negative ions are generated. The charge states for both positive and negative ions in the mass spectra are labeled, and the * denotes noise peaks in the spectra.

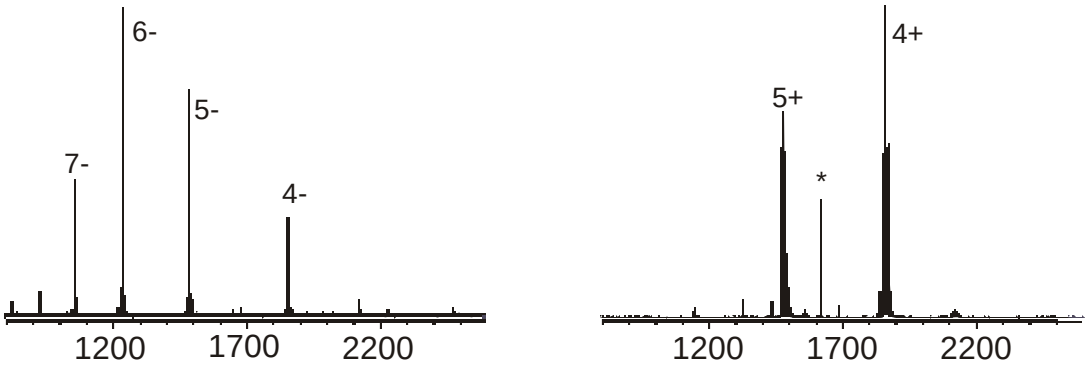
6-
5-
7-
4-
1200
1700
2200
4+
5+
*
1200
1700
2200

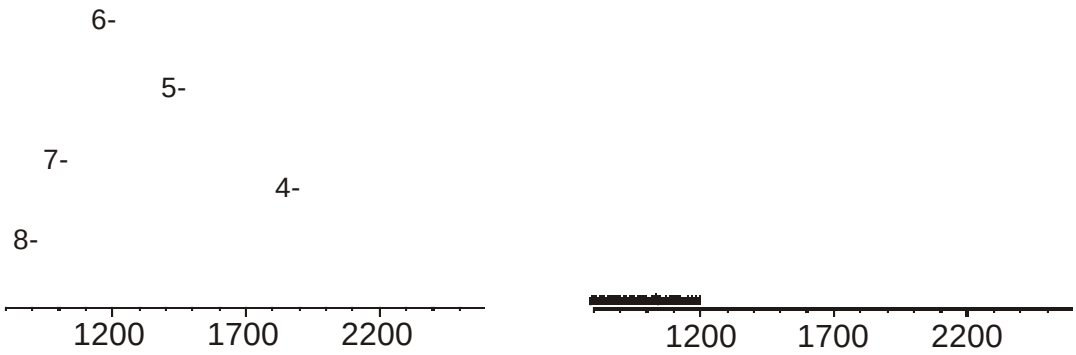
6-
5-
7-
4-
8-
1200
1700
2200
1200
1700
2200

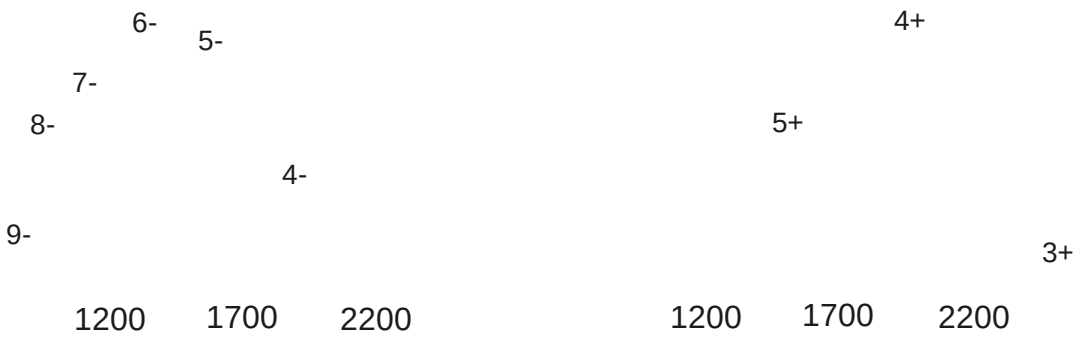
6-
5-
7-
8-
4-
9-
1200
1700
2200
4+
5+
3+
1200
1700
2200

Figure 5.3 ESI-FTICR mass spectra of an expanded charge state for each of the ferredoxin proteins obtained in positive and negative mode ESI. (a,d) [3Fe-4S]-containing ferredoxin from the 5- and 5+ charge states. For the negative ion mass spectrum, the [3Fe-4S] cluster appears as a stable ion, but as a positive ion, many degradation products are observed. Adducts of oxygen and sodium are also present in the mass spectra. (b) Gallium-substituted ferredoxin in the negative ion mode (4- charge state) showing a stable [3Ga-4S] peak with some degradation to the [3Ga-3S] form of the cluster. (e) The positive mode mass spectrum for gallium ferredoxin (4+ charge state) shows a stable [3Ga-3S] for of the cluster and degradation to a [3Ga-2S] form. Adducts of sodium and oxygen are also observed. (c,f) [4Fe-4S] ferredoxin protein showing stable, intact clusters with no degradation products for either mode of ionization (4- and 4+ charge state).

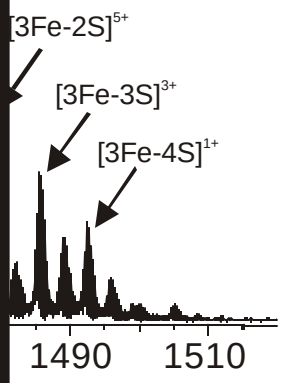
[3Fe-2S]5+
[3Fe-3S]3+
[3Fe-4S]1+
1490
1510

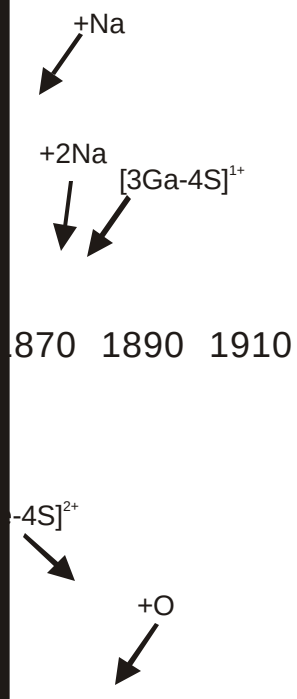
+Na
+2Na
[3Ga-4S]1+
870
1890
1910
-4S]2+
+O

The mass spectra of the [4Fe-4S] cluster protein, Figures 3c and 3f, exhibit stable molecular ions in both positive and negative mode ESI. The mass spectra contain peaks corresponding to the intact cluster with no degradation products. In contrast, the [3Fe-4S]-containing protein shows several degradation peaks in its positive ion mass spectrum. These peaks correspond to loss of sulfur (Figure 3d). Prior work has established that the sulfur loss is from the metal cluster [1]. These peaks correspond to [3Fe-nS], n=0-4. The negative mode ESI mass spectrum of the [3Fe-4S] ferredoxin shows a stable molecular ion and a smaller peak due to loss of one sulfur (Figure 3a). A comparison of the [3Fe-4S] cluster protein and the gallium-substituted form of the protein in negative ion mode illustrates that the [3Ga-4S] form of the ferredoxin produces a similar pattern of degradation. In the positive ion mass spectrum, Figure 3e, a fragmentation pattern showing [3Ga-3S] and [3Ga-2S] products is observed, indicative of [3Ga-4S] cluster degradation. In the negative ionization mode, Figure 3b, principally the [3Ga-4S] cluster is observed, but a small peak due to [3Ga-3S] is also found in both the iron and the gallium mass spectra.

By comparison, the mass spectrum of the gallium-substituted protein resembles that of the [3Fe-4S] ferredoxin rather than its [4Fe-4S] counterpart. In the gallium-substituted cluster, Figures 3b and 3e, some degradation is observed for both positive and negative ions; however, the protein appears more stable as a negative ion than as a positive ion. The major peak in the positive ion mss spectrum corresponds to a [3Ga-3S] cluster. The major ion in the negative mode mass spectrum corresponds to a [3Ga-4S] cluster. By comparison to the wild-type [3Fe-4S] protein, the gallium center is expected to be more stable as a negative ion than as a positive ion. The pattern of degradation for the gallium cluster is similar to the [3Fe-4S] cluster in both modes of ionization. Thus, the mass spectral data is consistent with a stoichiometry of the metal center of [3Ga-4S] rather than [4Ga-4S].

Conclusion

Electrospray ionization Fourier transform ion cyclotron resonance mass spectrometry was used to identify the stoichiometry of a gallium-substituted ferredoxin cluster in both positive mode and negative mode ionization. The results illustrate the significant variations in degradation that can occur during the formation of positive and negative ions during ESI. Although the [4Fe-4S] cluster ferredoxin from *Pf* is stable in both modes of ionization, a major difference in ion stability is observed for the [3Fe-4S] cluster form of the metalloprotein. The removal of the single iron atom from the cuboidal cluster is enough to decrease the cluster stability between the two modes of ionization. The mass spectra of the gallium-substituted protein greatly resemble those of [3Fe-4S] ferredoxin, both in positive and negative ionization modes.

Acknowledgment

We gratefully acknowledge funding provided by the National Science Foundation, CHE 9412334 and 9984579 (IJA) and MCB 9809060 (MWA). We thank Professor John R. Eyler at the University of Florida for providing the heated metal capillary interface used in these experiments. We thank Michael Johnson from the University of Georgia for discussions and insights regarding iron-sulfur proteins, as well as for providing several of the samples used for these studies.

References

1. Johnson, K. A.; Verhagen, M.; Adams, M. W. W.; Amster, I. J. *Anal. Chem.* **2000**, *72*, 1410-1418.
2. Johnson, K. A.; Verhagen, M.; Adams, M. W. W.; Amster, I. J. *Int. J. Mass Spectrom.* **2000**, *in press*.
3. Troxler, H.; Kuster, T.; Rhyner, J. A.; Gehrig, P.; Heizmann, C. W. *Anal. Biochem.*. **1999**, *268*, 64-71.

4. Bruce, J. E.; Smith, V. F.; Liu, C. L.; Randall, L. L.; Smith, R. D. *Protein Sci.* **1998**, *7*, 1180-1185.

5. Hay, M. T.; Milberg, R. M.; Lu, Y. *J. Am. Chem. Soc.* **1996**, *118*, 11976-11977.

6. Katta, V.; Chait, B. T. *J. Am. Chem. Soc.* **1991**, *113*, 8534-8535.

7. Loo, J. A. *Mass Spectrom. Rev.* **1997**, *16*, 1-23.

8. Veenstra, T. D. *Biophys. Chem.* **1999**, *79*, 63-79.

9. Lei, Q. P.; Cui, X. Y.; Kurtz, D. M.; Amster, I. J.; Chernushevich, I. V.; Standing, K. G. *Anal. Chem.* **1998**, *70*, 1838-1846.

10. Johnson, M. K. Iron-Sulfur Clusters. In *Encyclopedia of Inorganic Chemistry*. King, R. B. Ed; John Wiley and Sons: New York. **1994,** Vol 4, pp 1896-1913.

11. Forest, E. *J. Protein Chem.* **1997**, *16*, 527-532.

12. Breton, J. L.; Duff, J. L. C.; Butt, J. N.; Armstrong, F. A.; George, S. J.; Petillot, Y.; Forest, E.; Schafer, G.; Thomson, A. J. *Eur. J. Biochem.* **1995**, *233*, 937-946.

13. Petillot, Y.; Forest, E.; Mathieu, I.; Meyer, J.; Moulis, J. M. *Biochem. J.* **1993**, *296*, 657-661.

14. Petillot, Y.; Golinelli, M. P.; Forest, E.; Meyer, J. *Biochem. Biophys. Res. Commun.* **1995**, *210*, 686-694.

15. Armengaud, J.; Gaillard, J.; Forest, E.; Jouanneau, Y. *Eur. J. Biochem.* **1995**, *231*, 396-404.

16. Remigy, H.; Jaquinod, M.; Petillot, Y.; Gagnon, J.; Cheng, H.; Xia, B.; Markley, J. L.; Hurley, J. K.; Tollin, G.; Forest, E. *J. Protein Chem.* **1997**, *16*, 527-532.

17. Vo, E.; Wang, H. C.; Germanas, J. P. *J. Am. Chem. Soc.* **1997**, *119*, 1934-1940.

18. Conover, R. C.; Kowal, A. T.; Fu, W.; Park, J. B.; Aono, S.; Adams, M. W. W.; Johnson, M. K. *J. Biol. Chem.* **1990**, *265*, 8533-8541.

19. Koenig, S.; Haegele, K.; Fales, H. *Anal. Chem.* **1998**, *70*, 4453-4455.

20. He, F.; Hendrickson, C. L.; Marshall, A. G. *J. Am. Soc. Mass Spectrom.* **2000**, 120-126.

21. Douglas, D.; Konerman, L. *J. Am. Soc. Mass Spectrom.* **1998**, *9*, 1248-1254.

22. Konermann, L.; Douglas, D. J. *J. Am. Soc. Mass Spectrom.* **1997**, *9*, 1248-1254.

CHAPTER 6

CHEMICAL AND ON-LINE ELECTROCHEMICAL REDUCTION OF METALLOPROTEINS WITH HIGH RESOLUTION ELECTROSPRAY IONIZATION MASS SPECTROMETRY DETECTION[1]

[1]Keith A. Johnson, Brian A. Shira, James L. Anderson and I. Jonathan Amster. Anal. Chem. 2001. Accepted for publication.

Abstract

The observation of the reduced forms of several metal containing proteins using electrospray ionization (ESI) is reported for the first time. High resolution mass analysis using Fourier transform ion cyclotron resonance mass spectrometry allows the oxidized and reduced forms of the proteins to be distinguished. The metalloproteins are reduced both chemically and electrochemically. Under normal sample handling conditions, the proteins that are reduced in solution appear in their oxidized form in their ESI mass spectra. Rigorous exclusion of oxygen from the solution of the reduced protein allows the observation of the reduced form in the gas phase. The metal centers investigated include heme and non-heme iron proteins, copper, and a manganese-substituted iron-sulfur cluster of the form [3FeMn-4S]. The electrochemical method is shown to provide several advantages over chemical reduction. The oxidation state of the metal center is stable with respect to electrospray ionization in both positive and negative ionization modes.

Introduction

Mass spectrometry has been demonstrated to be a useful method for the analysis of metalloproteins.[1-6] Combined with electrospray ionization, many details of structure can be obtained including molecular weight, metal identity, and metal atom stoichiometry. Mass spectrometry has been used to examine structure and function relationships between proteins and metalloproteins and, with the implementation of electrospray ionization (ESI), has been used to compare solution- and gas-phase conformations of biological molecules.[7-10] ESI provides the means to study proteins and metalloproteins in their native conformation without loss of tertiary or quaternary structure, so there is no loss of weakly bound constituents under nondenaturing ESI. The retention of a protein's native conformation in the solution phase requires the use of nondenaturing solvents and experimental conditions.

The first mass spectrometric observations of the oxidized forms of heme from myoglobin and cytochrome *c* were conducted using ESI.[11] In those experiments, collision

induced dissociation (CID) was used to determine the oxidation state of the heme group that was ejected from the molecule. Several other groups have also investigated the oxidation state of the heme group in cytochrome *c* in its oxidized form using high resolution mass spectrometry.[2, 12, 13] In all of these studies, the iron was always observed in its highest oxidation state, Fe^{3+}. Metalloproteins other than those that contain heme have also been investigated by mass spectrometry and the oxidation states of their metal centers have been determined.[2] Several iron-sulfur cluster-containing proteins have been investigated using both positive and negative ion mode mass spectrometry and were found to exist in their highest possible oxidation state under biological conditions.[4] In fact, only the highest biologically relevant oxidation state has been observed in the ESI mass spectra of any metalloprotein to date. This observation raises the question of whether the ESI process itself causes the metal center to be oxidized or whether the observed oxidation state reflects the redox state present in solution.

Redox reactions at the ESI interface have been studied in detail by Van Berkel and co-workers.[14, 15] The behavior of small redox active compounds was examined, and it was shown that oxidation does occur during positive mode ESI. The electrospray current that is generated is maintained by the oxidation or reduction of species in solution, such as water electrolysis and analyte redox reactions, and is dependent on the magnitude of the ESI voltage. The solution flow rate, redox potential, and the concentration of the analyte are also factors that influence the redox reactions that occur during electrospray ionization. Bond et al. have investigated cytochrome *c* by both ESI-quadrupole mass spectrometry and cyclic voltammetry.[16] They considered the effect of pH, electrolyte composition, and solvent on protein charge and reduction potential. They noted changes in apparent molecular weight due to adducts with a variety of metal ions from solution and concluded that conditions for electrospray and cyclic voltammetry were mutually incompatible. They did not consider the effect of protein oxidation state on the mass spectrum. Spray voltage has only a small impact on the oxidation or reduction of species in solution even though 96-97% of the total electrospray voltage is dropped across the liquid-phase - gas-phase gap.[14, 15] Ferrocene was studied by ESI to

determine the extent of oxidation that occurs during the ionization process. Oxidation of the ferrocene and the electrolysis of H_2O were found to be the dominant redox processes.[15] Oxidation of polyaniline[14] and oxidation of methionine residues in polypeptide chains has been found to occur during ESI. Cole and co-workers have also shown that ESI has an inherent tendency to induce oxidation, although nitrobenzene reduction was detected along with reduction intermediates in both positive and negative mode electrospray ionization.[17, 18] It is thus possible that metalloproteins always appear in their most oxidized state because of the oxidative nature of the electrospray process. The work reported here addresses whether oxidation of proteins occurs during ESI and to what extent the ESI data reflects the oxidation state of the metal center of the protein in solution prior to analysis.

Experimental

The mass spectra were obtained using a Bruker BioApex FTICR mass spectrometer (Billerica, MA) with a 7-T magnet. The Analytica ESI source (Branford, CT) used with this instrument was modified by replacing the glass capillary interface with a heated metal capillary, which was maintained at 150 °C for all of the experiments except for superoxide reductase. Since this protein exists as a tetramer in solution, the capillary heat was increased to 250 °C to stimulate mild denaturation to yield the monomer. The samples were ionized by nanoelectrospray ionization with a maximum flow rate of 100 nL/min. The nanoelectrospray tips were fabricated in our laboratory using 100 μm inner diameter fused silica capillary tubing (Polymicro Technologies, Phoenix, AZ). The tips were pulled by heating with a hand held microtorch (Microflame, Inc., Minnetonka, MN) while applying a constant force of 0.112 N. Spray voltages ranged between 600 V and 1200 V (-600 V and -1200 V for negative ion mode) for the experiments. In this range, the spray voltage did not affect the oxidation state of the metalloproteins. The voltage was applied to the syringe needle that delivered the sample to the spray emitter, forming a liquid electrical junction.[19] The experimental parameters used to trap and store the ions are the same as described previously.[4] The monoisotopic mass was

assigned using the χ^2 statistical method, as described by McLafferty.[20] The oxidation state of the metal center was determined from the data as described previously.[4]

Proteins were produced by overexpression in *Escherichia coli*. Their production and purification have been described previously.[4, 21] Cytochrome *c* was purchased from Sigma. Protein samples were introduced at a concentration of 20 mM in water after removal of reducing agent (see below) for chemical reduction. For electrochemical reduction (see below), cytochrome *c* (20 mM) was reduced in 5 mM ammonium acetate. After the proteins are reduced, it is essential to exclude oxygen during all subsequent sample handling procedures in order to observe the reduced forms of the proteins in their mass spectra. Storage and trapping potentials and a description of the data analysis using the chi-squared test[21] have also been described previously.[4] Exclusion of oxygen during sample handling after reducing the protein samples was imperative in obtaining mass spectra for the reduced samples. Solutions of reduced metalloprotein that were not protected from ambient air and those not electrosprayed immediately after sample preparation reverted to their oxidized state during electrospray. Only those samples from which oxygen was rigorously excluded and electrosprayed promptly after reduction could be detected in their reduced form.

Chemical Reduction: Metalloprotein solutions (20 mM) were prepared for ESI by suspending them in water prior to reduction. Sodium dithionite was used to chemically reduce all of the protein samples except for superoxide reductase. Ascorbic acid was used to reduce this protein without loss of the iron center. The samples were placed in a glove bag with a microcentrifuge and degassed under a nitrogen atmosphere before reducing the proteins. The reducing agent was added to the metalloproteins in a ten fold excess and the color change was monitored for all of the samples except for the manganese-substituted protein, which is brown in both the oxidized and reduced forms. The presence of sodium dithionite in the spray solution created a broad distribution of multiply sodiated protein ions with overlapping isotope distributions. This greatly diminished the signal intensity and made the data uninterpretable. For

this reason, the reducing agent was removed prior to analysis by ultrafiltration using a microcentrifuge tube with a 5 kDa cutoff integral membrane filter (Millipore Corporation, Bedford, MA), using approximately 500 μL of degassed, 20 mM ammonium acetate solution. The protein was then resuspended in water, resulting in a final concentration of 20 μM. Typically, the chemical reduction step including resuspension of the protein in water lasted 2.5 to 3 h. The reduced protein (monitored visually) was transferred to a gastight syringe and introduced to the mass spectrometer via nanoelectrospray ionization.

Electrochemical Reduction: The electrochemical cell was fabricated in our laboratory using two 1 mL plastic syringes connected via a T-valve, shown schematically in Figure 1. The third leg of the T-valve was connected to the electrospray emitter tip so that the contents of either syringe could be selected for analysis. When the valve was set in the "off" position, the solution in the two syringes made electrical contact. The electrodes for the cathode and the anode were platinum wire that was forced through the plunger end of each syringe. This maintained a separation of the "reduction" end of the cell and the "oxidation" end of the cell and prevented mixing of oxidized and reduced protein. A micro stir bar was placed in the reduction end of the cell to aid in mass transfer to the electrode in that region, and to prevent protein precipitation. Cytochrome *c* was prepared in a solution of 2 mM ammonium acetate at a concentration of 20 μM. About 0.5 mL of the brown (oxidized) solution was transferred to the electrochemical cell. The resistance of the cell was measured at approximately 0.5 MΩ, between the reducing and oxidizing electrodes. Current was maintained at 30 μA for the reduction of cytochrome *c*. This corresponded to a voltage of 13.3 V across the cell, although most of this was dissipated as *iR* drop between the electrodes. After approximately 30 minutes, the solution in the reduction end of the capillary changed from brown to pink, indicating that the protein was reduced. The T-valve was then switched so that the oxidation end of the cell was closed. The reducing cell was placed on a syringe pump and its solution was delivered to the detectors.

Figure 6.1 Electrochemical cell used to reduce metalloproteins showing the oxidizing and reducing ends of the cell connected by a T-valve. Platinum electrodes were inserted through the plunger end of the syringes, as shown in the figure.

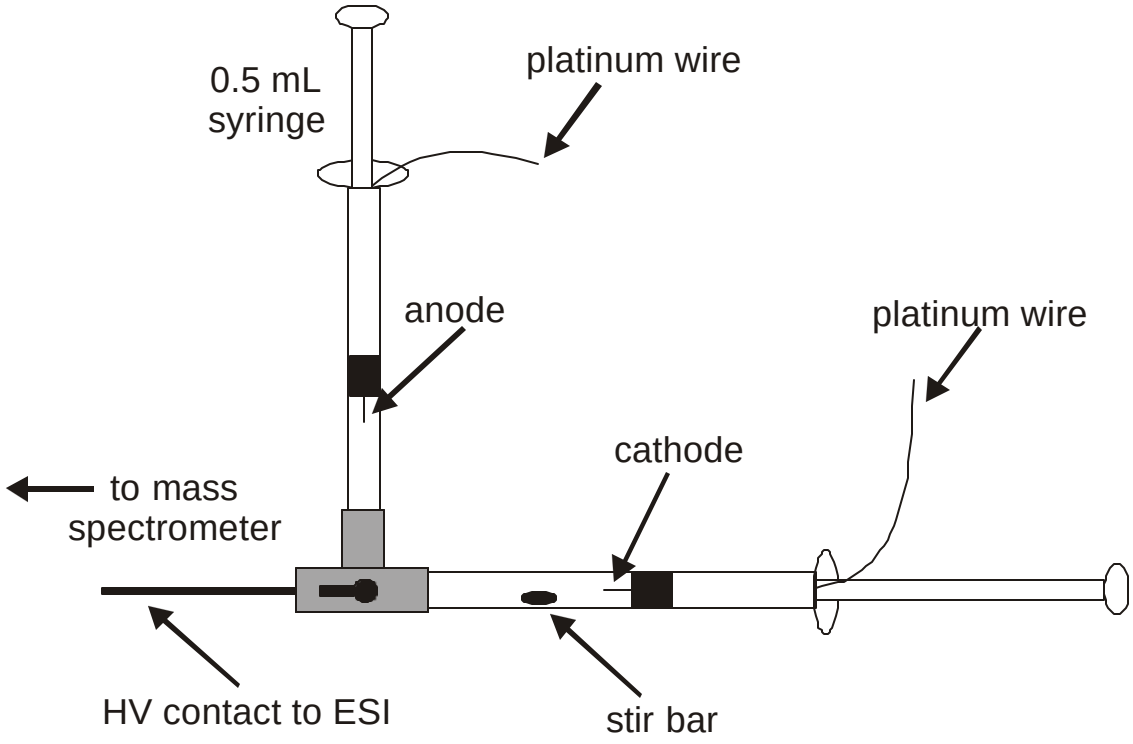
0.5 mL
syringe
platinum wire
anode
platinum wire
cathode
to mass
spectrometer
HV contact to ESI
stir bar

The voltage for electrospray was applied to the syringe needle, which forms a liquid electrical junction with the nanoelectrospray tip.

Results and Discussion

ESI-Fourier transform ion cyclotron resonance mass spectrometry is a valuable tool for identifying the small changes in mass associated with a metalloprotein's oxidation state or in counting disulfide bonds within a protein.[2, 4, 22, 23] The isotopically-resolved mass spectra provide the resolution sufficient to separate $^{13}C/^{12}C$ isotopes. The isotopes spacing allows for the calculation of charge state (i.e. the number of extra charges on an otherwise neutral protein), since the mass separation between the isotope peaks must be the mass difference between ^{13}C and ^{12}C, 1.0034 Da.[24] From the charge state information, the monoisotopic molecular weight of the protein can be assigned.[4] Monoisotopic molecular weight is defined as the sum of the lowest molecular weight isotopes in the molecular formula, and for typical proteins, this corresponds to ^{12}C, ^{1}H, ^{14}N, ^{16}O and ^{32}S. For the purpose of discussion, we define the monoisotopic mass of a metalloprotein as the sum of all of the lowest molecular weight isotopes in the molecular formula of the protein in addition to the most abundant isotope of the metal or metals that make up the metalloprotein. For example, we use ^{56}Fe instead of ^{54}Fe since their natural abundances are 91.8% and 5.82%, respectively, and the isotope peak corresponding to ^{54}Fe is not usually observable.

The molecular weight for a protein is normally calculated assuming that all of the ionizable sites in the amino acid sequence for the protein are neutral. However, the metals in metalloproteins exist in oxidation states other than zero, which makes this rule impractical. Using this rule for metalloproteins will result in molecular weights that vary according to the oxidation state of the metal center because metalloproteins of differing oxidation states will have different numbers of protons to achieve charge neutrality. For the purpose of discussion, we define the "apparent mass" as the mass that is derived from the data making the assumption that all of the charge of an ion is due to excess (or a deficit of, for negative ions) protons. The

apparent mass will differ from the actual mass by the number of protons equal to the charge present on the metal center. Thus, a comparison of apparent and calculated masses allows the oxidation state in the metalloprotein to be derived from the difference between the two values. A more complete description of this procedure has been recently published.[4]

An expansion of the 8+ charge state of cytochrome *c* obtained during positive ion mode ESI is shown in Figure 2. The top spectrum was obtained for the metalloprotein with the metal in the oxidized form of Fe^{3+}. The isotope distribution for the 8+ charge state is shown. From the apparent mass that is determined from the data, it is observed that five protons make up the 8+ charge state. The remaining charge is present on the metal center, allowing the oxidation state to be identified as Fe(III). The bottom spectrum shows chemically reduced cytochrome *c* obtained under the same ESI conditions. The spectrum is shifted to higher mass-to-charge for the reduced sample, indicating an increase in molecular weight due to the addition of one proton relative to the oxidized protein. Comparison with the theoretical distribution indicates that six protons are added to the metalloprotein to form the 8+ charge state. The reduced form of the metal, Fe^{2+}, is thus determined from the data. The reduced spectrum of cytochrome *c* was acquired only after performing reduction and the cleanup procedure under a nitrogen atmosphere. The sample was protected from reoxidation by exclusion from oxygen in a gastight syringe prior to and during electrospray ionization. Oxidized cytochrome *c* was determined from the mass spectra for "reduced" samples that were not electrosprayed immediately after reduction and cleanup. Cytochrome *c* was also electrosprayed in negative ion mode to confirm that neither reduction nor oxidation occurs during negative mode ionization. The mass spectra for the oxidized and chemically reduced metalloprotein are shown Figure 3. The expansion of the isotope distribution for the 6- charge state is shown for both oxidized (top) and reduced (bottom) protein. For the oxidized protein we measure $[M + Fe^{3+} - 9H^{+}]^{6-}$, and for the reduced protein $[M + Fe^{2+} - 8H^{+}]^{6-}$ causing an observable shift in mass-to-charge ratio. Thus, we see that the oxidation state of the protein in solution does not change during either positive mode or negative mode electrospray ionization.

Figure 6. 2 Positive ion mode ESI-FTICR mass spectra of the 8+ charge state for both oxidized (top) and chemically reduced (bottom) cytochrome *c* are shown. The centroid of each isotope distribution is marked with "●" to highlight the shift in mass corresponding to the change in the oxidation state of the metalloprotein.

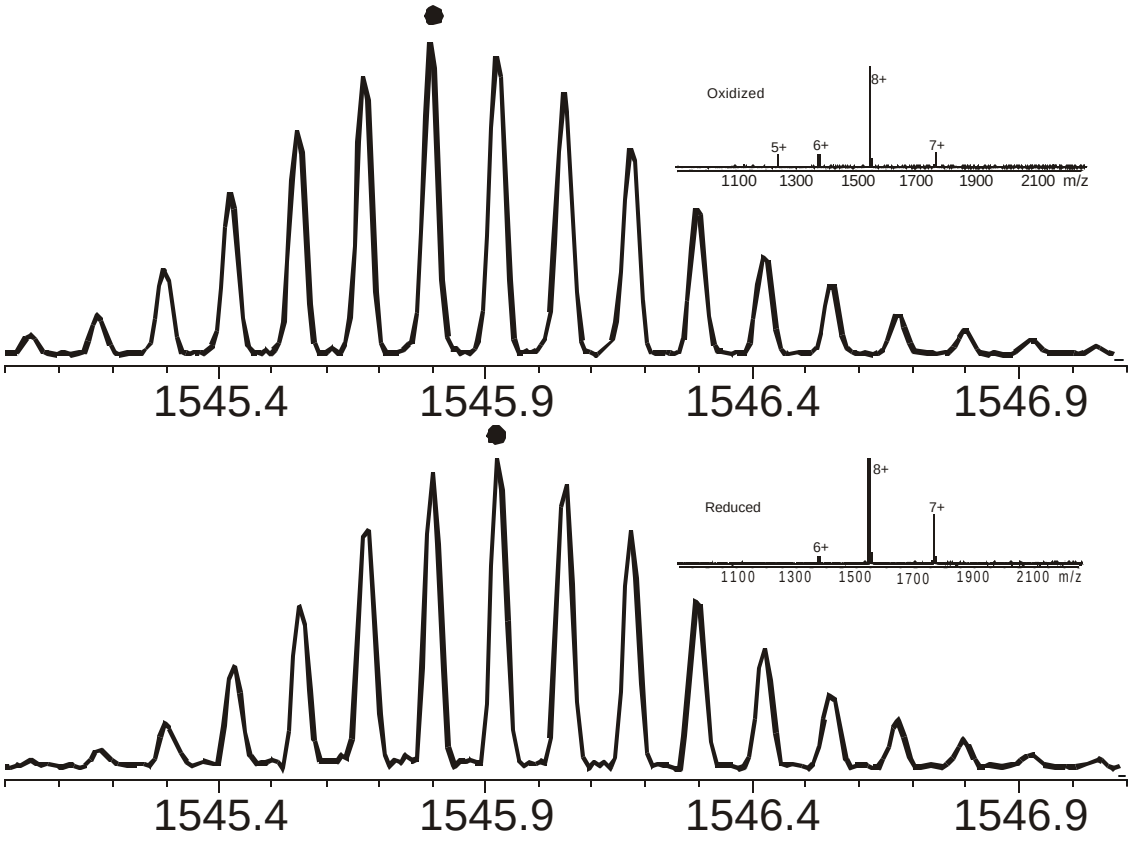
Oxidized
8+
5+
6+
7+
1100 1300 1500 1700 1900 2100 m/z
1545.4 1545.9 1546.4 1546.9
Reduced
8+
7+
6+
1100 1300 1500 1700 1900 2100 m/z
1545.4 1545.9 1546.4 1546.9

Figure 6.3 Negative ion mode ESI-FTICR mass spectra for the 6- charge state for both oxidized (top) and reduced (bottom) cytochrome *c*. The centroid of each isotope distribution is marked with "●", to highlight the mass shift resulting from the reduction of the metal center.

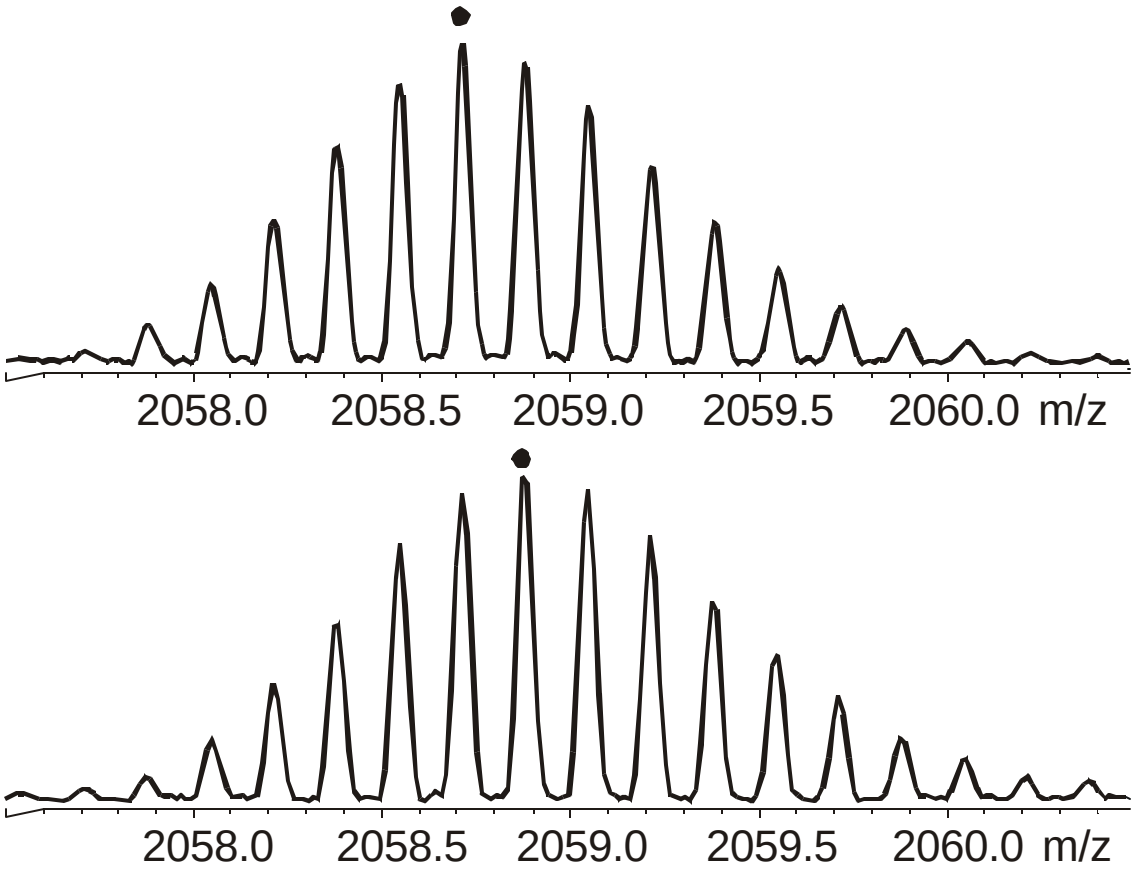
2058.0
2058.5
2059.0
2059.5
2060.0
m/z
2058.0
2058.5
2059.0
2059.5
2060.0
m/z

The ESI process has been compared to an electrochemical cell by Van Berkel and co-workers. Their research shows that ferrocene and polyaniline can become oxidized during positive mode ESI. The metalloproteins that are used in this research are much larger than the compounds used in their research and the metal centers are surrounded by the protein. Due to the shielding of the metal center from the electrode, its oxidation is too slow to occur on the timescale of the electrospray process. In fact, electrochemical measurements of metalloproteins usually require a mediator molecule to shuttle electrons between the electrode and the metal center.[25-27] Apparently oxygen can act as a mediator, as the reduced protein is oxidized during electrospray ionization unless oxygen is rigorously excluded from the solution. He et al. were unable to observe the reduced form of cytochrome *c*, even for dithionite-reduced samples that were kept in an oxygen-free environment.[2] One substantial difference between our experiments is the spray voltage. Our experiments utilized nanospray with an applied voltage of 600 - 1200 V through a liquid junction. He et al. used voltages higher than 2000 V. Unlike He's experiments, we did not try to exclude oxygen from the spray tip/capillary region, as this was not found to be necessary.

Other metal containing proteins have also been investigated including copper-containing azurin from *Pseudomonas aeruginosa*. The mass spectra for the 7+ charge state of the oxidized (top) and chemically reduced (bottom) metalloprotein are shown in Figure 4. The isotope peaks in the mass spectra in Figure 4 are shifted by one mass-to-charge unit between the oxidized and chemically reduced forms. The copper center of azurin can cycle between 1+ and 2+ oxidation states; the spectra show the addition of five protons in the case of the oxidized protein and six protons for the dithionite-reduced protein in the 7+ charge state, from which we derive 2+ and 1+ redox states for copper in the corresponding mass spectra.

High resolution is necessary for deriving the oxidation states of these compounds, and in our hands, only those metalloproteins having molecular weights below 20,000 can be assigned with confidence. Above ~20,000, the comparison of the theoretical isotope distribution to the experimentally determined isotope distribution becomes increasingly difficult because of a

Figure 6.4 ESI-FTICR mass spectra obtained for copper-containing azurin from *Pseudomonas aeruginosa* in the 7+ charge state for both oxidized (top) and dithionite-reduced (bottom) protein. Both spectra were obtained in positive ion mode. A shift in the most abundant peak of the isotope distribution, marked by "●" in both spectra, corresponds to a change from Cu^{2+} to Cu^{1+} in the metalloprotein.

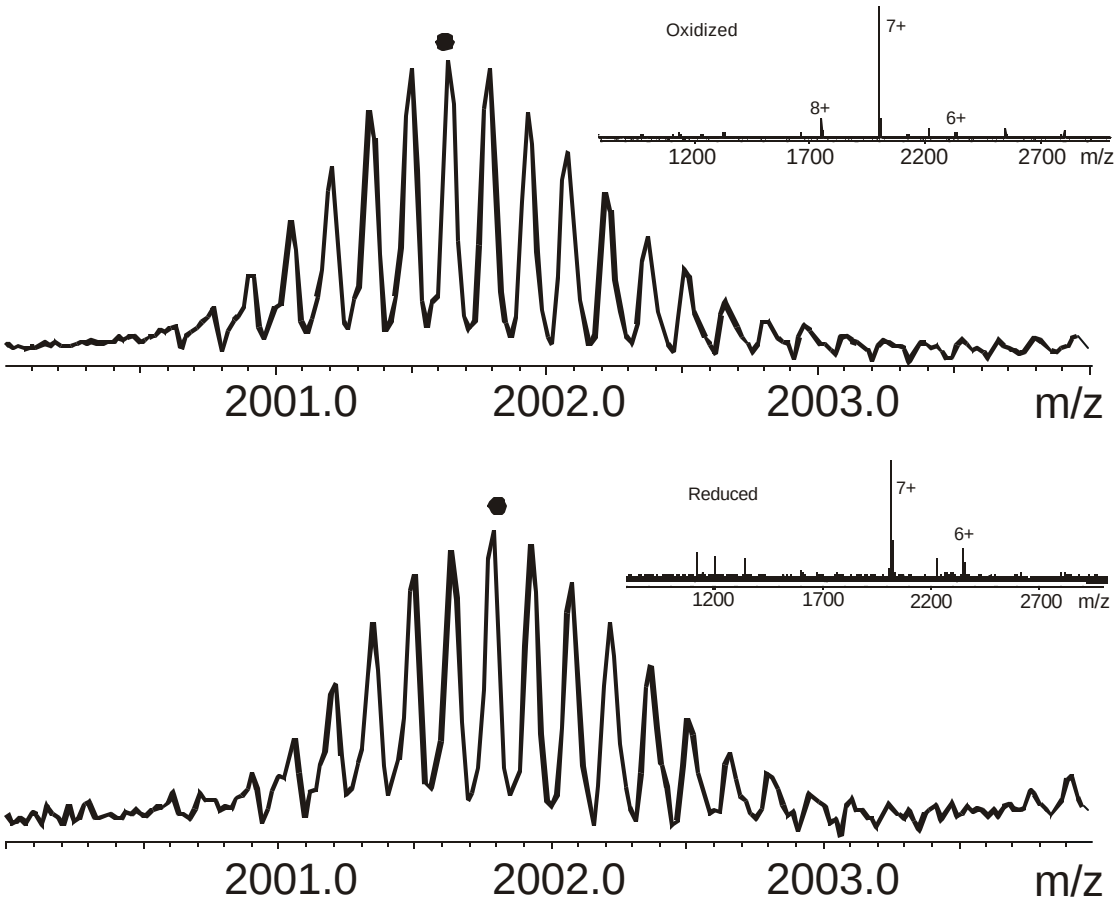
Oxidized
7+
8+
6+
1200
1700
2200
2700
m/z
2001.0
2002.0
2003.0
m/z
Reduced
7+
6+
1200
1700
2200
2700
m/z
2001.0
2002.0
2003.0
m/z

decrease in the accuracy of the isotope statistics. For example, superoxide reductase from *Pyrococcus furiosus* is a mononuclear iron-containing protein that exists as a tetramer in solution. Each subunit has a molecular weight of 14371.21 Da (Table 1). Although the tetramer can be observed in the mass spectrum (not shown), high accuracy in the isotope statistics could only be obtained from the monomer data. Dissociation of the tetramer to yield the monomer was achieved by increasing the metal capillary temperature from 150 °C to 250 °C. An expansion showing the isotope distributions for the monomer is shown in Figure 5. The top spectrum was obtained for the oxidized protein in the 9+ charge state. Only six excess protons are present in making up the 9+ charge state for the oxidized protein, while for the ascorbic acid reduced metalloprotein (bottom), seven excess protons are observed. From this, we derive oxidation states of Fe^{3+} and Fe^{2+} for the oxidized and reduced proteins, respectively. The decrease in resolution between the oxidized and the reduced spectra is caused by the desalting step.

Metalloproteins with mixed metal centers are of great interest to researchers in bioinorganic chemistry, and are difficult targets for analysis by other spectroscopic methods. The mass spectrum of manganese-substituted iron-sulfur cluster protein from *Pyrococcus furiosus* ferredoxin of the cuboidal form, [3FeMn-4S], is shown in Figure 6. The oxidized (top) and dithionite-reduced (bottom) forms of the metalloprotein are shown in the 4+ charge state. The highest possible oxidation state for the metal center in its biological environment is 2+. We observe the addition of only two excess protons during ESI to the oxidized protein, with the remainder of the charge present on the $[3FeMn\text{-}4S]^{2+}$ cluster. The ESI mass spectrum of the dithionite-reduced protein is shown in the bottom spectrum. It is also compared in its 4+ charge state and was found to contain only three excess protons for the 4+ charge state during positive mode ESI. The reduced cluster, $[3FeMn\text{-}4S]^{1+}$, is deduced from the data. Other spectroscopic methods are often used to investigate iron-sulfur proteins, including electron paramagnetic resonance (EPR) and magnetic circular dichroism (MCD). The manganese-substituted cluster is EPR silent, and its presence could only be inferred by the

Table 6.1 Metalloproteins are listed in order of discussion starting with a) Cytochrome *c* from the positive ion mode spectrum, b) Cytochrome *c* from the negative ion mode spectrum, c) Azurin, d) Superoxide reductase, e) Ferreodoxin containing a manganese substituted cluster, f) Cytochrome *c* for electrochemical reduction experiments. Monoisotopic mass measurements obtained for oxidized samples are shown with the oxidation form of the metal. Monoisotopic mass measurements for chemically reduced samples (a,b,c,d,e) and the electrochemically reduced sample (f) are shown with the reduced form of the metal. The calculated mass is the monoisotopic mass obtained from the amino acid sequence for the metalloproteins assuming a neutral molecule.

Metalloprotein	Oxidized Mass (Da)	Reduced Mass (Da)	Calculated Mass (Da)
[a]Cytochrome *c*	Fe(III) 12351.33	Fe(II) 12352.33	12354.33
[b]Cytochrome *c*	Fe(III) 12351.33	Fe(II) 12352.34	12354.33
[c]Azurin	Cu(II) 13995.51	Cu(I) 13996.42	13997.68
[d]Superoxide Reductase	Fe(III) 14368.28	Fe(II) 14369.39	14371.21
[e][Mn3Fe-4S] Ferredoxin	M(II) 7508.86	M(I) 7509.89	7510.86
[f]Cytochrome *c*	Fe(III) 12351.38	Fe(II) 12352.39	12354.33

Figure 6.5 ESI-FTICR mass spectra for mononuclear iron-containing superoxide reductase from *Pyrococcus furiosus*, shown in the 9+ charge state for oxidized (top) and ascorbic acid-reduced (bottom) protein. The shift in the isotope distribution between oxidized and reduced protein (most abundant peak labeled by "●") and corresponds to a change in oxidation state from Fe^{3+} to Fe^{2+}.

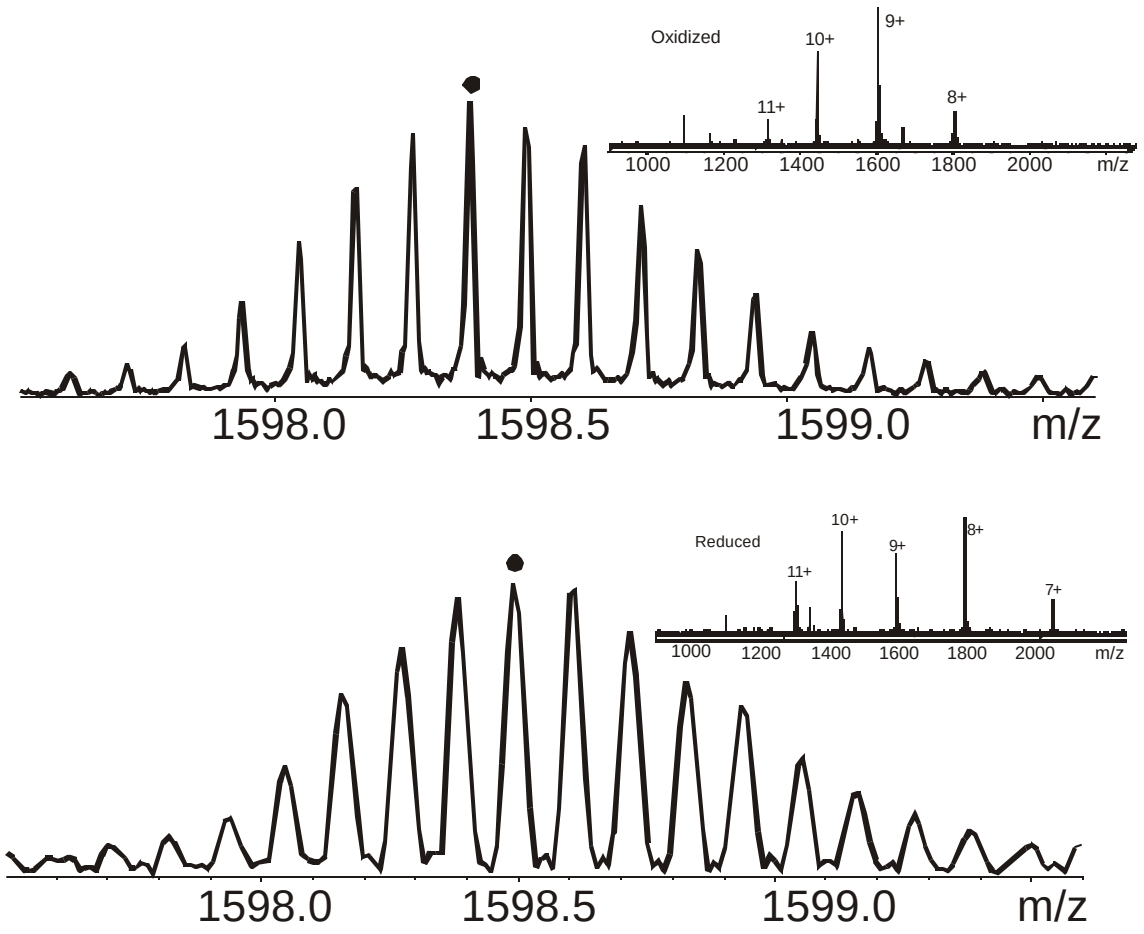
Oxidized
9+
10+
11+
8+
1000
1200
1400
1600
1800
2000
m/z
1598.0
1598.5
1599.0
m/z
Reduced
10+
11+
9+
8+
7+
1000
1200
1400
1600
1800
2000
m/z
1598.0
1598.5
1599.0
m/z

Figure 6.6 Manganese-substituted iron-sulfur-containing protein from *Pyrococcus furiosus* ferredoxin, obtained using positive ion mode ESI-FTICR mass spectrometry. The cluster has the composition [3FeMn-4S] and exhibits oxidation states of 2+ (top) 1+ form (bottom). The center of the 4+ charge state distribution is marked by "●" and shows the change in the mass due to reduction of the metal center.

absence of signal in the EPR spectrum. The appearance of the [3Fe-4S] cluster from the loss of manganese from the active site upon oxidation is monitored instead. Thus, this is the first direct evidence that this metal-substituted cluster is stable in the oxidized form.

In addition to chemical reduction, an electrochemical cell was used to reduce cytochrome *c*. The bulk electrochemical reduction of cytochrome *c* was monitored visually for a change in color from light brown in the oxidized state to pink in the reduced state. The electrochemical cell was placed on-line with a UV-visible absorbance detector and the nanoelectrospray source. The full absorbance spectrum between 375 nm and 625 nm is shown in Figure 7. The transition at 550 nm was monitored on-line prior to ionization. The exit end of the UV-visible detector was connected to the nanoelectrospray source. An increase in absorbance from 0.1410 AU to 0.4113 AU at 550 nm (pathlength, 1cm) was observed between the oxidized and reduced forms of the protein. Upon exiting the UV-visible absorbance detector, the solution entered the nanoelectrospray tip and was ionized in positive ion mode to obtain the mass spectrum in Figure 8. The top spectrum shows the expansion of the 7+ charge state for the oxidized protein. The same charge state is shown for the reduced protein in the bottom spectrum. The shift in the isotope distribution between the two forms corresponds to the change in the number of protons that are added during ESI to form the 7+ charge state. For the oxidized protein, four excess protons are observed from which we determined Fe^{3+} as the oxidation state of the metal center. In the reduced form of the protein, five excess protons are observed, indicating Fe^{2+}.

The electrochemical reduction was found to have several advantages over chemical reduction. First, the time needed for electrochemical reduction was 5 times shorter than for chemical reduction, principally because the lengthy process of removal of the reducing agent by ultrafiltration is required only for chemical reduction. Secondly, there is a risk of reoxidation of reduced protein by contact with ambient oxygen during the removal of the reducing agent from the protein solution for chemically reduced samples, so the samples must be handled in a glovebag during and after the reduction step (including the ultrafiltration process). In contrast,

Figure 6.7 The UV-visible absorbance spectrum for oxidized and reduced cytochrome *c*, from 375 nm and 625 nm. The transition at 550 nm (path length, 1 cm) was monitored during on-line electrospray ionization for the electrochemically reduced sample. The concentration of cytochrome *c* calculated from these data is ~13 μM..

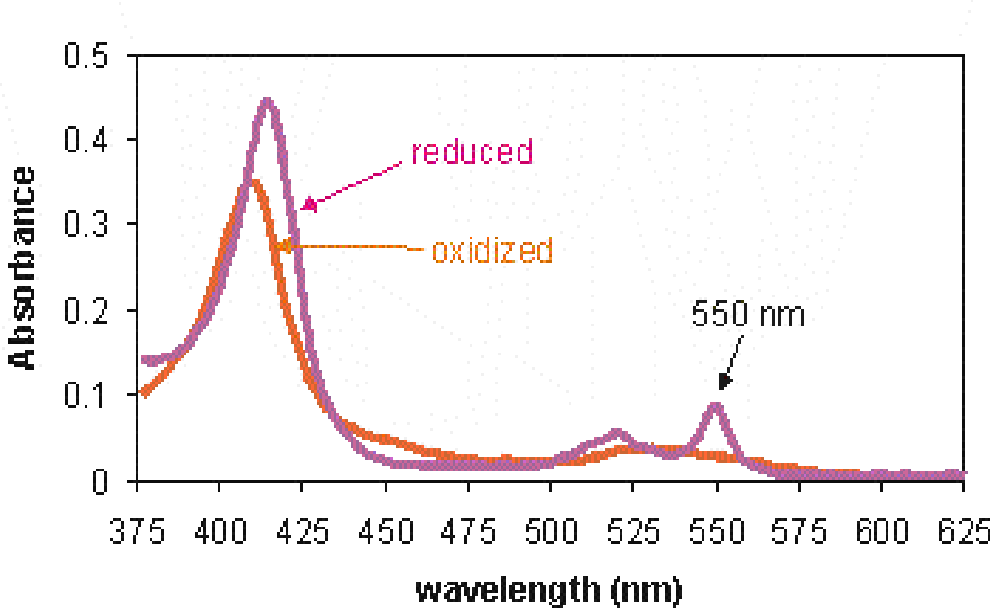
0.5
0.4
0.3
0.2
0.1
0
Absorbance
reduced
oxidized
550 nm
375 400 425 450 475 500 525 550 575 600 625
wavelength (nm)

Figure 6.8 ESI-FTICR mass spectra for oxidized (top) and on-line, electrochemically reduced (bottom) cytochrome *c*. The shift in the isotope distribution for the 7+ charge state between oxidized and reduced metalloprotein is easily discerned from the position of the center of the distribution, marked by "●".

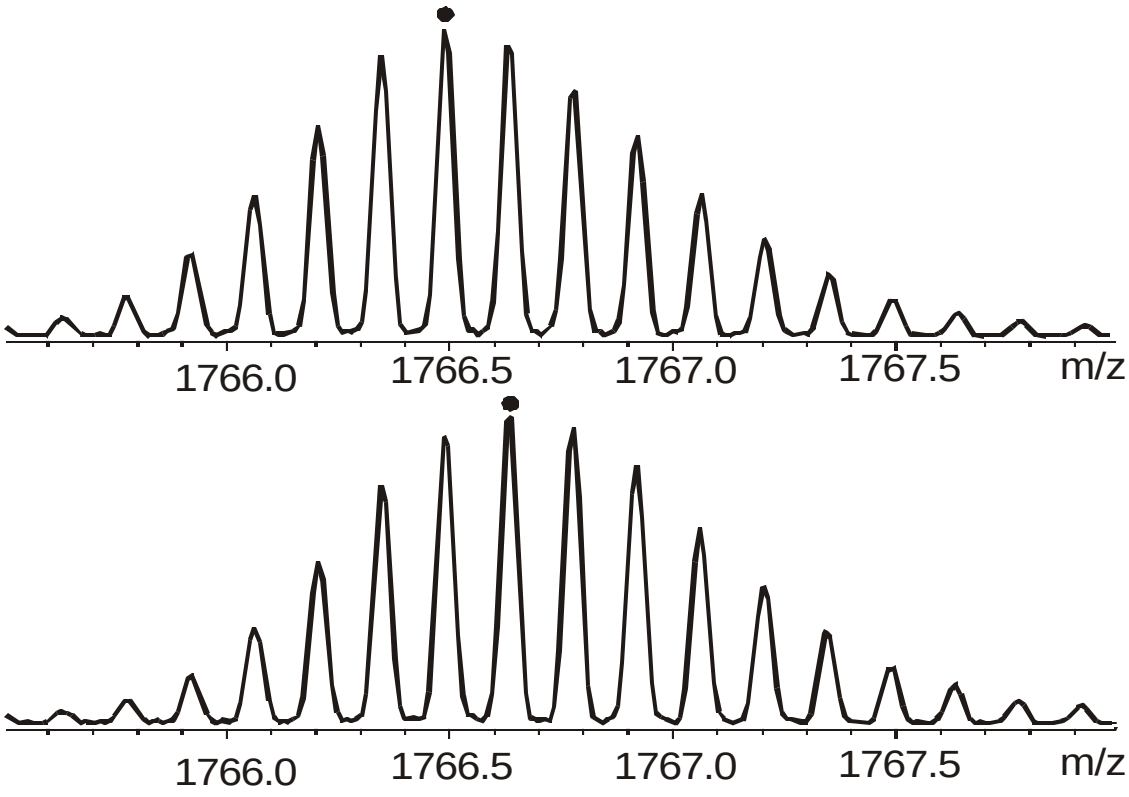
1766.0
1766.5
1767.0
1767.5
m/z
1766.0
1766.5
1767.0
1767.5
m/z

the “reducing” syringe remained in electrical contact until the solution was ejected, and the possibility of reoxidation was greatly diminished for the electrochemical method. Although the volume of the cell used here was quite large (0.5 mL), this could be reduced to a few microliters to provide a method for the analysis of the oxidation states of metalloproteins that are available only in limited quantities.

Conclusion

We have observed both oxidized and reduced forms of several metalloproteins using ESI-FTICR mass spectrometry. Reduction of the metalloproteins with sodium dithionite and bulk reduction in an electrochemical cell are both feasible methods; however, the electrochemical method is quicker and is less prone to reoxidation of the reduced protein. The mass spectra that are obtained for these metalloproteins reflect the solution-phase oxidation state. The data show that metalloproteins are not oxidized by the ESI process provided that oxygen is excluded from place during positive mode or negative mode ESI. The their solutions prior to and during analysis. Neither oxidation nor reduction is observed to take electrochemical method can be conducted on-line with ESI, since no cleanup of the protein is necessary after reduction. The online analysis of metalloproteins using thin-layer, low-volume electrochemical cells with ESI-MS detection will be useful for characterizing the active oxidation states of a wide variety of metalloproteins.

Acknowledgment

The authors thank Marc F.J.M. Verhagen, Francis Jenny and Mike W.W. Adams from the University of Georgia for providing superoxide reductase and the [3FeMn-4S] cluster protein and also Michael Hay and Yi Lu from the University of Illinois for providing the azurin used in this study. We gratefully acknowledge funding provided by the National Science Foundation (CHE-9974579).

References

(1) Remigy, H.; Jaquinod, M.; Petillot, Y.; Gagnon, J.; Cheng, H.; Xia, B.; Markley, J. L.; Hurley, J. K.; Tollin, G.; Forest, E. *J. Protein Chem.* **1997,** *16*, 527-532.

(2) He, F.; Hendrickson, C. L.; Marshall, A. G. *J. Am. Soc. Mass Spectrom.* **2000**, 120-126.

(3) Hu, P. F.; Loo, J. A. *J. Mass Spectrom.* **1995,** *30*, 1076-1082.

(4) Johnson, K. A.; Verhagen, M.; Adams, M. W. W.; Amster, I. J. *Anal. Chem.* **2000,** *72*, 1410-1418.

(5) Lei, Q. P.; Cui, X. Y.; Kurtz, D. M.; Amster, I. J.; Chernushevich, I. V.; Standing, K. G. *Anal. Chem.* **1998,** *70*, 1838-1846.

(6) Loo, J. A. *Mass Spectrom. Rev.* **1997,** *16*, 1-23.

(7) Ens, W.; Standing, K.; Chernushevich, I. In *NATO ASI series. Series C, Mathematical and Physical Sciences*; Dordrecht, Boston, 1998; Vol. 510, pp 149-156.

(8) Katta, V.; Chait, B. T. *J. Am. Chem. Soc.* **1991,** *113*, 8534-8535.

(9) Douglas, D.; Konerman, L. *J. Am. Soc. Mass Spectrom.* **1998,** *9*, 1248-1254.

(10) Smith, D. L.; Yang, H. H. *FASEB J.* **1997,** *11*, 276.

(11) Li, Y. T.; Hsieh, Y. L.; Henion, J. D.; Ganem, B. *J. Am. Soc. Mass Spectrom.* **1993,** *4*, 631-637.

(12) McLafferty, F. W.; Guan, Z.; Haupts, U.; Wood, T. D.; Kelleher, N. L. *J. Am. Chem. Soc.* **1998,** *120*, 4732-4740.

(13) Hunter, C. L.; Mauk, A. G.; Douglas, D. J. *Biochemistry.* **1997,** *36*, 1018-1025.

(14) Deng, H.; Van Berkel, G. J. *Anal. Chem.* **1999,** *71*, 4284-4293.

(15) Van Berkel, G. J.; Giles, G. E.; Bullock, J. S.; Gray, L. J. *Anal. Chem.* **1999,** *71*, 5288-5296.

(16) Bond, A. M.; Colton, R.; D'Agostino, A.; Traeger, J. C.; Downard, A. J.; Canty, A. J. *Inorg. Chim. Acta* **1998,** *267*, 281-291.

(17) Xu, X.; Lu, W.; Cole, R. B. *Anal. Chem.* **1996,** *68*, 4244-4253.

(18) Xu, X.; Lu, W.; Cole, R. B. *Anal. Chem.* **1997,** *69*, 2478-2484.

(19) Koenig, S.; Haegele, K.; Fales, H. *Anal. Chem.* **1998,** *70*, 4453-4455.

(20) Senko, M. W.;Beu, S. C.; McLafferty, F. W. *J. Am. Soc. Mass Spectrom.* **1995**, 6, 229-233.

(21) Hay, M. T.; Milberg, R. M.; Lu, Y. *J. Am. Chem. Soc*. **1996,** *118*, 11976-11977.

(22) Fabris, D.; Hathout, Y.; Fenselau, C. *Inorg. Biochem.* **1999,** *38*, 1322-1325.

(23) Troxler, H.; Kuster, T.; Rhyner, J. A.; Gehrig, P.; Heizmann, C. W. *Anal. Biochem.*. **1999,** *268*, 64-71.

(24) Henry, K. D.; McLafferty, F. W. *Org. Mass Spectrom.* **1990,** *25*, 490-492.

(25) Kuramitz, H.; Sugawara, K.; Kawasaki, M.; Hasebe, K.; Nakamura, H.; Tanaka, S. *Anal. Sci.* **1999,** *15*, 589-592.

(26) Cheng, G. J.; Dong, S. J. *J. Electroanal. Chem.* **1996,** *416*, 97-104.

(27) Parker, V. D.; Seefeldt, L. C. *Anal. Biochem.*. **1997,** *247*, 152-157.

CHAPTER 7

STUDIES OF LIGAND BINDING IN HEMOGLOBIN AND MYOGLOBIN BY ESI-FTICR MASS SPECTROMETRY: EVIDENCE FOR SMALL DEVIATIONS BETWEEN GAS-PHASE AND SOLUTION-PHASE STRUCTURES[1]

[1]Keith A. Johnson, and I. Jonathan Amster. Anal. Chem. 2001. To be submitted to Analytical Chemistry

Abstract

Cyanide-binding and carbon monoxide-binding to hemoglobin tetramer and cyanide-binding to myoglobin are observed by electrospray ionization Fourier transform ion cyclotron resonance mass spectrometry. Large variations in the stability of cyanide-bound myoglobin are observed depending on the capillary temperature used during ionization and the polarity of ionization. The allosteric nature of ligand-bound hemoglobin tetramer provides a means to compare the solution-phase structure to ions in the gas-phase. Slight changes in tertiary structure of tetrameric hemoglobin result in the dissociation of the ligands from the complex. We have observed noncooperative binding of CO and CN ligands to hemoglobin tetramer during electrospray ionization. Ligand binding to dimer and monomer has also been investigated. The results indicate that although the higher order protein structure is conserved enough during ionization to observe the tetramer, dimer, and monomer with heme intact, small changes in conformation during ionization cause the dissociation of ligands that were present in solution.

Introduction

A challenging and unresolved question in mass spectrometry is the degree of similarity between the structures of gas-phase protein ions and their condensed phase counterparts. A variety of experiments suggest a correspondence between the structures of proteins as they exist in solution versus the vacuum of a mass spectrometer.[1-3] For example, a number of noncovalent complexes have been observed to have the same stoichiometry in the gas-phase as in the condensed phase.[4, 5] These include observations of protein-protein, protein-peptide, and protein-substrate complexes.[3, 6-11] Such observations suggest that enough of the protein's three dimensional solution structure remains in the gas-phase to preserve the multiple noncovalent interactions that join a protein with its partner. Other experiments have been directed at measuring the conformations of gas-phase ions.[12-14] Ion mobility measurements probe molecular size and shape, for example distinguishing extended from compact structures.[15, 16] Gas-phase

hydrogen-deuterium exchange experiments provide a means to determine the number of exchangeable protons on the outside of a folded protein, and have provided examples of multiple folded conformations of cytochrome *c*. In this paper, we present another experiment that provides a means to evaluate the correspondence in gas-phase and solution structures of a protein, namely examining cooperativity in substrate binding by gas-phase protein ions. Binding cooperativity often occurs through small changes in the three dimensional structure of a protein, and so this provides a sensitive means to distinguish similarity or difference in structures between gas-phase and condensed phase structures for this protein.

In this article, we examine protein-substrate binding in the well-studied heme proteins, hemoglobin and myoglobin. Hemoglobin and myoglobin are proteins which enclose a noncovalently attached heme group. Both proteins reversibly bind oxygen, and provide a means to transport and store this molecule. The activity of the protein is dependent upon the oxidation state of the heme iron.[17] The ferric forms of these proteins, met-hemoglobin and met-myoglobin will not bind oxygen until they are reduced to the ferrous form, Fe^{2+}. Thus, these proteins serve as good models for examining the capability of ESI mass spectrometry to observe noncovalant interactions, and to discern whether such interactions are biologically relevant. We look at both cyanide binding and carbon monoxide binding to hemoglobin and myoglobin. Ligand binding to hemoglobin, in particular, is sensitive to structural changes in the protein's three dimensional structure. Several studies have confirmed the allosteric nature of hemoglobin.[17-20] This characteristic begins when a molecule of O_2 binds to the heme group. The iron in the heme group is drawn into the plane of the porphyrin ring, which causes a slight change in three dimensional structure in the protein. The movement in one subunit triggers tertiary structural changes in adjacent subunits, increasing their affinity for oxygen. This increases the probability of observing a 1:1, protein-to-ligand ratio. These changes can be examined during ESI mass spectrometry by measuring the extent of cooperative binding to hemoglobin in its reduced and oxidized forms. Myoglobin, on the other hand, exists as a monomer under native conditions. Although the reduced protein's function is to store O_2, the

heme group can easily become oxidized. The protein's tertiary structure serves to cradle the heme group, protect the heme iron atom from oxidation, and it provides a pocket into which the O_2 can fit.[18]

The investigation of protein noncovalent complexes such as the hemoglobin tetramer studied here requires that particular care be taken to avoid denaturation of the sample during its ionization and introduction to the mass spectrometer. Electrospray ionization (ESI) mass spectrometry has been widely used for the investigation of protein-protein and protein-metal complexes because of its gentle transformation of these species from the solution-phase into the gas-phase.[2, 10, 21] Studies of these complexes have ranged from monitoring conformational changes of protein complexes by mass spectrometry, to investigations of metal-protein stoichiometry, cooperativity, and oxidation states.[7, 22-26] The detection of noncovalent complexes requires that the solution conditions are compatible with the biological environment of the native protein complex. The solvents usually used for ESI analysis (49% methanol, 49% water and 2% acetic acid) cause a loss of tertiary and quaternary structure of the protein and ultimately denaturation, which for a metalloprotein results in the loss of the metal center. With advances in ESI, pure aqueous solution can be utilized successfully yielding mass spectra of protein complexes.[25, 27-29]

The substrate binding behavior of the heme proteins studied here can be affected by the oxidation state of the metal center. Studies of the redox behavior of ESI have shown that there is a tendency for the ESI source to function similar to an electrolytic flow cell.[30, 31] In one study, small molecules underwent redox reactions during electrospray ionization. Factors that affect the redox process are flow rate, electrospray voltage, and analyte concentration. Other groups have investigated the effect of ESI mass spectrometry on metalloproteins after the reduction of the metal centers; however, in those studies, only the oxidized forms of the metalloproteins could be observed in the mass spectra.[25, 29, 32-34] We have recently shown that the reduced forms of several metalloproteins including cytochrome *c*, ferredoxin, superoxide reductase, and azurin can be observed during ESI-FTICR mass spectrometry only after eliminating oxygen

from solution.[35, 36] These observations permit redox biochemistry to be studied by ESI mass spectrometry. The hemoglobin and myoglobin systems examined here serve as models for the analysis of reduced versus oxidized protein-substrate complexes. However, we have not been able to examine oxygen as a substrate, as it easily auto-oxidizes heme iron.[37] For this reason, we have chosen to examine the binding behavior of carbon monoxide and cyanide, and the structural changes that are necessary for the substrates to exhibit cooperativity in binding to hemoglobin. Cyanide binds both hemoglobin and myoglobin more strongly in the ferric form rather than in the reduced, ferrous form.[17, 19] Alternatively, carbon monoxide binds the proteins only in their ferrous forms, which requires that the proteins are maintained in their reduced states prior to and during ionization.[20] Several groups have reported the detection of heme-globin complexes during ESI mass spectrometry.[38-41] These well studied proteins make good models to examine the question of gas-phase protein conformation.

Experimental

A Bruker BioApex FTICR mass spectrometer (Billerica, MA) with a 7-T magnet equipped with an Analytica ESI source (Branford, CT) was used to obtain all of the mass spectra. The Analytica ESI source was modified by replacing the glass capillary interface with a heated metal capillary. The temperature of the heated metal capillary was adjusted for each sample to obtain a maximum protein-ligand ratio before the mass spectra were collected. This temperature was typically 80 °C for positive ions or 100 °C for negative ions. Nanoelectrospray was used to ionize the samples at a flow rates of 1-5 μL/h. The nanoelectrospray tips were fabricated in our lab using fused silica capillary tubing (100 μm i.d., L=4 cm) (Polymicro Technologies, Phoenix, AZ). The tips were pulled by heating the capillary tubing with a hand held micro-torch (Microflame, Inc., Minnetonka, MN) while applying a constant force of approximately 10 g. Spray voltages were 900 to 1100 V for positive ion mode and -950 to -1150 V for negative ion mode. The spray voltage did not affect the protein-ligand ratio in this range, although the signal intensity could be adjusted slightly

depending on the electrospray voltage. The voltage was applied to the syringe needle that delivered the sample to the spray emitter, forming a liquid electrical junction.[31]

Horse heart myoglobin and ferrous human hemoglobin were obtained from Sigma (St. Louis, MO). Metalloprotein solutions (20 μM) were prepared for ESI by suspending them in water prior to chemical reduction. For cyanide-bound experiments, several crystals of KCN were added to the ferric form of the proteins, and the excess reagent was removed by aerobic ultrafiltration using a microcentrifuge tube (10 kDa cutoff for myoglobin, 30 kDa cutoff for hemoglobin) with an integral membrane filter (Millipore Corporation, Bedford, MA) using approximately 500 μL of degassed, 20 mM ammonium acetate solution. After removal of excess KCN, the sample was resuspended in water to a concentration of 20 μM. A portion of the sample was transferred to a gastight syringe and introduced to the mass spectrometer via nanoelectrospray ionization. The remaining sample was placed in a 500 μL UV-visible absorbance cell and monitored for ligand-bound protein, as CN-binding produces a characteristic shift in the UV spectrum.

Human hemoglobin was obtained in the crystallized, ferrous (reduced) form, and it remained reduced upon dissolution in nitrogen-purged ammonium acetate (20 mM). Ultrafiltration with a 30 kDa cutoff membrane was necessary to remove the protein stabilizers introduced by the manufacturer. Solutions of myoglobin and hemoglobin were prepared in a nitrogen-filled glovebag and purged with nitrogen prior to chemical reduction by sodium dithionite. The reducing agent was added to the metalloproteins in a ten fold excess and a color change from brown to red was monitored visually for both proteins in their transformation from the ferric to the ferrous form. For carbon monoxide experiments, carbon monoxide gas was added to the headspace above the protein solution in a nitrogen-purged glass container with a rubber stopper. The gas was introduced via a syringe needle with a second needle placed in the stopper to vent the excess pressure. The reduced sample changed from a red color to a bright “cherry-red” color that is characteristic of carbon monoxide-bound hemoglobin.[20] Sodium dithionite creates a plethora of sodium adduct peaks which dominate the mass

spectrum, and greatly diminishes the signal intensity to a point where interpretable data can not be acquired. Therefore, after reduction, sodium dithionite was removed prior to analysis by anaerobic ultrafiltration in a nitrogen-purged glovebag using a microcentrifuge tube as described above. The protein was then resuspended in water, resulting in a final concentration of 20 μM. A portion of the reduced, CO-bound protein was transferred to a gastight syringe and introduced to the mass spectrometer via nanoelectrospray ionization. The remainder of the reduced solution was used for spectroscopic analysis to confirm the presence of ligand-bound protein.

Protein samples were introduced to the mass spectrometer at a concentration of 20 μM in water after removal of reducing agent (see below) for chemical reduction. For electrochemical reduction (see below), cytochrome *c* (20 μM) was reduced in 5 mM ammonium acetate. Exclusion of oxygen during sample handling after reducing the protein samples was imperative in obtaining mass spectra for the reduced hemoglobin and carbon monoxide-bound hemoglobin. The samples were ionized by nanoelectrospray and stored in the hexapole region of the source for 0.5 s. For positive ion mode experiments, the source parameters were as follows: skimmer, -3.00 V; dc offset, 1.89 V, extraction from hexapole, -2.00 V, hexapole trap, -6.89 V. A 15 ms ion pulse introduced the ions to the ICR cell where trapping voltages of -0.9V and -1.0 V were used to trap the ions. For positive ions, the parameters were as follows: skimmer, 2.03 V; dc offset, -2.71 V; extraction from hexapole, 1.68 V; hexapole trap, 5.83 V. The ions were trapped in the ICR cell by 0.90 V and 1.00 V on the trapping plates after an 8 ms ionization pulse from the source. A description of the data analysis using the χ^2 test [42] have been discussed previously.[35] Calculations of isotope distributions for the proteins were made by using IsoPro software available from (http://www.members.aol/msmssoft). The time domain signal (transient) was collected by averaging approximately 100 scans. The summed transient was apodized prior to application of the Fourier transform, followed by calibration to yield a mass spectrum.

Results and Discussion

Previous studies of metalloproteins in positive and negative ion mode ESI have shown that positive ions are more labile than negative ions during their transformation into the gas-phase.[5, 25, 36, 43, 44] Myoglobin and hemoglobin have also been found to be more stable as negative ions during ESI.[38] The myoglobin-CN complex was electrosprayed in both positive and negative ion modes. Complexation of myoglobin with cyanide was ascertained by UV-visible absorbance, as shown in Figure 1. It is known that the oxidized forms of hemoglobin and myoglobin bind cyanide more strongly than the reduced forms. In contrast, only the reduced forms of either proteins form complexes with carbon monoxide.[17] The positive ion mode mass spectrum of CN-bound met-myoglobin (that is, the ferric form) is shown at the top of Figure 2. Although the UV spectrum confirms that the ligand is bound to the heme group of myoglobin, only about 25% of the protein appears as the complex in the mass spectrum. The negative ion mode mass spectrum for the same sample is shown at the bottom of Figure 2. In contrast to the positive ion mode mass spectrum, mostly CN-bound protein is detected, with little unbound holomyoglobin observed. Both of the mass spectra were obtained under the same electrospray conditions, with a capillary temperature of 110 °C and an electrospray voltage of ± 1000 V. The monoisotopic molecular weight of myoglobin, based on a neutral protein, is 17557.14 Da. The apparent mass for the measured protein, derived assuming that all of the charge on the metalloprotein is in the form of protons, is 17556.18 Da. The difference in the two weights suggests the iron is in the ferric form, Fe^{3+}, or $[heme]^{+}$. The calculated monoisotopic mass of CN-bound myoglobin is 17583.18 Da, and matches well with the apparent mass of 17583.20 Da. The data shows that the heme-cyanide complex has an overall charge of zero, which shows that iron is in its oxidized form, Fe^{3+}.

The temperature of the heated metal capillary in the electrospray interface region was found to affect the amount of complex that is observed. It is possible that small changes in tertiary structure at various capillary temperatures dissociates the ligand from the protein. Figure 3 shows a graph of percentage complex versus temperature for both positive and

Figure 7.1 UV-visible absorbance spectrum for CN-bound myoglobin, which shows CN-bound versus unbound myoglobin. The peaks are labeled as such in the figure.

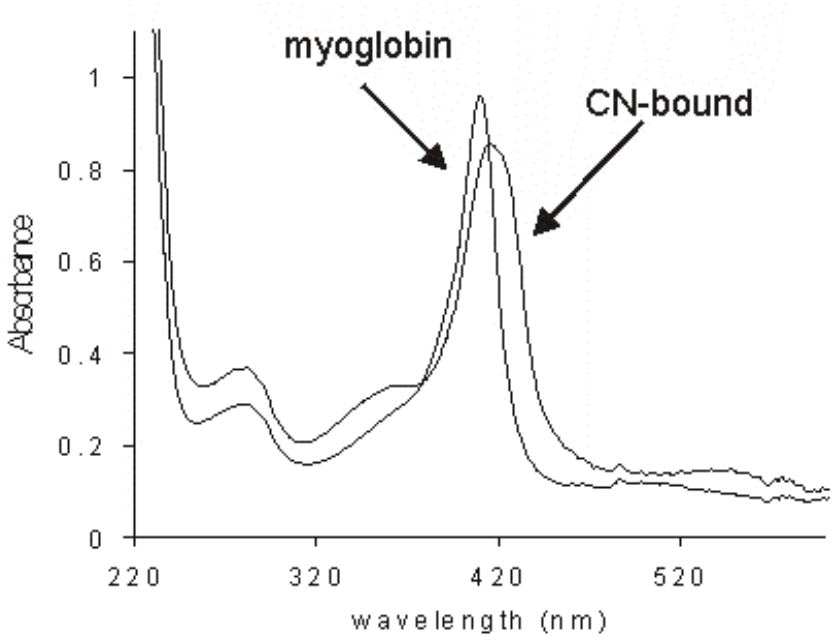
myoglobin
CN-bound
Absorbance
1
0.8
0.6
0.4
0.2
0
220
320
420
520
wavelength (nm)

Figure 7.2 ESI-FTICR mass spectra for myoglobin reacted with KCN in positive ion mode (top) and negative ion mode (bottom). The complex as a negative ion is shown to be more stable than the complex in positive ion mode with a capillary temperature of 110 °C.

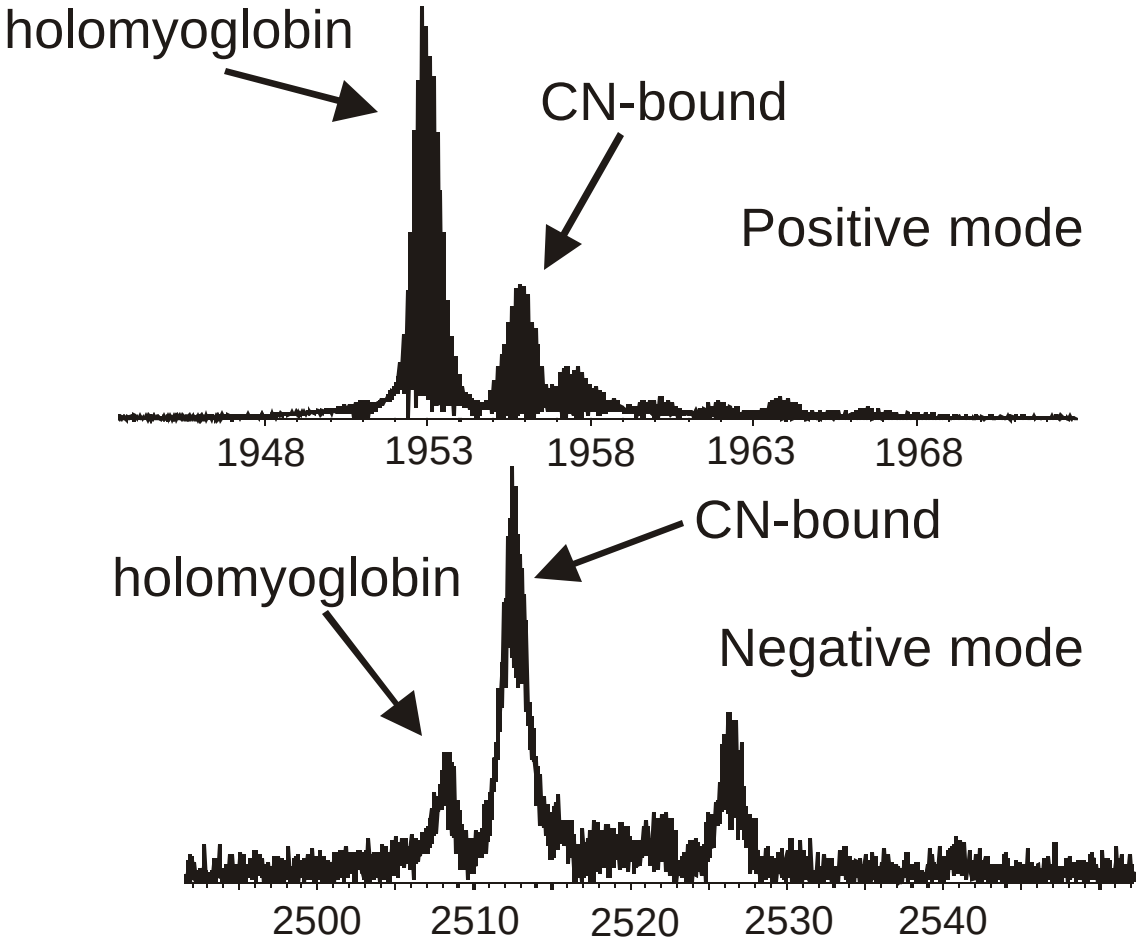
holomyoglobin
CN-bound
Positive mode
1948
1953
1958
1963
1968
CN-bound
holomyoglobin
Negative mode
2500
2510
2520
2530
2540

Figure 7.3 The graph showing the percentage of intact complex versus temperature is shown for both positive and negative ion mode. The optimum conditions for protein-ligand analysis for myoglobin are in negative ion mode at temperatures less than 120 °C.

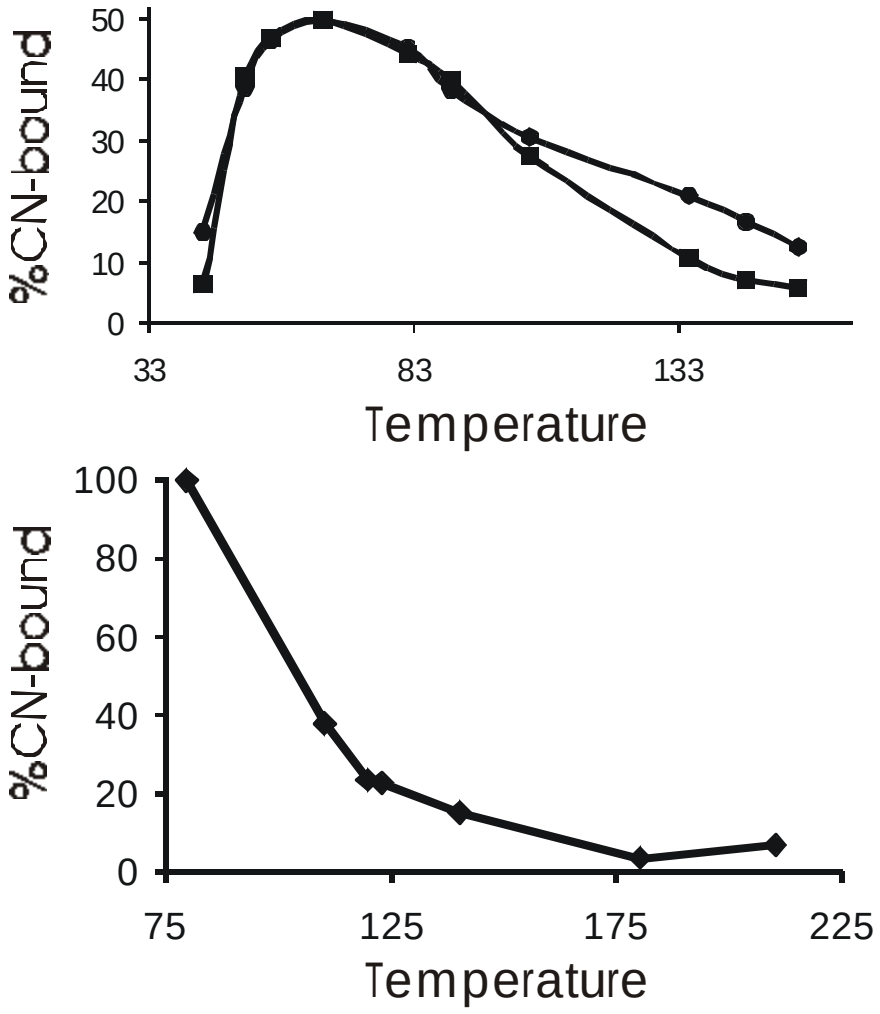
%CN-bound
50
40
30
20
10
0
33
83
133
Temperature
%CN-bound
100
80
60
40
20
0
75
125
175
225
Temperature

negative modes of ionization of myoglobin with cyanide. The optimum temperature for the complex in positive ion mode is ~75 °C, although at that temperature, only half of the detected protein is bound to its ligand. Alternatively, in negative ion mode there are a wide range of temperatures for which the complex is more abundant than the unbound holoprotein. The complex is 100% of the protein signal at an interface temperature of 80 °C in negative ion mode. A constant capillary temperature of 80 °C was used for the investigation of hemoglobin samples in positive ion mode. Although myoglobin data shows that there is an increase in the preservation of ligand-bound protein for negative ions, there is a tradeoff with signal-to-noise. Much weaker, less stable ion signal was observed during negative ion mode experiments. This characteristic made the application of negative ion mode electrospray to hemoglobin difficult even in denaturing solvent. The data for hemoglobin presented in this article was thus obtained by positive ion mode ESI. We also attempted to produce CO-bound myoglobin to observe its binding characteristics during ESI. Upon addition of sodium dithionite to the protein solution to reduce the metal to the ferrous state, the protein precipitated from solution. Reduction was not attempted with any other reducing reagents for these studies.

Carbon monoxide is known to bind only to ferrous hemoglobin, and this was examined first. To establish the oxidation state of heme, and to monitor binding of the substrate, the UV-visible absorbance spectrum was obtained for the CO-bound hemoglobin used in the mass spectrometry studies, and was compared to that of met-hemoglobin and deoxyhemoglobin (ferrous). The shift in λ_{max} from ferric hemoglobin (415 nm) to CO-bound hemoglobin (419 nm) is well known, and indicates that CO is bound to the protein after the anaerobic preparation of the protein.[17] Figure 4 shows the mass spectrum obtained for chemically reduced hemoglobin with carbon monoxide. Tetramer, dimer, and monomer can be observed in the mass spectrum. The principal set of peaks correspond to hemoglobin minus its N-terminal methionine. This amino acid was probably processed off during the overexpression of the protein, and this modification is not expected to change the folding of the protein or its ligand binding properties.

Figure 7.4 The ESI-FTICR mass spectrum showing tetramer, dimer, and monomer of CO-bound hemoglobin. The expansions of the monomer (8+ charge state), dimer (12+ charge state), and tetramer (17+ charge state), in addition to the carbon monoxide-bound protein, are labeled in the figure. The CO-bound monomer is measured in its reduced form, but the unbound protein is found to be in its oxidized form.

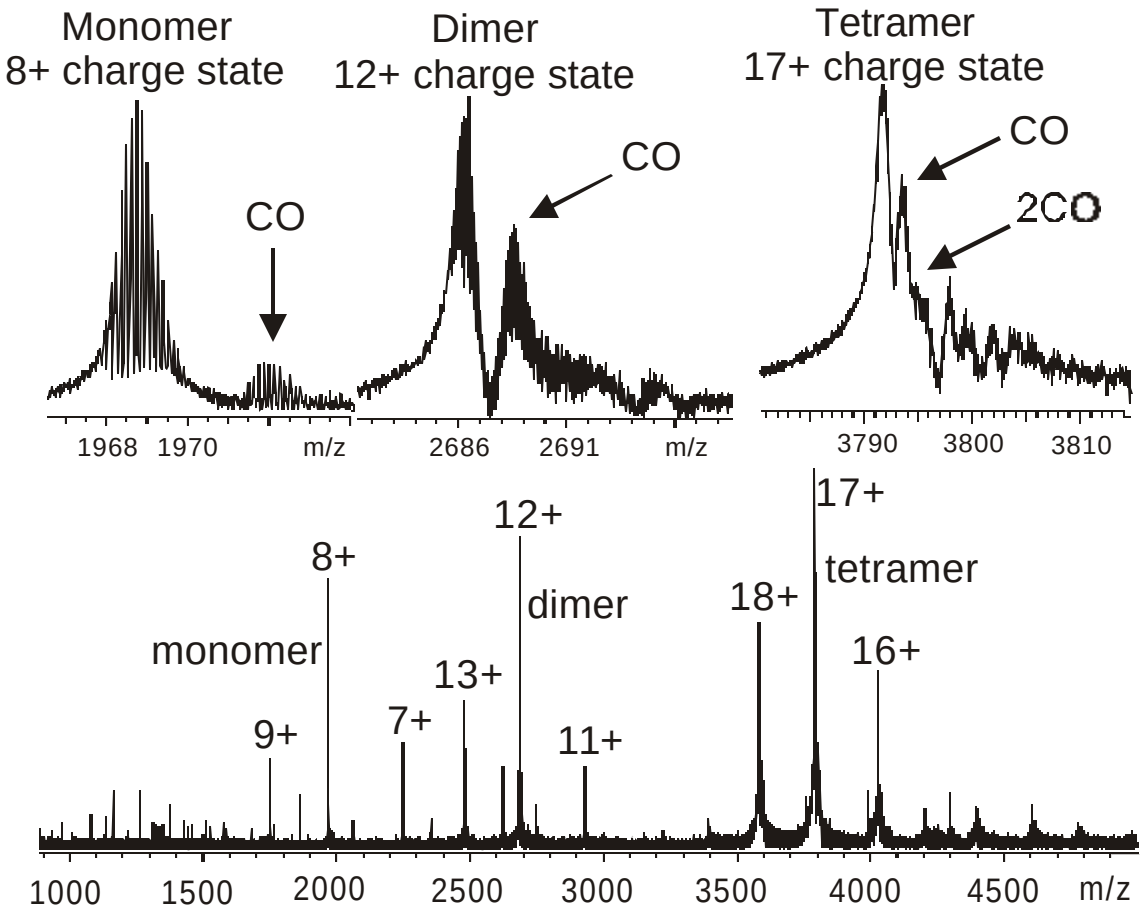
Monomer
8+ charge state
CO
Dimer
12+ charge state
CO
Tetramer
17+ charge state
CO
2CO
1968 1970 m/z
2686 2691 m/z
3790 3800 3810
8+
monomer
9+
7+
13+
12+
dimer
11+
18+
17+
tetramer
16+
1000 1500 2000 2500 3000 3500 4000 4500 m/z

The monomer, dimer, and tetramer all are observed to bind CO, although more non-bound protein is observed in the spectrum. For tetramer, a maximum of 2 ligands per tetramer are observed. For dimer, one or possibly two ligands per dimer are observed, although most of the protein that is detected contains no carbon monoxide. For the monomer, the ratio of CO-bound protein to unbound protein is even lower. The apparent mass for the monomeric hemoglobin is 15731.95 Da versus the calculated value of 15733.05 Da, a difference of 1 Da, suggesting ferric heme. The CO-bound monomeric protein has an apparent mass of 15760.99 Da and the theoretical mass for this protein is 15761.05 Da, corresponding to CO-bound hemoglobin in the ferrous form, $[heme]^0$-CO. This observation is consistent with the known oxidation state preference for the binding of CO to hemoglobin.[20h thef 0 T36 known]

The binding of cyanide to hemoglobin is not dependent on the redox state of heme.[17, 47] We thus examined the cyanide-hemoglobin complex to eliminate the heme redox state as an influence in the observed binding behavior. UV-absorbance spectrophotometry was used to monitor the oxidation state and ligand binding in cyanide-hemoglobin solution, as the λ_{max} for each is known.[17] UV-visible spectra of human hemoglobin with and without bound CN are shown in Figure 5. Met-hemoglobin (Fe^{3+}) is easily distinguished from CN-bound hemoglobin by the shift in λ_{max} from 406 nm to 420 nm in the spectra. The ferric form of CN-bound hemoglobin is more stable than the ferrous form of the complex.[19] Also shown in the mass spectrum is deoxyhemoglobin, or ferrous hemoglobin. The deoxyhemoglobin sample (λ_{max}=430 nm) was prepared by adding sodium dithionite directly to the cuvette before measurement of wavelength. This reduced ferric heme to the ferric form.[17] The presence of sodium dithionite causes the increase in absorbance observed at wavelengths below 350 nm. These spectra are consistent with published data for these forms of hemoglobin[17], and confirm the state of the protein that exists in the solutions that were subsequently analyzed by ESI mass spectrometry.

Figure 6 shows a positive ion mode ESI-FTICR mass spectrum of human hemoglobin that has been treated with potassium cyanide and electrosprayed under nondenaturing (10% methanol) and denaturing (25% methanol) conditions. In the nondenatured spectrum (top), tetramer ($\alpha_2\beta_2$), dimer ($\alpha\beta$), and monomer are observed, each of which bind cyanide. The denaturing solution (bottom) includes peaks corresponding to apoprotein and holoprotein. Peaks corresponding to the α-subunit of hemoglobin, the β-subunit of hemoglobin, α-holoprotein and α-apoprotein with loss of N-terminal methionine, and β-holoprotein are observed in the mass spectrum. The most abundant distribution in the mass spectrum corresponds to α-apoprotein (minus N-terminal methionine). The intact protein appears as a small peak ~130 Da higher. The less denatured mass spectrum (Figure 6, top) shows some small amount of CN binding. Sufficient tertiary structure is conserved to allow the heme group

Figure 7.5 UV-visible absorbance spectrum for hemoglobin showing wavelengths from 230 nm to 590 nm. Met-hemoglobin, CN-bound hemoglobin, and deoxyhemoglobin are labeled in the figure. The reducing agent was not removed from deoxyhemoglobin so a large increase in absorbance can be seen for dithionite at lower wavelengths.

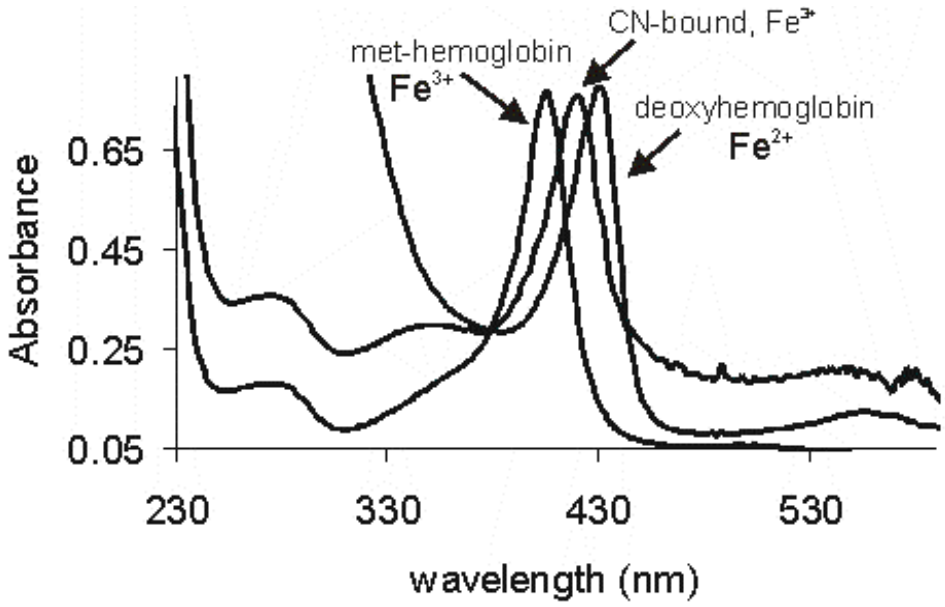
CN-bound, Fe3+
met-hemoglobin
Fe3+
deoxyhemoglobin
Fe2+
Absorbance
0.65
0.45
0.25
0.05
230
330
430
530
wavelength (nm)

Figure 7.6 The ESI-FTICR mass spectra for cyanide-bound hemoglobin in 10% and 25% methanol solutions are shown. Monomer, dimer, and trimer are each observed for the spectrum obtained under nondenaturing conditions (10% methanol), but only monomer is observed for the denatured protein (25% methanol). In both spectra, methionine cleaved hemoglobin is detected, but it still binds CN in its holo form.

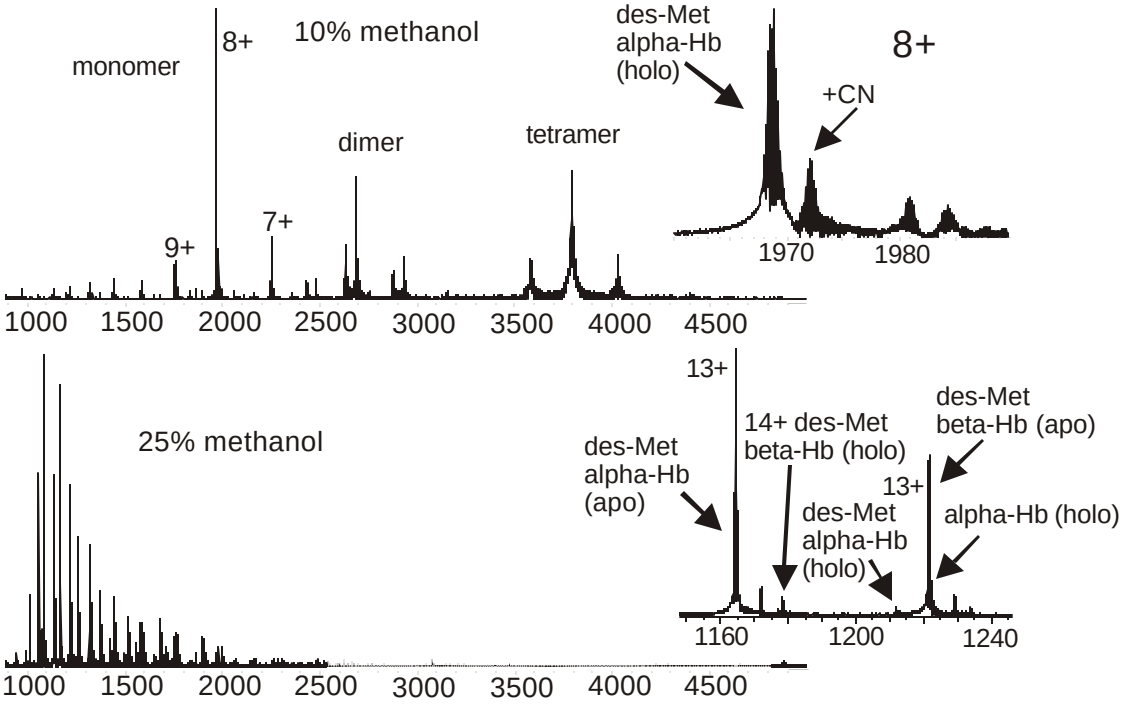
10% methanol
monomer
8+
9+
7+
dimer
tetramer
des-Met
alpha-Hb
(holo)
8+
+CN
1970
1980
1000 1500 2000 2500 3000 3500 4000 4500
25% methanol
13+
14+ des-Met
beta-Hb (holo)
des-Met
beta-Hb (apo)
des-Met
alpha-Hb
(apo)
13+
des-Met
alpha-Hb
(holo)
alpha-Hb (holo)
1160
1200
1240
1000 1500 2000 2500 3000 3500 4000 4500

to be retained. The apparent monoisotopic molecular weight obtained for the hemoglobin-methionine (prepared as reduced protein in 10% methanol) monomer is 15732.10 Da. The calculated molecular weight for this protein is 15733.05 Da, a difference of 1 Da, which indicates that the iron in the heme is present in its oxidized form, Fe^{3+}, and the heme is present as $[heme]^{+}$. The CN-bound form of the protein has an apparent molecular weight of 15759.13 Da and is compared to the theoretical molecular weight of 15759.06 Da, which suggests ferric iron, $[Fe^{3+}CN^{-}]^{2+}$ or oxidized heme, $[heme^{+}\ CN^{-}]^{0}$.

Tetrameric ferric hemoglobin is shown in the mass spectrum in Figure 7. The CN-bound protein discussed previously was dissolved in solutions of 10% and 25% methanol, which may be slightly denaturing to the protein. We electrosprayed CN-bound hemoglobin from a nondenaturing solution to preserve the native conformation of the protein, which is more characteristic of its biological environment. In this way, we hoped to conserve the conformation, and in doing so, prevent dissociation of the ligands in solution caused by alterations in the tertiary structure caused by organic solvents. Charge states of 16+, 17+, and 18+ are observed, and an expansion of the 17+ charge state is shown in the inset. Up to 2 ligands per tetramer are seen in the mass spectrum. Other adducts, possible potassium, sodium, and variations of the two with cyanide can be seen at slightly higher mass-to-charge. Ligand binding to hemoglobin is known to be cooperative,[17] so one would expect to observe four substrate molecules binding with higher abundance. These data suggest that the tertiary structure of the ion is not the same as that of the protein ion in solution. The structures are similar enough to allow the normal stoichiometry of the subunits to be observed ($\alpha_2\beta_2$).

Conclusion

These experiments build on our previous finding that reduced metalloproteins can be analyzed by ESI mass spectrometry provided that oxygen is excluded.[35, 36] Unfortunately, this precludes the study of oxygen binding to these heme proteins. Myoglobin binds cyanide in both positive and negative modes of ionization, although the complex is much more stable as a

Figure 7.7 The ESI-FTICR mass spectrum for the 16+, 17+ and 18+ charge states of tetrameric cyanide-bound hemoglobin are shown. The sample was prepared as the ferric form of CN-hemoglobin and was electrosprayed from a solution of water. The inset shows the expansion of the 17+ charge state. CN-bound hemoglobin is labeled and binds the protein in a ratio of 2 CN per tetramer. Adducts of potassium are also seen in the mass spectrum.

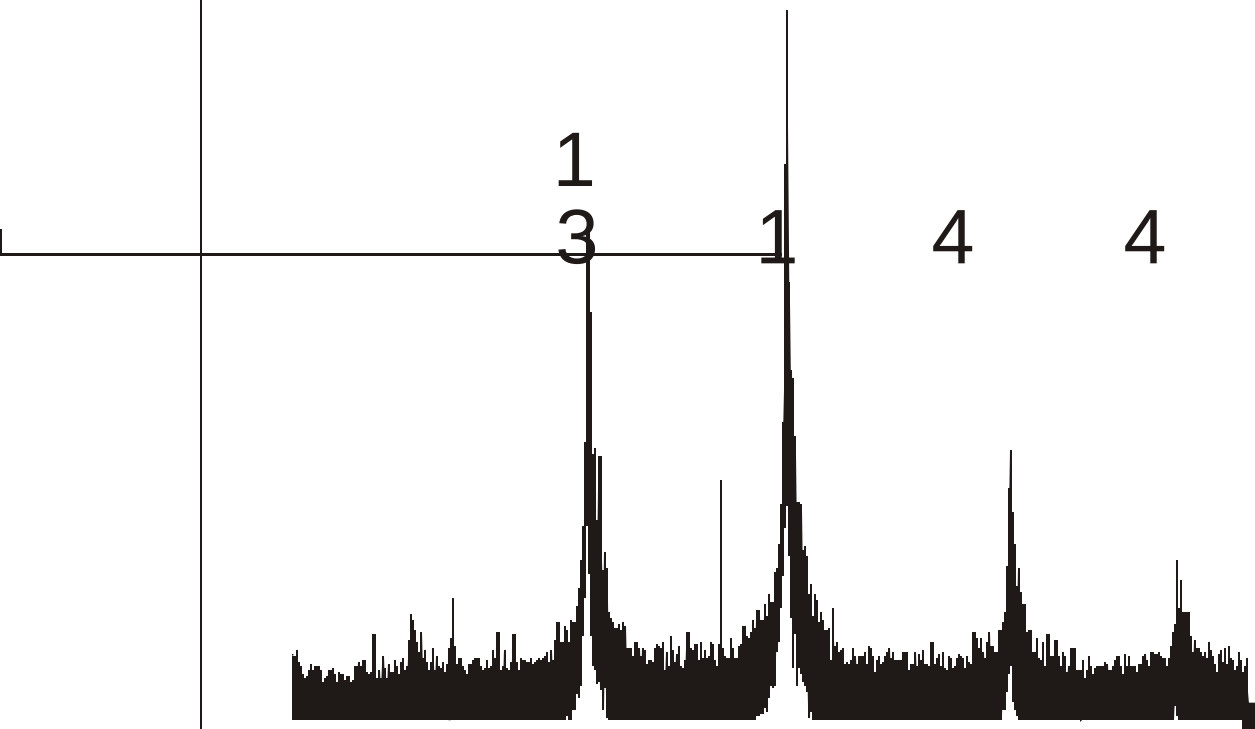
1
3
1
4
4

negative ion. The heated metal capillary temperature has a large effect on the stability of the complex in positive ion mode, in contrast to negative ionization mode, for which the ligand complex is stable over a wider range of temperatures. The redox state of iron in hemoglobin and myoglobin plays an important role in the binding of ligands such as CO and O_2. We have shown that this characteristic of a metalloprotein can be examined by controlling the redox state of the protein under investigation.[25, 35, 36] The studies with CO show that the oxidation state preference of this ligand exists in the gas-phase as well as in solution. There is no evidence of cooperative binding in any of the ligand-hemoglobin complexes that were examined here. These data suggest that small but significant differences exist between the gas-phase and condensed phase structures of hemoglobin holoprotein.

Acknowledgment

The authors would like to thank Brian Shira, Mike Clay, Jeff Agar, and Michael Johnson at the University of Georgia for helpful discussions and for providing reducing agents and carbon monoxide used in these experiments. We gratefully acknowledge funding provided by the National Science Foundation (CHE-9974579).

References

1 Veenstra, T. D.; Johnson, K. L.; Tomlinson, A. J.; Kumar, R.; Naylor, S. *Rapid Commun. Mass Spectrom.* **1998,** *12*, 613-619.

2 Loo, J. A. *Mass Spectrom. Rev.* **1997,** *16*, 1-23.

3 Veenstra, T. D. *Biophys. Chem.* **1999,** *79*, 63-79.

4 Petillot, Y.; Golinelli, M. P.; Forest, E.; Meyer, J. *Biochem. Biophys. Res. Commun.* **1995,** *210*, 686-694.

5 Petillot, Y.; Forest, E.; Mathieu, I.; Meyer, J.; Moulis, J. M. *Biochem. J.* **1993,** *296*, 657-661.

6 Bruce, J. E.; Smith, V. F.; Liu, C. L.; Randall, L. L.; Smith, R. D. *Protein Sci.* **1998,** *7*, 1180-1185.

7 Chazin, W.; Veenstra, T. D. *Rapid Commun. Mass Spectrom.* **1999,** *13*, 548-555.

8 Jaquinod, M.; Leize, E.; Potier, N.; Albrecht, A. M.; Shanzer, A.; Vandorsselaer, A. *Tetrahedron Lett.* **1993,** *34*, 2771-2774.

9 Lei, Q. P.; Cui, X. Y.; Kurtz, D. M.; Amster, I. J.; Chernushevich, I. V.; Standing, K. G. *Anal. Chem.* **1998,** *70*, 1838-1846.

10 Pramanik, B. N.; Bartner, P. L.; Mirza, U. A.; Liu, Y. H.; Ganguly, A. K. *J. Mass Spectrom.* **1998,** *33*, 911-920.

11 Nemirovskiy, O. V.; Ramanathan, R.; Gross, M. L. *J. Am. Soc. Mass Spectrom.* **1997,** *8*, 809-812.

12 Remigy, H.; Jaquinod, M.; Petillot, Y.; Gagnon, J.; Cheng, H.; Xia, B.; Markley, J. L.; Hurley, J. K.; Tollin, G.; Forest, E. *J. Prot. Chem.* **1997,** *16*, 527-532.

13 Neubert, T. A.; Walsh, K. A.; Hurley, J. B.; Johnson, R. S. *Protein Sci.* **1997,** *6*, 843-850.

14 Wang, F.; Li, W. Q.; Emmett, M. R.; Marshall, A. G.; Corson, D.; Sykes, B. D. *J. Am. Soc. Mass Spectrom.* **1999,** *10*, 703-710.

15 Shelimov, K. B.; Jarrold, M. F. *J. Am. Chem. Soc.* **1997,** *119*, 2987-2994.

16 Shelimov, K. B.; Clemmer, D. E.; Hudgins, R. R.; Jarrold, M. F. *J. Am. Chem. Soc.* **1997,** *119*, 2240-2248.

17 Antonini, E.; Brunori, M. In *Frontiers of Biology*; Neuberger, A., Tatum, E. L., Eds.; American Elsevier Publishing Company: New York, 1971; Vol. 21, pp 436.

18 Garrett, R. H.; Grisham, C. M. *Biochemistry*; Harcourt Brace College Publishers: New York, 1995.

19 Bellelli, A.; Antonini, G.; Brunori, M.; Springer, B. A.; Sligar, S. G. *J. Biol. Chem.* **1990,** *31*, 19989-18901.

20 Egan, W. J.; Brewer, W. E.; Morgan, S. L. *Appl. Spectrosc.* **1999,** *53*, 218-225.

21 Winston, R. L.; Fitzgerald, M. C. *Mass Spectrom. Rev.* **1997,** *16*, 165-179.

22 Hu, P. F.; Loo, J. A. *J. Mass Spectrom.* **1995,** *30*, 1076-1082.

23 Yu, X. L.; Wojciechowski, M.; Fenselau, C. *Anal. Chem.* **1993,** *65*, 1355-1359.

24 Thorvaldsen, J. L.; Sewell, A. K.; Tanner, A. M.; Peltier, J. M.; Pickering, I. J.; George, G. N.; Winge, D. R. *Biochemistry.* **1994,** *33*, 9566-9577.

25 Johnson, K. A.; Verhagen, M.; Adams, M. W. W.; Amster, I. J. *Anal. Chem.* **2000,** *72*, 1410-1418.

26 Randall, L. L.; Hardy, S. J. S.; Topping, T. B.; Smith, V. F.; Bruce, J. E.; Smith, R. D. *Protein Sci.* **1998,** *7*, 2384-2390.

27 Wilm, M.; Mann, M. *Int. J. Mass Spectrom. Ion Process.* **1994,** *136*, 167-180.

28 Wilm, M.; Mann, M. *Anal. Chem.* **1996,** *68*, 1-8.

29 He, F.; Hendrickson, C. L.; Marshall, A. G. *J. Am. Soc. Mass Spectrom.* **2000**, 120-126.

30 Van Berkel, G. J.; Giles, G. E.; Bullock, J. S.; Gray, L. J. *Anal. Chem.* **1999,** *71*, 5288-5296.

31 Deng, H.; Van Berkel, G. J. *Anal. Chem.* **1999,** *71*, 4284-4293.

32 Bond, A. M.; Colton, R.; Dagostino, A.; Traeger, J. C.; Downard, A. J.; Canty, A. J. *Inorg. Chim. Acta* **1998,** *267*, 281-291.

33 McLafferty, F. *J. Am. Chem. Soc.* **1998,** *120*, 4732-4740.

34 Johnson, K. A.; Amster, I. J. *J. Am. Soc. Mass Spectrom.* **2000**, Submitted.

35 Johnson, K. A.; Shira, B. A.; Anderson, J. A.; Amster, I. J. *Anal. Chem.* **2000**, Submitted.

36 Johnson, K. A.; Verhagen, M.; Adams, M. W. W.; Amster, I. J. *Int. J. Mass Spectrom.* **2001,** *204*, 77-85.

37 Schweitzer, R.; Stenner, D.; Wedekind, D.; Dreybrodt, W. *Biophys. J.* **1989,** *55*, 703-712.

38 Schmidt, A. J.; Karas, M. *Communication* **1999**.

39 Lippincott, J.; Fattor, T. J.; Lemon, D. D.; Apostol, I. *Anal. Biochem.*. **2000,** *284*, 247-255.

40 Apostol, I. *Anal. Biochem.*. **1998,** *272*, 8-18.

41 Schaaff, T. G.; Cargile, B. J.; Stephenson, J. L.; McLuckey, S. A. *Anal. Chem.* **2000,** *72*, 899-907.

42 Senko, M. W.; Beu, S. C.; McLafferty, F. W. *J. Am. Soc. Mass Spectrom.* **1995,** *6*, 229-233.

43 Petillot, Y.; Forest, E.; Meyer, J.; Moulis, J. M. *Anal. Biochem.*. **1995,** *228*, 56-63.

44 Veenstra, T. D.; Johnson, K. L.; Tomlinson, A. J.; Naylor, S.; Kumar, R. *Biochemistry.* **1997,** *36*, 3535-3542.

45 Gryczynski, Z.; Gering, H.; Bucci, E. *Anal. Biochem.*. **1998,** *255*, 176-182.

46 Balasubramanian, S.; Lambright, D. G.; Simmons, J. H.; Gill, S. J.; Boxer, S. G. *Biochemistry.* **1994,** *33*, 8355-8360.

47 Brunori, M.; Antonini, G.; Castagnola, M.; Bellelli, A. *J. Biol. Chem.* **1992,** *267*, 2258-2263.

CHAPTER 8

CONCLUSIONS AND FUTURE DIRECTIONS

Metalloproteins provide many interesting challenges to electrospray ionization Fourier transform ion cyclotron resonance mass spectrometry. These challenges begin with the transfer of the solution phase metalloprotein into the gas phase without disrupting the native conformation of the protein-metal complex. This problem is overcome by suspending the metalloprotein in a solution that is compatible with the conditions of the protein in its biological environment that will not denature the protein and result in loss of the noncovalently bound metal prosthetic group. By achieving ionization of a nondenatured metalloprotein, measurements of stoichiometry and conformation are made, and its identity can be confirmed.

We have illustrated these concepts using metalloproteins that include ferredoxins, metal-substituted ferredoxins, and rubredoxin. Measurements in positive ion mode have shown that upon denaturation, accompanied by loss of the metal center, a much wider distribution of ions is detected. The stoichiometry is determined simply by measurements of the protein under denaturing and nondenaturing conditions. The iron-sulfur clusters from *Pyrococcus furiosus* and *Thermotoga maritima* have been shown to contain metalloprosthetic centers that range from mononuclear iron centers to [4Fe-4S] clusters and even multiple [4Fe-4S] centers as in the case of pyruvate oxidoreductase. Measurements of stoichiometry of mixed metal and metal-substituted ferredoxin clusters have also been conducted during these studies. Metal centers of interest have included [3FeNi-4S] from *Thermococcus litoralis*, [3FeMn-4S] from *Pyrococcus furiosus*, and the gallium-substituted [4Ga-4S] cluster from *Pyrococcus furiosus*.

Electrospray ionization is used for biological molecules because it is a “soft” method of ionization. Many comparisons between solution phase and gas phase have been made since the advent of the method. The comparisons have been taken one step further by ionizing metalloproteins in both positive and negative modes, which create positive ions and negative ions to be analyzed. The high resolution comparisons have shown that the formation of disulfide bonds, the solution phase oxidation state, and the retention of the metal center are not affected by changes between positive and negative modes of ionization; however, variations in the charge state distributions and stability of protein ions do occur. Mononuclear metal-containing

proteins ions and [3FeM-4S]-containing (M = Fe, Ni, Mn) proteins ions are stable in both modes of ionization, but protein ions consisting of [2Fe-2S] and [3Fe-4S] clusters are only stable as negative ions. The positive ion forms of these metalloproteins degrade during ionization forming products with losses of inorganic sulfide.

The substitution of manganese into the iron-sulfur cluster from *Pyrococcus furiosus* generates a [3FeMn-4S] cluster that is only stable in its reduced form. Upon oxidation of the metalloprotein, manganese is ejected from the cluster. This research provides the first direct evidence that this cluster exists. In addition, this is the first time that a metalloprotein has been observed in its reduced form during electrospray ionization mass spectrometry.

These experiments have led to interesting structural studies, in which some metalloproteins change drastically depending on the mode of ionization. In particular, the [3Fe-4S] cluster from *Pyrococcus furiosus* ferredoxin degrades during positive ion mode, but remains stable during ionization as a negative ion. This same observation is true for the same protein with either manganese-substitution, [3FeMn-4S], and the gallium substituted form, [4Ga-4S]. These studies provide the first direct evidence of the existence of the [3FeMn-4S] cluster in both the oxidized and the reduced form. The degradation of some metal clusters in positive mode has led to studies conducted in negative ion mode because of the increased stability of the negative ions. The importance of this finding is illustrated in the study of the stoichiometry of the gallium-substituted cluster from *Pf*. Studies in positive mode resulted in an assignment of the cluster as [3Ga-3S], but a more stable ion in negative mode allowed the

spectrometric measurements. The oxidation or reduction of the metal or metal cluster of a metalloprotein can change the measured molecular weight by 1 Da, the mass of a proton that is substituted for charge on a reduced metal (compared to the oxidized form of the electrosprayed metalloprotein ion) ion during positive ion mode, for example. These small variations in mass become more complex when dealing with metalloproteins that contain post-translational modifications, however, those situations can be resolved using proteomic methods of sample preparation like enzymatic or chemical digestion before mass spectrometric analysis.

We have found that the oxidation state that is detected by ESI mass spectrometry is the highest biologically relevant oxidation state for the metalloprotein under biological conditions. We have observed oxidation states that range from 0, in the case of heme in cytochrome *c*, for example, to 3+, in the case of HiPIP from *Cv*. For HiPIP, the initial measurements of oxidation state was 4+, which is not the biologically relevant redox state for the protein. The chemical and enzymatic digestion of the HiPIP from *Cv* allowed the confirmation of the post-translational modification, amidation, which differed in mass by 1 Da compared to the published amino acid sequence. After accounting for the modification, the redox state for HiPIP was assigned as 3+.

We have also shown that the reduced forms of several proteins can be observed by ESI mass spectrometry by reducing the metalloproteins prior to ESI by chemical or electrochemical methods. We found that removal of the reducing agent (sodium dithionite or ascorbic acid) could be achieved in an oxygen-free environment without oxidation of the metal center. The preparation and analysis time was greatly reduced by using an electrochemical cell that was fabricated in our laboratory for metalloprotein reduction. This cell also lowered the risk of reoxidation of the metalloprotein in solution prior to ESI.

Electron transfer and other redox active metalloproteins with a wide range of reduction potentials should be investigated to determine the limits of use by ESI mass spectrometry. One of the main limiting factors for metalloprotein analysis by ESI mass spectrometry is the possible exposure of reduced protein to oxygen before or during analysis. The exposure before analysis may be resolved by miniaturizing the electrochemical cell that is described in Chapter 6.

Exposure during ionization may be overcome by using a sheath of non-reactive gas such as nitrogen or argon, or an oxygen-free box that isolates the ionization source from the ambient environment. Since there seemed to be no effect on the proteins that we have examined so far, this procedure may only be necessary for metalloproteins with lower reduction potentials.

There are several caveats that are revealed from the completion of the work presented here. These areas of interest result from the study of metalloproteins by FTICR mass spectrometry and the data that show the process by which the redox active proteins are ionized does not affect the oxidation state of the protein in solution. We have shown that this characteristic of a metalloprotein can be exploited by using hemoglobin in both of its redox forms to study ligand binding. Although cyanide is found to bind both oxidized and reduced forms of hemoglobin, carbon monoxide only binds to hemoglobin in its reduced form.[1] There are many examples of increased stability of proteins in negative mode versus positive mode ESI,[2-7] and we have shown that this stability is necessary for the observation of several ferredoxin proteins as well as the myoglobin-cyanide complex.[8]

The study of reduced metalloproteins and their ligands does not limit itself to hemoglobin. A variety of other metalloprotein-ligand complexes could be studied by mass spectrometry, such as nitrogenase, the enzyme complex which performs the conversion of N_2 to ammonia and consists of an iron protein and a molybdenum-iron protein. The reactions occur while N_2 is bound to the complex, but the protein is inactivated in the presence of oxygen. Another potential candidates for analysis is superoxide reductase, which can bind ligands similar to heme-protein ligands.

The high-potential iron-sulfur protein from *Chromatium vinosum* is another candidate for further exploration of these concepts. The systematic mutation of the active site amino acid residues provides insight into their functional roles in maintaining the redox characteristics and stability of the iron-sulfur center. A change in redox state for some metalloproteins is also accompanied by change in their structure. Hemoglobin, because of its allosteric effects (i.e. its subunit cooperativity in binding ligands), is an example of a protein whose structure relies on its

oxidation state.[1] Cowan and co-workers found that for a particular mutant form of the HiPIP, C77S, the stability of the metal cluster was affected depending on which redox state the protein was in.[9] The [4Fe-4S] cluster protein was found to degrade within a few hours in its oxidized form to resemble a [3Fe-4S]-type cluster by EPR. Measurements of labile clusters can be made using ESI mass spectrometry in either positive or negative ion mode to investigate not only the mutations, but also metal binding efficiency simultaneously.

The experiments presented here provide a foundation for the further analysis of metalloproteins by ESI mass spectrometry. These experiments include information from many aspects of metalloprotein structure ranging from primary to tertiary structure, metal stoichiometry, oxidation state, and protein-metal-ligand binding. Several examples of experiments applicable to these studies are included, which take advantage of the gentle ionization conditions that ESI provides.

References

1 Antonini, E.; Brunori, M. In *Frontiers of Biology*; Neuberger, A., Tatum, E. L., Eds.; American Elsevier Publishing Company: New York, 1971; Vol. 21, pp 436.

2 Petillot, Y.; Forest, E.; Meyer, J.; Moulis, J. M. *Anal. Biochem.*. **1995,** *228*, 56-63.

3 Remigy, H.; Jaquinod, M.; Petillot, Y.; Gagnon, J.; Cheng, H.; Xia, B.; Markley, J. L.; Hurley, J. K.; Tollin, G.; Forest, E. *J. Prot. Chem.* **1997,** *16*, 527-532.

4 Schmidt, A. J.; Karas, M. *Communication* **1999**.

5 Lippincott, J.; Fattor, T. J.; Lemon, D. D.; Apostol, I. *Anal. Biochem.*. **2000,** *284*, 247-255.

6 Apostol, I. *Anal. Biochem.*. **1998,** *272*, 8-18.

7 Schaaff, T. G.; Cargile, B. J.; Stephenson, J. L.; McLuckey, S. A. *Anal. Chem.* **2000,** *72*, 899-907.

8 Johnson, K. A.; Verhagen, M.; Adams, M. W. W.; Amster, I. J. *Anal. Chem.* **2000,** *72*, 1410-1418.

9 Agarwal, A.; Li, D.; Cowan, J. A. *J. Am. Chem. Soc.* **1996,** *118*, 927-928.